MOLECULAR CHARACTERISATION AND FUNCTIONAL ANALYSES OF *Musa acuminata Pathogenesis-related 10* (*MaPR10*) GENE

ARULLTHEVAN A/L RAJENDRAM

FACULTY OF SCIENCE
UNIVERSITI MALAYA
KUALA LUMPUR

2022

MOLECULAR CHARACTERISATION AND FUNCTIONAL ANALYSES OF *Musa acuminata* *Pathogenesis-related 10* (*MaPR10*) GENE

ARULLTHEVAN A/L RAJENDRAM

DISSERTATION SUBMITTED IN FULFILMENT OF THE REQUIREMENTS FOR THE DEGREE OF MASTER OF SCIENCE

INSTITUTE OF BIOLOGICAL SCIENCES
FACULTY OF SCIENCE
UNIVERSITI MALAYA
KUALA LUMPUR

2022

UNIVERSITI MALAYA

ORIGINAL LITERARY WORK DECLARATION

Name of Candidate: **ARULLTHEVAN A/L RAJENDRAM**

Matric No: **17051477/2**

Name of Degree: **MASTER OF SCIENCE**

Title of Dissertation ("this Work"):

MOLECULAR CHARACTERISATION AND FUNCTIONAL ANALYSES OF *Musa acuminata Pathogenesis-related 10* (*MaPR10*) GENE

Field of Study:

BIOCHEMISTRY AND BIOTECHNOLOGY

I do solemnly and sincerely declare that:

(1) I am the sole author/writer of this Work;
(2) This Work is original;
(3) Any use of any work in which copyright exists was done by way of fair dealing and for permitted purposes and any excerpt or extract from, or reference to or reproduction of any copyright work has been disclosed expressly and sufficiently and the title of the Work and its authorship have been acknowledged in this Work;
(4) I do not have any actual knowledge nor do I ought reasonably to know that the making of this work constitutes an infringement of any copyright work;
(5) I hereby assign all and every rights in the copyright to this Work to the University of Malaya ("UM"), who henceforth shall be owner of the copyright in this Work and that any reproduction or use in any form or by any means whatsoever is prohibited without the written consent of UM having been first had and obtained;
(6) I am fully aware that if in the course of making this Work I have infringed any copyright whether intentionally or otherwise, I may be subject to legal action or any other action as may be determined by UM.

Candidate's Signature Date: 31.01.2022

Subscribed and solemnly declared before,

Witness's Signature Date: 31.01.2022

Name:

Designation:

MOLECULAR CHARACTERISATION AND FUNCTIONAL ANALYSES OF *Musa acuminata Pathogenesis-related 10* (*MaPR10*) GENE

ABSTRACT

Plant immunity to pathogen infections is a dynamic response that involves multiple organelles and defence signalling systems such as induced systemic resistance (ISR) and systemic acquired resistance (SAR). The latter is mediated by pathogenesis-related proteins (PR), a common type of plant protein known for its diverse role in plant innate immunity. In this study, two novel PR protein variants were isolated from two *Musa acuminata* cultivars namely Berangan and Grand Naine (ITC 1256). Sequence characterisation study carried out on 69 genomic and transcript clones of *M. acuminata PR* (*MaPR*) gene revealed that the *PR1-like* gene that was reported to involve in *Meloidogyne incognita* - Grand Naine (ITC 1256) interaction in Al-Idrus *et al.* (2017) actually belongs to *PR10* gene group despite showing 81–95 % similarity with *M. acuminata PR1* sequences in the GenBank and Banana Genome Hub database. This discrepancy was further discussed and linked to miss-curation of the previous sequence data entered in the two sequence databases, hence the isolated clones were denoted as *MaPR10* instead. Phylogenetic analysis revealed that the deduced amino acid sequences from 69 genomic and transcript clones of *MaPR10* clustered into four distinct groups, while 44 genomic clones clustered into three distinct groups. Southern blot result corroborated that of found in phylogenetic analysis confirming that *MaPR10* gene was present in at least three copies in both Berangan and Grand Naine genomes studied. Two sequence variants i.e., *MaPR10-BeB5* and *MaPR10-GNA5,* were chosen for a subcellular localisation study in onion epidermal cells. Meeting the expectation of the *in silico* prediction, this study confirmed that the two protein variants were localised intracellularly. In addition, functional analyses confirmed that both protein variants function as β-1,3-glucanases and ribonucleases. While the former is novel, the latter is a common function of the members of *PR10* gene family in plants. When tested on three

economically important fungal species *Aspergillus fumigatus*, *Aspergillus niger*, and *Fusarium oxysporum* f. sp. *cubense*: Tropical Race 4, both protein variants only significantly ($p < 0.05$) inhibited the growth of *A. fumigatus*. This study reports MaPR10 protein variants as the first plant protein to exhibit antagonistic effect towards *A. fumigatus* and the first member of PR10 protein family to exhibit β-1,3-glucanase function.

Keywords: Antifungal enzyme, β-1,3-glucanase, *Musa acuminata*, *Pathogenesis-related 10* gene, ribonuclease.

PENCIRIAN MOLEKULAR DAN ANALISIS FUNGSI GEN *Berkait Pathogenesis 10 Musa acuminata (MaPR10)*

ABSTRAK

Imuniti tumbuhan terhadap serangan patogen merupakan satu tindak balas dinamik yang melibatkan pelbagai organel dan sistem isyarat pertahanan seperti rintangan sistemik teraruh (RST/*ISR*) dan rintangan yang diperoleh secara sistemik (RDSS/*SAR*). Sistem RDSS dikawal oleh protein berkait patogenesis (BP/*PR*), satu protein tumbuhan yang diketahui untuk peranannya yang pelbagai dalam imuniti tumbuhan. Dalam kajian ini, dua varian protein BP baharu telah berjaya diasingkan daripada dua kultivar *Musa acuminata* iaitu Berangan dan 'Grand Naine' (ITC 1256). Kajian pencirian jujukan telah dilaksanakan terhadap 69 klon genomik dan transkrip *MaPR* menunjukkan bahawa identiti sebenar gen serupa *PR1* yang dilaporkan terlibat dalam interaksi *Meloidogyne incognita* – 'Grand naine' (ITC 1256) dalam Al-Idrus (2017) sebenarnya tergolong dalam kumpulan gen *PR10* walaupun menunjukkan 81–95 % persamaan dengan jujukan gen *PR1 M. acuminata* dalam pangkalan data GenBank dan Banana Genome Hub. Percanggahan ini telah dibincangkan dan dikaitkan dengan kurasi tidak tepat pada data sebelumnya yang telah dimasukkan ke dalam kedua-dua pangkalan data tersebut. Oleh itu, semua klon yang diasingkan dirujuk sebagai gen *MaPR10.* Analisis filogenetik yang dijalankan terhadap 69 jujukan asid amino PR10 yang diterjemahkan daripada klon genomik dan trankrip terbahagi kepada empat kumpulan berbeza, manakala 44 klon genomik terbahagi kepada tiga kumpulan berbeza. Analisis sap 'Southern' menyokong hasil dapatan analisis filogenetik, menunjukkan terdapat sekurang-kurangnya tiga salinan gen *MaPR10* dalam genom kultivar Berangan dan 'Grand Naine'. Dua varian iaitu *MaPR10-BeB5* dan *MaPR10-GNA5* telah dipilih untuk kajian persetempatan subsel dalam sel epidermis bawang. Kajian tersebut memenuhi jangkaan ramalan simulasi komputer dan mengesahkan bahawa kedua-dua varian protein bersetempat di dalam sel. Di samping itu, analisis fungsi mengesahkan bahawa kedua-dua varian protein berfungsi

sebagai β-1,3-glukanase dan ribonuklease. Sementara fungsi gen ini sebagai β-1,3-glukanase adalah satu penemuan baharu bagi ahli keluarga gen *PR10*, fungsi ribonuklease pula merupakan antara fungsi yang kerap dikaitkan dengan gen *PR10.* Apabila potensi anti-kulat kedua-dua varian protein ini diuji dengan tiga jenis kulat, iaitu *Aspergillus fumigatus*, *Aspergillus niger*, dan *Fusarium oxysporum* f. sp. *cubense*: Tropical Race 4, kedua-dua varian protein hanya berjaya merencatkan pertumbuhan kulat *A. fumigatus* secara ketara ($p < 0.05$). Kajian ini melaporkan varian protein MaPR10 sebagai protein tumbuhan pertama yang menunjukkan interaksi antagonis jelas terhadap *A. fumigatus* dan ahli pertama dalam keluarga protein PR10 yang berfungsi sebagai β-1,3-glukanase.

Kata kunci: β-1,3-glukanase, enzim anti-kulat, gen *berkait patogenesis 10*, *Musa acuminata*, ribonuklease.

ACKNOWLEDGEMENTS

First and foremost, I would like to express my deepest and sincere gratitude to my main research supervisor, Dr. Syarifah Aisyafaznim Sayed Abdul Rahman and co-supervisor, Dr. Nur Ardiyana Rejab for their patience, supervision, and guidance in this research project as well as for the many ideas and constructive criticisms offered during the completion of this thesis. I appreciate the training I have received from both supervisors in molecular laboratory technical works, analytical works and in scientific writing. Special thanks to Dr. Walftor Dumin, a post-doctoral research fellow from MP 2.0 Genetics Laboratory, who is now working in National Institute of Horticultural and Herbal Science, Rural Development Administration in Republic of Korea for the analytical knowledge offered. A special thanks to the dear members of the MP 2.0 Genetics Laboratory; Professor Dr. Zulqarnain Mohamed, Dr. Sally Teh Ser Huy, Dr. Yeoh Suat Hui, Dr. Ili Syazwana Abdullah, Dr. Fiqri Dizar Khaidizar, Dr. Nur Nadiah Roslan, Amirah Assyiqqin, Nur Ayuni Dayana, Nurfairuz Abdul Latiff, Mohamad Taufiq Ahmad, Yvonne Cashinn Chia, Nurhafizah Dahniar Afandi, Ahmad Husaini Suhaimi, Fatin Nurshuhada, Nur Fatin Husna Mohd Yunos, Ong Sheue Ni and importantly, Nur Hikmah Mostaffa for the wonderful moments and the support given throughout my postgraduate life and research journey. Thanks also to Dr. Khanom Simarani and Dr. Mushafau Adebayo Oke for providing the assistance and technical knowledge on antifungal study in this project. Not to forget Dr. Zuliana Razali and Associate Professor Dr. Chandran Somasundram who helped me in the biochemical study for this research. Lastly, I would like to thank my family: Rajendram Annamalai, Vasanthi G. Arokiasamy, Ananthakrishan Rajendram, Arunnvinthan Rajendram and Vinotha Sharmini Nagooru, and my close friends: Aruna Suframanyam and Prasad Malaimany, for their unconditional love, support and sacrifices given along the research journey.

TABLE OF CONTENTS

ABSTRACT ..... **iii**

ABSTRAK ..... **v**

ACKNOWLEDGEMENTS ..... **vii**

TABLE OF CONTENTS ..... **viii**

LIST OF FIGURES ..... **xvi**

LIST OF TABLES ..... **xix**

LIST OF SYMBOLS AND ABBREVIATIONS ..... **xx**

LIST OF APPENDICES ..... **xxiii**

CHAPTER 1: INTRODUCTION **1**

1.1 Background study 1

1.2 Aim and objectives 4

CHAPTER 2: LITERATURE REVIEW **5**

2.1 Banana and its economic value 5

2.2 Biotic stresses on banana plants 5

2.3 Plant-parasitic nematodes (PPN) 7

2.4 *Meloidogyne incognita* and the current practice to manage PPNs in banana plantations 8

2.5 Plant defence system 9

2.6 Systemic acquired resistance (SAR) and induced systemic responses (ISR) 12

2.7 Pathogenesis-related (PR) proteins 13

2.8 Pathogenesis-related 10 (PR10) protein 14

2.9 Subcellular localisation of PR proteins 16

2.10 Functional analyses of a gene 17

2.10.1 Dinitrosalicylic acid (DNS) assay 19

2.11 Opportunistic and pathogenic fungi 20

2.11.1 *Aspergillus fumigatus* 20

2.11.2 *Aspergillus niger* 21
2.11.3 *Fusarium oxysporum* f. sp. *cubense* 22
2.11.4 Antifungal susceptibility test 23
CHAPTER 3: METHODOLOGY 25
3.1 Data mining 25
3.2 Plant tissue culture and transplantation 25
3.3 Propagation of *M. incognita* in plants 26
3.4 DNA isolation from banana leaf tissues 27
3.5 RNA isolation from plant tissues 28
3.5.1 Diethylpyrocarbonate (DEPC) treatment on the apparatus used for RNA isolation experiment 28
3.5.2 RNA isolation from *M. incognita*-infected banana root tissues 29
3.5.3 RNA isolation from *A. thaliana* leaf tissues 30
3.6 Quantification and quality assessment of nucleic acid samples 31
3.7 Agarose gel electrophoresis 31
3.7.1 Gel electrophoresis of DNA sample 31
3.7.2 Gel electrophoresis of RNA sample 31
3.8 Isolation of Musa acuminata pathogenesis-related 1-like (MaPR1-like) gene from banana DNA samples 32
3.8.1 Primer design for the isolation of *MaPR1-like* gene 32
3.8.2 PCR amplification of *MaPR1-like* gene from banana genomic samples 32
3.8.3 DNA purification 33
3.8.4 Preparation of *Escherichia coli* strain JM109 competent cells using calcium chloride ($CaCl_2$) 34
3.8.5 T-A Cloning 35
3.8.6 Plasmid isolation using alkaline lysis with sodium dodecyl sulfate (SDS) 37

3.8.7 Restriction enzyme (RE) digestion assay 38
3.8.8 Cycle sequencing 39
3.8.9 Sequence and phylogenetics analyses of the isolated genomic clones 39
3.9 Copy number analysis of *MaPR1-like* gene in the two banana genomes 40
3.9.1 Hybridisation probe design 40
3.9.2 Southern blot assay 41
3.10 Isolation of *MaPR1-like* transcript from RNA samples 42
3.10.1 Reverse transcriptase-PCR of *MaPR1-like* transcript and cloning of the isolated fragment 42
3.10.2 Sequence analysis of putative *MaPR1-like* transcript clones using deduced amino acid sequences 43
3.10.3 Phylogenetic analysis of the deduced amino acid cloned sequences of MaPR10 44
3.11 *Agrobacterium tumefaciens*-based infiltration study using inner epidermal onion cells 45
3.11.1 Propagation and cloning of *MaPR10-BeB5* and MaPR10-*GNA5* transcript fragments into pCAMBIA1304 expression vector 45
3.11.2 Amplification and purification of *MaPR10-BeB5* and *MaPR10-GNA5* transcript fragments 46
3.11.3 Purification of the *Nco*I-digested *MaPR10* transcript fragments and *Nco*I-digested pCAMBIA1304 vector 46
3.11.4 Directional cloning 47
3.11.5 Plasmid isolation and restriction enzyme digestion assay 48
3.11.6 Sequence analysis on the cloned fragment 49
3.11.7 Propagation of pCAMBIA1304::CaMV35S::*MaPR10-BeB5/GNA5*::*mgfp5*::*GUS*::6xHis vector into *A. tumefaciens* strain LB4404 49

3.11.8 β-glucuronidase (GUS) histochemical assay on transformed *A. tumefaciens* cells 50
3.11.9 *In vivo* subcellular localisation of MaPR10-BeB5 and MaPR10-GNA5 protein variants in inner epidermal onion cells 51
3.12 Overexpression of *MaPR10-BeB5* and *MaPR10-GNA5* transcripts in *Escherichia coli* strain BL21 cells 52
3.12.1 Amplification and fragment purification of *Nco*I-digested *MaPR10-BeB5* and *MaPR10-GNA5* transcript fragments and pET30a(+) expression vector 52
3.12.2 DNA ligation, transformation, and bacterial screening of transformed *E. coli* strain JM109 cells via colony PCR 53
3.12.3 Propagation of pET30a(+)::T7promoter::6xHis::*MaPR10*-BeB5*/GNA5* vector in *Escherichia coli* strain BL21(E3) cells 54
3.12.4 Induction of heterologous gene expression in *E. coli* strain BL21(E3) cells 54
3.12.5 Purification of MaPR10-BeB5 and MaPR10-GNA5 protein variants using nickel His Gravitrap™ affinity column 55
3.12.6 Precipitation of the purified MaPR10-BeB5 and MaPR10-GNA5 protein variants 56
3.12.7 Bradford assay 56
3.12.8 SDS-PAGE and western blot analysis 57
3.13 Functional analyses of MaPR10-BeB5 and MaPR10-GNA5 protein variants 60
3.13.1 Ribonuclease activity assay 60
3.13.2 Laminarin-dinitrosalicylic acid assay of purified MaPR10-BeB5 and MaPR10-GNA5 protein variants 61

3.14 Antifungal susceptibility assay of MaPR10-BeB5 and MaPR10-GNA5 protein variants against *Aspergillus fumigatus*, *Aspergillus niger* and *Fusarium oxysporum* f. sp. *cubense*: Tropical Race 4 62

3.14.1 Fungal culture growth 62

3.14.2 Morphological-based identification of *A. fumigatus*, *A. niger* and *F. oxysporum* 62

3.14.3 Molecular-based identification of *A. fumigatus*, *A. niger* and *F. oxysporum* 63

3.14.4 Well-diffusion method for antifungal susceptibility assay of MaPR10-BeB5 and MaPR10-GNA5 protein variants against *A. fumigatus, A.* niger and *F. oxysporum* 65

3.14.5 Statistical analysis 66

CHAPTER 4: RESULTS 67

4.1 Isolation of putative *Musa acuminata Pathogenesis-related 1-like* gene 67

4.1.1 Data mining and primer design for the isolation of *MaPR1-like* gene from Berangan and Grand Naine (ITC 1256) cultivars 67

4.1.2 DNA isolation from Berangan and Grand Naine (ITC 1256) cultivars 68

4.1.3 Isolation and purification of *MaPR1-like* gene from Berangan and Grand Naine (ITC 1256) cultivars 69

4.1.4 T-A cloning: Colony screening for the cloned *MaPR1-like* gene fragment 70

4.1.5 Isolation of pGEM-T Easy plasmids containing the cloned *MaPR1-like* DNA fragment 71

4.1.6 Restriction enzyme digestion of pGEM-T Easy vector harbouring *MaPR1-like* DNA fragment 72

4.1.7 Sequence analyses of the isolated *MaPR1-like* gene fragment 73

4.1.8 Phylogenetic analysis of *MaPR1-like* cloned sequences 75

4.1.9 Southern blotting analysis 77
4.2 Isolation of *MaPR1-like* transcript fragment 78
4.2.1 RNA isolation of total RNA sample from the banana root tissues infected with *M. incognita* 78
4.2.2 Reverse transcription-PCR and purification of *MaPR1-like* transcript 79
4.2.3 Colony PCR for the detection of cloned *MaPR1-like* transcript fragment in the transformed JM109 *Escherichia coli* cells 80
4.2.4 Isolation of pGEM-T Easy Vector plasmids harbouring *MaPR1-like* transcript fragment 82
4.2.5 Restriction enzyme digestion of pGEM-T Easy Vector plasmids harbouring *MaPR1-like* transcript fragment 82
4.2.6 Sequence analysis of the putative *MaPR1-like* transcript fragments 83
4.2.7 BLAST analysis of *MaPR1-like* transcript fragment in the GenBank and Banana Genome Hub database 84
4.2.8 Conserved domain analysis on the deduced MaPR1-like amino acid cloned sequences 87
4.2.9 Sequence alignment of the deduced amino acid MaPR1-like clonal variants with plant PR10 amino acid sequences 87
4.2.10 Phylogenetic analysis of the deduced amino acid sequences of MaPR10, banana PR1 reference sequences, and plant PR10 reference sequences ... 89
4.3 Subcellular localisation of MaPR10 protein in *A. cepa* inner epidermal cell 92
4.3.1 *In silico* subcellular localisation of MaPR10 protein variants 92
4.3.2 *In vivo* subcellular localisation of MaPR10 protein variants in the inner epidermal cell of *A. cepa* 93
4.4 Purification of MaPR10-BeB5 and MaPR10-GNA5 protein variants from *Escherichia coli* strain BL21 cells 100

4.4.1 Propagation and cloning of *MaPR10-BeB5* and *MaPR10-GNA5* transcript into pET30a(+) expression vector 100
4.4.2 Isolation of pET30a(+)::T7promoter::6xHis::*MaPR10-BeB5/GNA5* vector from transformed *E. coli* strain JM109 cells and sequence characterisation of the isolated plasmids 102
4.4.3 Detection of pET30a(+)::T7promoter::6xHis::*MaPR10-BeB5/GNA5* in transformed *E. coli* strain BL21 cells via PCR 103
4.4.4 Expression and purification of pET30a(+)::T7promoter::6xHis::*MaPR10-BeB5/GNA5* heterologous proteins from *E. coli* 104
4.5 Functional analyses of MaPR10-BeB5 and MaPR10-GNA5 protein variants 105
4.5.1 RNA isolation of *A. thaliana* (Col-0) 105
4.5.2 Ribonuclease (RNase) activity of MaPR10 protein variants 106
4.5.3 β-1,3-glucanase activity of MaPR10-BeB5 and MaPR10-GNA5 protein variants 109
4.6 Antifungal susceptibility test of MaPR10 protein variants against human and plant opportunistic fungal pathogens 110
4.6.1 Morphological characterisation of *A. fumigatus*, *A. niger* and *F. oxysporum* 110
4.6.2 Molecular characterisation of *A. fumigatus*, *A. niger* and *F. oxysporum* 112
4.6.3 Antifungal susceptibility test of MaPR10-BeB5 and MaPR10-GNA5 protein variants against *A. fumigatus*, *A. niger*, and *F. oxysporum* 115
CHAPTER 5: DISCUSSION 118
CHAPTER 6: CONCLUSION 125
6.1 Concluding remarks 125
6.2 Future prospect 125
REFERENCES 127
LIST OF PUBLICATIONS AND PAPERS PRESENTED 147

APPENDICES 149

LIST OF FIGURES

Figure 2.1 : A schematic representation of plant defence pathway against a pathogen infection..... 11

Figure 2.2 : Intracellular PR10 protein structure..... 16

Figure 3.1 : Diagram showing the positions of forward and reverse degenerate primers targeting *MaPR1-like* gene..... 32

Figure 3.2 : Diagram showing the positions of forward and reverse specific primers targeting *MaPR1-like* transcript..... 43

Figure 3.3 : pCAMBIA1304 expression cassettes harbouring *MaPR10-BeB5/GNA5* transcripts..... 48

Figure 3.4 : pET30a(+) expression cassette harbouring *MaPR10-BeB5/GNA5* transcript..... 53

Figure 4.1 : PCR primer stats result..... 68

Figure 4.2 : DNA extraction result from banana cultivars..... 69

Figure 4.3 : PCR amplification of *MaPR1-like* gene fragment from banana cultivars..... 70

Figure 4.4 : Detection of the presence of cloned *MaPR1-like* gene fragment in *E. coli* strain JM109 transformed cells by colony PCR..... 71

Figure 4.5 : Plasmid isolation from bacterial colonies containing clones of *MaPR1-like* gene fragment..... 72

Figure 4.6 : Restriction enzyme digestion assay on the isolated plasmids to verify the presence of cloned *MaPR1-like* gene fragment in the plasmids..... 73

Figure 4.7 : Sequence verification of *MaPR1-like* gene fragment..... 74

Figure 4.8 : BLASTn analysis of *MaPR1-like* gene fragment in sequence databases..... 75

Figure 4.9 : Phylogenetic analysis of the clones of *MaPR1-like* gene fragment..... 76

Figure 4.10 : Estimation of the copy number of *MaPR10* gene via Southern blot assay..... 78

Figure 4.11 : RNA extraction from Berangan and Grand Naine (ITC1256).. 79

Figure 4.12 : PCR amplification and purification of *MaPR1-like* transcript fragment..... 80

Figure 4.13 : Detection of the presence of the cloned *MaPR1-like* transcript fragment in the *E. coli* strain JM109 cells by colony PCR..... 81

Figure 4.14 : Isolation of the plasmids containing the cloned *MaPR1-like* transcript fragment..... 82

Figure 4.15 : Restriction digestion assay to verify the presence of cloned *MaPR1-like* transcript fragment in plasmid..... 83

Figure 4.16 : Sequence verification of *MaPR1-like* transcript fragment..... 84

Figure 4.17 : BLAST analysis of *MaPR1-like* transcript fragment in sequence databases..... 86

Figure 4.18 : Conserved domain analysis of the deduced amino acid sequences of MaPR10 protein variants..... 87

Figure 4.19 : Alignment of the deduced amino acid sequences of *MaPR1-like* gene (BeB5 and GNA5), representing Berangan and Grand Naine (ITC 1256) genomes, respectively, with representative PR10 amino acid sequences from four other plant species..... 89

Figure 4.20 : Phylogenetic analysis of the deduced amino acid sequences from the transcript and genomic clones of *MaPR10* fragment, banana PR1 reference sequences and plant PR10 reference sequences…….. 92

Figure 4.21 : *In silico* analysis of protein subcellular localisation prediction using the deduced amino acid sequences..... 92

Figure 4.22 : PCR amplification, restriction enzyme digestion assay, and purification of *MaPR10-BeB5* and *MaPR10-GNA5* transcript fragments..... 94

Figure 4.23 : Plasmid isolation of pCAMBIA1304 expression vector harbouring the *MaPR10-BeB5/GNA5* transcript..... 95

Figure 4.24 : Sequence verification of *MaPR1-like* transcript fragment..... 96

Figure 4.25 : Detection of pCAMBIA1304::CaMV35S::*MaPR10-BeB5/GNA5*::*mgfp5*::*GUS*::6xHis plasmids in *A. tumefaciens* strain LB4404 via colony PCR..... 97

Figure 4.26 : GUS assay on the transformed *A. tumefaciens* strain LB4404.. 98

Figure 4.27 : Subcellular localisation analysis of MaPR10 protein variants in the inner epidermal onion cell..... 99

Figure 4.28 : Purification of *NcoI-digested MaPR10-BeB5/GNA5* transcript fragment, *NcoI* restriction enzyme assay of pCAMBIA vector, and detection of cloned *MaPR10-BeB5* and *MaPR10-GNA5* transcript in *E. coli* strain JM109 cells via colony PCR... 101

Figure 4.29 : Plasmid isolation of pET30a(+) expression vector harbouring the *MaPR10-BeB5/GNA5* transcript..... 102

Figure 4.30 : Sequence verification of *MaPR1-like* transcript fragment..... 103

Figure 4.31: : Detection of pET30a(+)::T7promoter::6xHis::*MaPR10-BeB5/GNA5* plasmids in *A. tumefaciens* strain LB4404 via colony PCR..... 104

Figure 4.32: : Detection of the purified MaPR10 protein variants..... 105

Figure 4.33 : RNA extraction from *A. thaliana* (Col-0)..... 106

Figure 4.34 : Agarose gel electrophoresis showing the denaturation of *A. thaliana* total RNA sample upon treatment with each MaPR10 protein isoform..... 108

Figure 4.35 : Laminarin-dinitrosalicylic (DNS) acid assay on the purified MaPR10 protein variants..... 110

Figure 4.36 : Morphological characteristics of *A. fumigatus* and *A. niger* observed under a compound microscope..... 111

Figure 4.37 : Morphological characteristics of *F. oxysporum* f. sp. *cubense*: TR4 observed under compound microscope..... 112

Figure 4.38 : Fungal DNA extraction..... 112

Figure 4.39 : PCR amplification of isolated fragments from *A. fumigatus, A. niger and F. oxysporum*..... 113

Figure 4.40 : Sequence analysis of the isolated gene fragments from three fungal species in the GenBank..... 115

Figure 4.41 : Antifungal susceptibility assay of MaPR10 protein variants against *A. fumigatus*, *A. niger* and *F. oxysporum*..... 117

LIST OF TABLES

Table 4.1 : Quantification of the soluble crude MaPR10 protein variants, and purified MaPR10 protein variants based on the standard curve generated from bovine serum albumin (BSA) standard solution..... 105

Table 4.2 : RNase activity of the purified MaPR1-BeB5 and MaPR10-GNA5 protein variants..... 108

Table 4.3 : Quantitative analysis of the laminarin-DNS assay using purified MaPR10 protein variants..... 110

LIST OF SYMBOLS AND ABBREVIATIONS

β	:	Beta
g	:	Gram
h	:	Hour
kDa	:	Kilo Dalton
µg	:	Microgram
µL	:	Microlitre
µM	:	Micromolar
mL	:	Millilitre
mM	:	Millimolar
min	:	Minute
sec	:	Second
ATP	:	Adenosine triphosphate
BAP	:	6-Benzylaminopurine
bp	:	Base pair
BSA	:	Bovine serum albumin
CDC	:	Centre of disease control and prevention
cDNA	:	Complementary deoxyribonucleic acid
CLSI	:	Clinical and Laboratory Standards Institute
CTAB	:	Cetrimonium bromide
DAMP	:	Damage-associated molecular pattern
DEPC	:	Diethyl pyrocarbonate
DNA	:	Deoxyribonucleic acid
DNase	:	Deoxyribonuclease
DNS	:	Dinitrosalicylic acid

dNTPs	:	Deoxynucleotide triphosphates
DTT	:	Dithiothreitol
EtBr	:	Ethidium bromide
ETI	:	Effector triggered immunity
EUCAST	:	European Committee on Antimicrobial Susceptibility Testing
g	:	Genomic
GH16	:	Glycoside hydrolases family 16
HCl	:	Hydrochloric acid
HR	:	Hypersensitivity response
IGS	:	Intergenic spacer
ISR	:	Induced systemic response
IPTG	:	Isopropyl β- d-1-thiogalactopyranoside
ITS	:	Internal transcribed spacer
IUPAC	:	International Union of Pure and Applied Chemistry
JA	:	Jasmonic acid
LB	:	Luria-Bertani
LiCl	:	Lithium chloride
MaPR1	:	*Musa acuminata Pathogenesis-related 1*
MaPR1-like	:	*Musa acuminata Pathogenesis-related 1-like*
MaPR10	:	*Musa acuminata Pathogenesis-related 10*
MgCl2	:	Magnesium chloride
MgSO4	:	Magnesium sulfate
mRNA	:	Messenger ribonucleic acid
NaCl	:	Sodium chloride
NaEDTA	:	Disodium ethylenediaminetetraacetate dihydrate
NaOAc	:	Sodium acetate

Na3PO4	:	Sodium phosphate
PAMP	:	Pathogen-associated molecular pattern
PCR	:	Polymerase chain reaction
PPN	:	Plant parasitic nematode
PPI	:	Plant-pathogen interaction
PR	:	*Pathogenesis-related*
PR1	:	*Pathogenesis- related 1*
PR1-like	:	*Pathogenesis-related 1-like*
PR10	:	*Pathogenesis-related 10*
PTI	:	Pathogen triggered immunity
PVP	:	Polyvinylpyrrolidone
RE	:	Restriction enzyme
RKN	:	Root-knot nematode
RNA	:	Ribonucleic acid
RNase	:	Ribonuclease
ROS	:	Reactive oxidative species
SA	:	Salicylic acid
SAR	:	Systemic acquired resistance
SDS	:	Sodium dodecyl sulphate
sdH2O	:	Sterilised distilled water
TBE	:	Tris/Borate/EDTA
Tris-HCl	:	Tris-Hydrochloride

LIST OF APPENDICES

Appendix A-1	:	The map of pCAMBIA1304::CaMV35S::*MaPR10-BeB5/GNA5*::*mgfp5*::GUS::6xHis expression vector.....	149
Appendix A-2	:	The map of pET30(a)+::*T7*Promoter::S-tag::6XHis::*MaPR10-BeB5/GNA5* expression vector.....	150
Appendix A-3	:	BSA standard curve generated to estimate protein concentration.....	151
Appendix B-1	:	Data mining result of ITC587_Bchr9_P26466_MUSABA peptide reported by Al-Idrus *et al.* (2017).....	151
Appendix B-2	:	Amino acid alignment of ITC1587_Bchr9_P26466_MUSBA banana PR sequence with six reference sequences obtained from the GenBank and Banana Genome Hub.....	152
Appendix B-3	:	Alignment of ITC1587_Bchr9_P26466_MUSBA banana *PR* nucleotide sequence with six reference sequences obtained from the GenBank and Banana Genome Hub.....	154
Appendix B-4	:	Quantification result of total DNA samples isolated from Berangan and Grand Naine (ITC1256) leaf tissues.....	156
Appendix B-5	:	Quantification results of the plasmid DNA samples containing *MaPR1-like* gene clone fragment isolated from Berangan and Grand Naine (ITC1256).....	156
Appendix B-6	:	PCR Primer Stats result of *PR1-like* primer pairs designed in this study using Sequence Manipulation Suite software...	157
Appendix B-7	:	Quantification result of total RNA samples extracted from *M. incognita*-infected root tissues from Berangan and Grand Naine (ITC1256) cultivars.....	157
Appendix B-8	:	Quantification result of the isolated plasmid DNA samples from 25 *MaPR1-like* transcript clones of Berangan (Be) and Grand Naine (ITC1256).....	157
Appendix B-9	:	Alignment of amino acid sequences of PR1 and PR10 with randomly chosen deduced MaPR1-like amino acid sequences of BeB5 and GNA5.....	160
Appendix B-10	:	Colony PCR to detect the presence of MaPR10-BeB5/GNA5 fragment in the transformed *Escherichia coli* strain JM109 cells.....	162
Appendix B-11	:	Quantification result of the three isolated pCAMBIA1304 plasmid vectors harbouring *MaPR10-BeB5* and *MaPR10-GNA5* transcript clones.....	162
Appendix B-12	:	Nucleotide alignment of *MaPR10-BeB5/GNA5* transcripts and the isolated pCAMBIA1304 plasmid verified to harbour the *MaPR10-BeB5/GNA5* fragment.....	163

Appendix B-13 : Quantification result of the five isolated pET30a(+) plasmid vectors harbouring *MaPR1-BeB5* and *MaPR10-GNA5* transcript clones..... 164

Appendix B-14 : Nucleotide alignment of *MaPR10-BeB5/GNA5* transcripts and the isolated pET30a(+) plasmid verified to harbour the *MaPR10-BeB5/GNA5* fragment..... 164

Appendix B-15 : Quantification result of total RNA samples extracted from *Arabidopsis thaliana* (Col-0) leaf tissues..... 165

Appendix B-16 : Quantification result of total DNA samples isolated from *A. fumigatus*, *A. niger* and *F. oxysporum* f.sp. *cubense*: TR4.... 165

Appendix B-17 : An example of chromatograms obtained after sequencing using (a) an ITS1-*5.8S* forward primer, (b) an ITS1-*5.8S* reverse primer, (c) *28S-18S* rDNA IGS forward primer and (d) *28S-18S* rDNA IGS reverse primer..... 166

CHAPTER 1: INTRODUCTION

1.1 Background study

Bananas are consumed as staple food in the tropics and subtropics, mainly because they are rich in carbohydrate (Aurore *et al.,* 2009). In Malaysia, banana is the second most grown crop (Mohamad *et al.,* 2012). Worldwide banana export revenue was estimated at USD 12 billion with 116 million tonnes produced annually (Banana Market Review Snapshot February 2020, 2020). This revenue reflected only 15 % of the total banana production as the rest of bananas are consumed locally. The same report also suggested that the increasing threat of plant pathogens caused reduction in total banana production. Plant pathogens such as fungi (Fones *et al.,* 2020) and nematodes (Davide, 1996) were recognised as challenges for banana production worldwide. It was reported that plant-parasitic nematodes (PPN), alarming pathogens that infect both monocotyledon and dicotyledon plants (Mejias *et al.,* 2019) caused 20 % losses in total banana production worldwide (Carlier *et al.,* 2002).

In Malaysia, *Meloidogyne incognita,* a species belonging to the root-knot nematode (RKN) group was found predominant in sampled banana roots (Rahman *et al.,* 2014). Like other PPNs, infestation by RKNs in banana plants caused the plants to topple over at young stages (Speijer and De Waale, 1997). RKN infestations occur when the infective stage-2 juvenile (J2) nematodes invade banana root tips and develop long-term feeding sites that appear as galls on infected roots (Holbein *et al.,* 2016) known as coenocytic giant cells. As a defence mechanism, the infected plant will in turn activate its basal defence system against the invasion by detecting pathogen-associated molecular pattern (PAMP). This defence mechanism is known as pattern triggered immunity (PTI) (Zhang & Zhou, 2010). However, pathogens such as nematodes (Vieira & Gleason, 2019) and fungi (Lo Presti *et al.,* 2015) were reported to have the ability to surpass plant's basal defence by secreting effector molecules into plant's apoplast and cytoplasm which

suppress this defence system. Following that, the invaded plant develops a heightened defence system that is known as effector triggered immunity (ETI). One such implication of this immunity is the hypersensitivity response (HR).

HR is the development of programmed cell deaths at/and surrounding the region of an infected cell (Mantelin *et al.,* 2015). This response is induced by pathogens such as fungi, oomycetes, bacteria, viruses, insects, and nematodes (Balint-Kurti, 2019) and can occur within a few hours after plants were in contact with pathogens. HR is known to restrict the biotrophic pathogen infection (Mur *et al.,* 2008) and is generally associated with race-specific resistance in plants (Balint-Kurti, 2019). This pathogen-induced defence response is accompanied by the generation of reactive oxygen species (ROS), oxidative cell wall protein cross linking, and eventually the production of pathogenesis-related (PR) proteins (Van Baarlen *et al.,* 2007). PR proteins belong to a diverse protein family (Van Loon *et al.,* 1994) which are vital for systemic acquired resistance (SAR) that forestalls further infection to non-infected regions of the host. SAR is known to be mediated by PR proteins.

Plant PR proteins, encoded by the *PR* genes were initially isolated from tobacco leaves that were infected by tobacco mosaic virus (Linthorst & van Loon, 1991). These proteins were found to be strongly induced upon pathogen infection (Van Loon *et al.,* 1994). Although their expression is upon pathogenic stress, some *PR* genes were constitutively expressed in flowers or leaves (Linthorst *et al.,* 1990), or during developmental stages of a flower (Lotan *et al.,* 1989), suggesting that PR proteins display organ specificity (Kombrink *et al.,* 2001; Edreva, 2005). These non-defence-regulated proteins are regarded as PR-like proteins because of their sequence homology with PR protein sequences (Sinha *et al.,* 2014). PR proteins are low-molecular weight proteins ranging from 6 to 43 kDa and are usually resistant to proteases (Jain & Khurana, 2018).

Depending on their isoelectric points, PR proteins can either be acidic or basic, and are either vacuolar or apoplastic (Sels *et al.,* 2008). Currently, 17 PR protein families have been characterised based on the similarity of their amino acid sequences, enzymatic activities, or other biological properties (Van Loon *et al.,* 2006). Although the proteins share a common name, they possess a great level of diversity in terms of specificity against pathogens, and the mechanism of action (Sinha *et al.,* 2014).

A proteomics study conducted on banana-*M. incognita* compatible interaction revealed that PR1-like protein was present at a significantly low abundance level in nematode-inoculated root samples at the 30th day after inoculation (dai) when compared to control samples (Al-Idrus *et al.,* 2017). This finding substantiates the hypothesis of this current study that *PR1-like* gene is involved in banana defence system, which warrants a characterisation and functional study on this subjected gene. Upon characterisation and isolation of the reported protein from two banana varieties namely Berangan and Grand Naine (ITC 1256), the current study confirmed that this *PR1-like* gene is in fact a *PR10* gene instead. The results obtained from Southern blot analyses suggested that more than one copy of *PR10* gene were present in the two banana genomes studied. This was corroborated by the result obtained from phylogenetic analysis where 84 deduced PR10 amino acid sequences obtained in this study together with ten banana *PR10* reference sequences clustered into four phylogenetic groups. Based on this analysis, two protein variants were chosen for further analyses namely MaPR10-BeB5 and MaPR10-GNA5, representing Berangan and Grand Naine cultivars, respectively. In addition, agroinfiltration of both MaPR10 protein variants into the inner epidermal cells of *Allium cepa* suggested that both variants were of intracellular type as it was found scattered throughout the cytoplasm. Functional analyses carried out on the two protein variants confirmed that they possess both ribonuclease and β-1,3-glucanase activities. This is the first report to highlight the function of PR10 group members as β-1,3-glucanases. When

both protein variants were subjected to antifungal susceptibility test on *Aspergillus fumigatus*, *Aspergillus niger* and *Fusarium oxysporum* f. sp. *cubense*: Tropical Race 4, they both inhibit the growth of *A. fumigatus*, a human opportunistic fungus. As far as the author is concerned, the discovery of MaPR10 protein as a β-1,3-glucanase with an inhibitory effect on *A. fumigatus* is at present, novel.

1.2 Aim and objectives

The general aim of this study was to characterise and assess the functionality of *MaPR10* gene isolated from two *M. acuminata* cultivars namely Berangan and Grand Naine (ITC 1256).

The specific objectives of this study were:

i. to isolate and characterise *MaPR10* gene and transcript sequences from two banana cultivars namely Berangan and Grand Naine (ITC 1256);
ii. to express and purify the isolated MaPR10 protein variants;
iii. to determine the subcellular localisation of the isolated MaPR10 protein variants.
iv. to assess the function of the isolated MaPR10 protein variants as ribonuclease (RNase) and β-1,3-glucanase;
v. to determine the antifungal effect of the isolated MaPR10 protein variants against important fungal species.

CHAPTER 2: LITERATURE REVIEW

2.1 Banana and its economic value

Bananas and plantains (henceforth will be referred to as 'banana') belong to the genus *Musa* (*Musaceae*, *Zingiberales*). The word 'banana' was originated from the Arabic word 'banan' which means finger (Boning, 2006). This giant perennial herb is consumed as the staple food in the tropics and subtropics, mainly because they are rich in carbohydrate (Aurore et al., 2009). As banana are consumed worldwide, in terms of economic value, banana is known as one of the leading crops among tropical fruits (EST, 2019). Banana, as a perennial plant, can be grown in warm humid environments and produce fruits throughout the year (Britannica, 2020). The total banana production worldwide was estimated at over 116 million tonnes per annum (Banana Market Review Snapshot February 2020, 2020). From the same report, the worldwide economic value of banana industry was estimated at USD 12 billion. However, only 15 % from the total production of banana were traded internationally while the rest were consumed locally as apart of daily diet, mainly in Asia and Africa (Voora *et al.,* 2020). Cavendish banana plants are known to be highly exported worldwide and accounts for nearly half from the total banana production worldwide (EST, 2019). In Malaysia, the Cavendish and Berangan are the most marketed banana varieties. Khazanah Research Institute recorded that banana made up 24 % of the total fruit production in year 2017 (Tumin & Ahmad Shaharudin, 2019). Approximately, 35,000 hectares of land with a production of 350,000 metric tonnes was recorded for banana plantation in Malaysia.

2.2 Biotic stresses on banana plants

The global mass production of banana as food crops is based on a large-scale vegetative propagation of a small number of genotypes, derived from limited ancient sexual recombination events of *M. acuminata* (AA) and *Musa balbisiana* (BB). These events restricted the recombination of genes in banana clones. The restriction and

inflexibility present in the genomes of banana clones made them susceptible to diseases, pests, and current ecological changes (Perrier *et al.,* 2011). Since bananas are vegetatively propagated, each banana plant would have the same genetic composition as their parents' (Heslop-Harrison & Schwarzacher, 2007). Therefore, if any of the banana plants in a plantation was found susceptible to a disease/pathogen, the disease/infection could spread throughout the whole plantation within days or perhaps hours. Therefore, to circumvent this problem, Gold *et al.* (1999) suggested to replace the susceptible variety(s) with a resistant variety.

In 1960, the banana variety 'Gros Michel' dominated banana production and its export trades worldwide (Ploetz, 2005). Unfortunately, this variety was found to be susceptible to *F. oxysporum* f. sp. *cubense*. This fungus caused a severe damage to Gros Michel production by causing Panama disease (Fusarium wilt) and nearly destroyed the whole population of this banana variety worldwide (Ploetz, 2000). To solve this problem, the banana variety 'Cavendish' (AAA) which was resistant to the *F. oxysporum* f. sp. *cubense* infection was used to replace Gros Michel. Other than fungal infections, bacterial infections were also known to cause a significant damage to the growth of banana plants. One of the most detrimental diseases is the Moko disease (bacterial wilt disease) caused by a soil borne betaproteobacteria, *Ralstonia solanacearum* (N'guessan *et al.,* 2013). The bacteria are transmitted into the host by insects during pollination or through wounds that occurred on the root tissues (Teng *et al.,* 2016). Typical symptoms of the disease include yellowing on affected leaves, appearance of bacterial ooze, and rotting of infected-plant parts (Riley *et al.,* 2002). Addy *et al.* (2016) reported that this bacterial species could cause approximately 80–100 % yield loss in a banana plantation. Other than *R. solanacearum*, *Xanthomonas vasicola* pv. *Musacearum* is another bacterial species that causes similar morphological symptoms on an infected banana plant known as Xanthomonas wilt disease (Bloome *et al.,* 2017). Viral infection is also known to cause

severe damages to banana plants. *Banana bunchy top virus* (BBTV) caused a devastating viral disease in banana plantation, affecting its production (Jooste *et al.,* 2016). Watanabe *et al.* (2013) suggested banana aphid *Pentalonia nigronervosa* as the vector that spreads the virus. This single-stranded DNA virus infected edible banana cultivars and was identified to cause bunchy top disease in approximately forty banana-growing countries (Ploetz *et al.,* 2015). Infected plants could never be recovered and had to be destroyed before it became the source of BBTV (Ferreira et al., 1997). Symptoms for this viral infection can be observed on the leaf tissues such as the narrowing of leaves with discontinuous dark-green streaks, chlorosis of leaf margins, and dwarfing (Mware, 2016). Along with other pathogens causing stress in banana, Gowen *et al.* (2005) suggested plant-parasitic nematodes as one of the severe damaging pathogens.

2.3 Plant-parasitic nematodes (PPN)

Plant-parasitic nematodes (PPN) can either be ectoparasitic or endoparasitic. The former migrates through the soil but will never enter the host and only feed on the root system of the host (Jones *et al.,* 2013) while the latter invade plant tissues and feed on the plant's inside. Endoparasitic nematodes can further be divided into two groups namely the migratory nematodes and the sedentary nematodes. The migratory endoparasitic nematodes such as *Radopholus similis* and *Pratylenchus coffeae* intracellularly migrate through the host's root tissues and cause extensive damage on the host. On the other hand, the juvenile stage 2 of sedentary endoparasitic nematodes such as *Meloidogyne incognita* intercellularly migrate in plant's root tissues and establish a permanent feeding site in the host and morph into adult egg-laying females (Carlier *et al.,* 2002). PPNs are critical threats to agriculture industry due to their compatibility with a wide range of plant crops. PPN infestation in plants contributed to approximately 78 billion USD of annual crop yield losses (Porazinska *et al.,* 2014). In addition, it was recorded that nematode infections are responsible for 20 % of yield loss in most banana plantations worldwide,

every year (Carlier *et al.,* 2002). Although *R. similis* is known to be the most important species infecting banana plants globally, *Meloidogyne* spp. (root-knot nematodes) namely *M. incognita* and *Meloidogyne javanica* were reported to be the commonly found nematodes infecting bananas in Asia and dessert bananas of the Cavendish subgroup (De Waele & Davide, 1998). In addition, these root-knot nematodes (RKNs) were listed as the most economically important pathogens (reviewed by Jones *et al.* 2013) and ranked amongst the top 10 important PPN species in molecular plant pathology. Bunch-bearing plants such as bananas that are severely infected with RKNs can be uprooted due to poor root anchorage and this leads to a total yield loss of unripe fruits. In Peninsular Malaysia, Rahman *et al.* (2014) reported that *M. incognita* was predominant in banana root samples isolated from their distribution study.

2.4 *Meloidogyne incognita* and the current practice to manage PPNs in banana plantations

Meloidogyne incognita is a sedentary plant-parasite which manipulates host cell's biological machinery to its own benefit (Jaouannet *et al.,* 2012). In a compatible plant-pathogen interaction, this parasite forms multinucleated nematode feeding cells (giant cells) due to re-differentiation of cells induced by the nematode (Sato *et al.,* 2019), facilitating the nutrient absorption to the nematode (Mejias *et al.,* 2019). A gall-like structure is formed on the plant root tissues as a result of the proliferation and enlargement of the cells surrounding the giant cells (Favery *et al.,* 2016). This nematode infection leads to a severe impact on the plant anchorage system. *Meloidogyne incognita* was reported to have a wide host range. Approximately 3,000 plant species including agricultural crops (Jepson, 1987) such as bananas are hosts to this pathogen. Therefore, it is crucial to develop an efficient management protocol to control the spread of this nematode species especially, and others along the way. The current practices to manage *M. incognita* infestation and other nematode species in general include the usage of

chemical nematicides, adoption of cultural practices such as crop rotations, and biological controls (Timper *et al.,* 2014). Nematicide has been an effective solution to this problem for decades (Mokrini *et al.,* 2019). In South Africa, the routine application of nematicide to counter the infestation of *Pratylenchus brachyurus* and *M. javanica* recorded an average increase in pineapple yield of 34 % per harvest (Coyne, 2016). However, due to toxicity and carcinogenicity of nematicides, its usage was banned in several countries (Danchin *et al.,* 2013). Therefore, identifying the gene(s) that involves in plant defence/resistance against RKN species to develop resistant banana line is seen as an attractive alternative to manage RKN infestation in bananas. In this regard, a baseline study was carried out to screen for banana proteins involved in a compatible banana-*M. incognita* interaction (Al-Idrus *et al.,* 2017) and PR1-like protein (ITC1587_Bchr9_P26466_MUSBA) was found to be present at a significantly low abundant level at the 30th day after inoculation (dai). This result substantiated the isolation and characterisation of *PR* gene from two banana varieties in the current study.

2.5 Plant defence system

Plants lack the motility to evade extreme environments that may affect their growth and reproduction (Dangl & Jones, 2001). As opposed to vertebrates, plant lack specialised mobile immune cells with specific recognition system to target the pathogens (Yakura *et al.,* 2020). To make up for these inadequacies, plants have evolved to establish a highly specific and sophisticated defence system to provide a long-lasting resistance against pathogens (Spoel & Dong, 2012) in order to survive. Studies on plant-pathogen interaction (PPI) offers a grasp of knowledge on how plants resist pathogenic invasions. Plant-pathogen interaction is classified into two types, i.e., incompatible and compatible interactions, depending on the speed and the severity of a visible damage that is caused by a pathogen (Ponzio *et al.,* 2016). The ability of a plant to limit pathogen invasion is also important in determining the host resistance or susceptibility state (Pagán & García-

Arenal, 2018). The current understanding on plant defence is based on the 'zig-zag' model proposed by Dangl & Jones (2006). This model branches the defence mechanism into two immunity systems namely basal defence mechanism against pathogens which also acts as the innate immunity while the latter is an acquired immunity, an evolved version of plant immune system that utilises disease-related proteins to correspond to the effector molecules secreted by the pathogens (Han, 2019).

Plant's basal defence system provides the first layer of defence against a wide range of pathogens (Gururani *et al.,* 2012). Most pathogens are defeated by the plant's basal defence system that recognises pathogen-associated molecular patterns (PAMPs). PAMPs are conserved molecules secreted by pathogens that can be recognised by the host's cell surface pattern recognition receptors (PRRs) that can activate pattern triggered immunity (PTI). Besides that, damaged-associated molecular patterns (DAMPs) can also trigger innate immunity (Mantelin *et al.,* 2015). The evolutionary arms race between plants and pathogens has shaped pathogens' genome to produce virulent factors called effector molecules, encoded by the *Avirulence* (*Avr*) genes. These effector molecules suppress PTI. Plants, in turn, have evolved a highly specific and strong immune response towards the effectors called effector-triggered immunity (ETI), which leads to hypersensitive response (HR) (Menna *et al.,* 2015). HR is described as a rapid cell death event that occurs at and around the site of infection (Balint-Kurti *et al.,* 2019). ETI is activated when specific R proteins encoded by the *Resistance* (*R*) genes recognise specific effector alleles within a pathogen population (Pumplin & Voinnet, 2013). This recognition process is termed as incompatible plant-pathogen interaction and conversely, a compatible reaction occurs when the *Avr* gene in pathogen is not recognised by the host's *R* gene due to mutations or the absence of the *Avr* gene, resulting in disease development. As a result of recognition of an effector allele by the *R* gene, a signal transduction cascade of mobile immune signal prompts the initiation of a variety of plant

defence responses such as production of a wide range of pathogenesis-related (PR) proteins in and around the infected plant cells, and the synthesis of chemical substances such as salicylic acid (SA), ethylene (ET), jasmonic acid (JA), and compounds which contributes to the lignification and strengthening of the cell wall (Patel *et al.,* 2020). The accumulation of SA and JA would trigger pathogen-induced resistance's signalling pathway (Yi *et al.,* 2014). The whole event of plant defence against the pathogen attack discussed above was represented in the Figure 2.1.

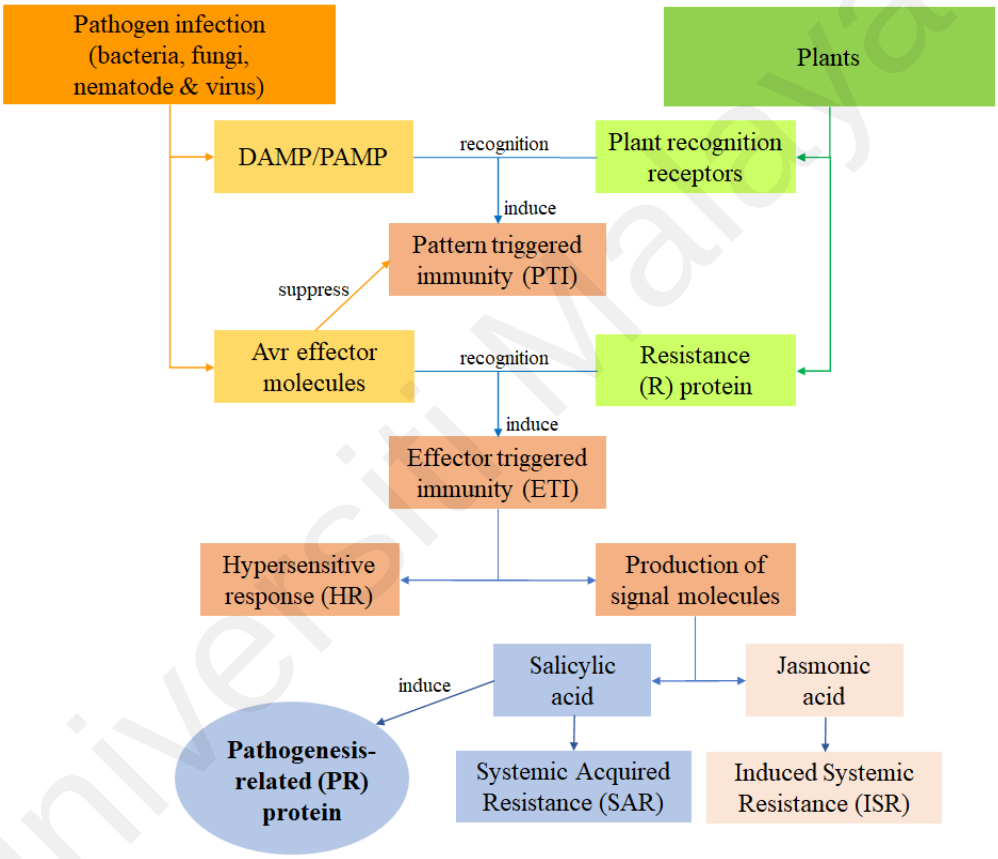

Figure 2.1: A schematic representation of plant defence pathway against a pathogen infection. The pathway above depicts the activation of pattern triggered immunity (PTI) by the host plant's reception receptors upon the recognition of the damage-associated molecular pattern (DAMP)/pathogen-associated molecular pattern (PAMP) released by the pathogens. Some pathogens evade the PTI with presence of Avirulence (Avr) effector molecules, thus, the plant instead produces specific Resistance (R) proteins to perceive the specific Avr effectors to trigger the effector-triggered immunity (ETI). ETI leads to the activation of the hypersensitive response (HR), a localized cell death which restricts the growth of pathogen. Along with the HR, mobile immune signals are also released, i.e., salicylic acid (SA) which activates the systemic acquired resistance (SAR), and jasmonic acid which activates induced systemic resistance (ISR). SA also induced the production of pathogenesis-related (PR) proteins, a vital protein family known to produce pathogen-toxic proteins.

2.6 Systemic acquired resistance (SAR) and induced systemic responses (ISR)

Pathogenic-induced resistance comprised of two main responses: (i) systemic acquired resistance (SAR), and (ii) induced systemic resistance (ISR) (Vallad & Goodman, 2004). ETI initiates a systemic spread of mobile defence signal transductions from an infection site throughout the plant tissues which results in increased resistance to secondary infections of the same pathogen in other parts of the infected plant (Thakur & Sohal, 2012). This event is termed as systemic acquired resistance (SAR). The ability of a plant to develop acquired immunity or increased resistance against reinfection of a pathogen (either complete or partial immunity) suggested that SAR may play a crucial role in controlling outburst of plant diseases (Chester, 1933). The effects of acquired immunity were observed in the report by Ross (1961) that SAR caused a smaller magnitude of secondary infection observed in tobacco mosaic virus (TMV)-infected *Nicotiana tabacum* leaves. The exact mechanism or signalling molecules were not identified then as Van Loon (1983) proposed that SAR leads to the accumulation of PR proteins. Raskin *et al.* (1990) provided enough evidence to link SA accumulation with SAR in their study on thermogenesis regulation factors in voodoo lily. Subsequently, Malamy & Klessig (1992) reported that endogenous SA serves as the signalling molecule for SAR. Further research supported the notion that SA functions as the pathogen-induced molecule and moves through the apoplast in *Arabidopsis thaliana* resulting in increased resistance of a plant (Lim *et al.,* 2016). However, Fu & Dong (2013) reviewed that SA may not be the critical mobile signal for SAR although its accumulation is required for the immunity, instead, mobile signals such as methyl salicylic acid, lipid-transfer protein DIR1 and glycerol-3-phosphate are involved in the signal cascade for SAR.

On the other end of the defence spectrum is induced systemic responses (ISR). This pathogen-induced response is dependent on the phytohormones ethylene and JA as the response is not associated with SA and PR proteins (Vallad & Goodman, 2004). ISR is

mediated by beneficial microbes such as plant growth-promoting rhizobacteria (PGPR) to prime plant defence against pathogens (Pieterse *et al.,* 2014). This signalling pathway is effective in mediating resistance against herbivores and necrotrophic pathogens (Gimenez-Ibanez *et al.,* 2016). Choudhary *et al.* (2007) and Fallath *et al.* (2017) suggested that both ISR and SAR could be integrated to elevate plant defence against a wider spectrum of pathogens, rather than the defence achieved by each response alone. In addition, both SAR and ISR signalling molecules were reported to be associated to each other (Shigenaga *et al.,* 2016), further suggesting the possibilities of SAR-ISR crosstalk in plant defence.

2.7 Pathogenesis-related (PR) proteins

Pathogenesis-related (PR) proteins were first isolated from tobacco mosaic virus (TMV)-infected tobacco plants in two independent studies conducted by Van Loon & Van Kammen (1970), and Gianinazzi *et al.* (1970). PR proteins could either be secreted or vacuole-targeted, and possess antimicrobial activities (Fu & Dong, 2013). These proteins usually accumulate locally in surrounding pathogen-infected cells, and in remote uninfected tissues in order to prevent further infections (Ebrahim *et al.,* 2011). Acidic PR proteins are commonly expressed extracellularly because the proteins are well-adapted in the acidic environment, while the basic ones are usually found in the vacuoles (Jain & Khurana, 2018). The expression of acidic PR proteins is regulated by certain signalling molecules such as salicylic acid (Pokotylo *et al.,* 2019) and reactive oxygen species (Chamnongpol *et al.,* 1998), suggesting that these proteins could be involved in SAR. As for the basic PR proteins, Xu *et al.* (1994) reported that methyl jasmonate and phytohormone ethylene regulate their production upon pathogen invasion.

PR proteins are usually expressed upon pathogenic stress on plants. However, it was reported that certain internal stimuli such as naturally occurring phytohormones (Jain &

Khurana, 2018) could as well induce PR proteins in plants, suggesting that *PR* gene expression could be organ specific (Kombrink *et al.,* 2001; Edreva, 2005). On the other hand, pathogen-induced PR proteins are classified into 17 families based on their properties and amino acid homology (Sels *et al*., 2008). Each protein family encodes for pathogen-toxic proteins with diverse functions such as chitinases, glucanases, lysozyme-active proteins, or proteins that involve in cell wall fortification such as hydroxyproline-rich glycoproteins (Linthorst & Van Loon, 1991; Ebrahim *et al.,* 2011). The diverse functions of PR protein family prompted Ali *et al.* (2018) to suggest that *PR* gene could be the fundamental factor in improving plant disease resistance in plants and as such have been experimentally overexpressed in many plants. Overexpression of *PR1* or *PR1-like* genes was reported to enhance disease resistance in pepper against multiple pathogens such as *Phytophthora nicotianae* and *R. solanacearum* (Alexander *et al.,* 1993; Sarowar *et al.,* 2005). Similar overexpression studies were conducted on other *PR* gene families such as *PR3* gene in *N. tabacum* against *R. solanacearum* (Tang *et al.,* 2017), *PR4* gene in *Vitis pseudoreticulata* against *Erysiphe necator* (Dai *et al.,* 2016), *PR5* gene in *Oryza sativa* against *Rhizoctonia solani* (Datta *et al.,* 1999), *PR10* gene in *O. sativa* against *Magnaporthe oryzae* (Wu *et al.,* 2016), and *PR12* gene in *Raphanus raphanistrum* subsp. *sativus* against *Raphanus raphanistrum* (Terras *et al.,* 1995). All studies pointed to the crucial role PR proteins played in plant defence system upon pathogen attacks.

2.8 Pathogenesis-related 10 (PR10) protein

PR10 proteins were initially described as PR1 proteins in parsley (Warner *et al.,* 1992) despite being structurally unrelated to PR1 proteins. PR10 proteins were found to be closely related to a group of major tree pollen allergens and food allergens based on sequence homology (~50 % identity) to the classic PR10 proteins such as white birch Bet v 1 allergen (Breiteneder *et al.,* 1989). Based on the amino acid sequences, cellular localisation, and protein function studies, PR10 proteins were classified into two distinct

groups i.e., intracellular pathogenesis-related proteins (IPR), and (S)-norsoclaurine synthase (NCS) (Agarwal & Agarwal, 2014). The former was associated with ribonuclease activities due to the presence of the conserved P-loop domain and Bet v 1 motif with a shorter open reading frame (ORF) (~480 bp), while the latter was known as the precursor molecule in benzylisoquinoline alkaloids (BIAs) biosynthesis, possessing a longer open reading frame (~650 bp). It is noteworthy that the current study focused on the IPR class. In plants, the members of this group are generally small acidic proteins with a molecular mass ranging from 16–17 kDa consisting of approximately 160 amino acids sequence (Hoffmann-Sommergruber *et al.,* 1997). PR10 proteins lack signal peptide, therefore are intracellular and cytosolic (Gao, 2019). In addition, Liu & Ekramoddoullah (2006), and Fernandes *et al.* (2013) reviewed that the members of this plant PR10 protein group share a similar gene structure with a highly conserved ORF of 456 to 489 bp that is interrupted by an intron from the 76^{th}–359^{th} nucleotide position. There are three signature motifs that characterise a PR10 protein namely the glycine-rich loop domain (GXGGXGXXK), Bet v 1 motif (with three conserved amino acid residues E96, E148, and Y150), and a PR10 specific domain (KAXEXYL) (reviewed by Jain & Kumar*,* 2015) (Figure 2.2). The glycine-rich loop domain has high sequence similarity to a P-loop domain, known as a phosphate-binding loop found in nucleotide binding proteins (Wu *et al.,* 2003), suggesting that these motifs are associated with ribonuclease activity. Chadha and Das (2006) reported that mutations in the P-loop domain resulted in the production of a defective ribonuclease in their antifungal study on peanut PR10 protein against *Fusarium* spp., highlighting the significance of this motif and the gene function in plant defence. This notion was supported by Jain & Kumar (2015) in their review, which suggested that the conformational differences in glycine-rich loop (P-loop) domain of PR10 sequences caused a lack of affinity to ATP and loss of ribonuclease function. On the other hand, ribonuclease activity of PR10 proteins has been linked to plant defence

response (Bantignies *et al.*, 2000; Wu *et al.,* 2003; Xu *et al.,* 2014) which either has a direct antagonistic interaction with pathogens or mediates increased plant immunity via programmed cell deaths occurring at the surrounding of the infected site. It is noteworthy that many reports have associated ribonuclease activity of the PR10 proteins with antifungal properties (Chadha & Das, 2006; Chen *et al.,* 2006; Agarwal *et al.,* 2013).

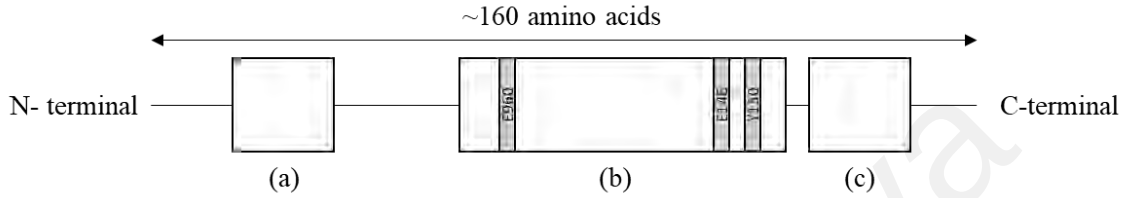

Figure 2.2: Intracellular PR10 protein structure. Plant PR10 proteins share three conserved motifs namely glycine-rich domain (a), Bet v 1 motif with three conserved amino acid residues E96, E148, and Y150 (b), and PR10 specific domain (c).

Although PR10 proteins are ubiquitous in plants, their biochemical properties are yet to be clearly defined, hence, the definitive role of PR10 proteins in plant genomes is yet unravelled . However, many reports had pointed out an indispensable role of PR10 protein in plant defence system (Filipenko *et al.,* 2013; Sinha *et al.,* 2014; Castro *et al.,* 2016; Finkina *et al.,* 2017; Ali *et al.,* 2018). In addition, Aglas *et al.* (2020) reported that PR10 proteins can bind to different ligands with different binding sites. The physiological role of ligand-specific binding activity has been demonstrated for PR10 proteins in several species. Examples of ligands bound by PR10 proteins include cytokinins (Fujimoto *et al.,* 1998; Gonneau *et al.,* 2001; Mogensen *et al.,* 2002), brassinosteroids (Marković-Housley *et al.,* 2003), fatty acids, and flavonoids (Mogensen *et al.,* 2002), suggesting the possibility of PR10 behaving as multifunctional proteins.

2.9 Subcellular localisation of PR proteins

The information on subcellular localisation of a protein is crucial to understand the basic function of the protein under investigation (Meissner *et al.,* 2011). PR proteins were found to either be extracellularly or intracellularly localised. Usually, the presence or absence of signal peptide or localisation signals (Arnoys & Wang, 2007) on the protein

sequences determines which region (extra, or intracellular) they are categorised. On the other hand, recent advances in bioinformatics suggested the use of computational approaches to predict protein localisation based on factors such as total amino acid compositions, presence of signal peptides, sequence homology with well-established protein references, and a hybrid method utilising the listed factors (Dönnes & Höglund, 2004). It is noteworthy that although proteins are synthesised in the cells, the presence of signal peptides directs the proteins to be brought to targeted locations such as extracellular matrices, the nucleus, mitochondria, chloroplasts, and other organelles in a cell (Schatz & Dobberstein, 1996; Neumann *et al.,* 2003). In the absence of the signal peptides, the proteins remain within the cytoplasmic region. Once the proteins reach the target destination, signal peptides will be cleaved from the protein by specific proteases (Jarvis & Robinson, 2004).

In plant defence system, the most abundant proteins found in the extracellular matrices are PR proteins (Guerra-Guimarães *et al.,* 2016) suggesting that PR proteins are expressed extracellularly. In addition to that, Kaur *et al.* (2020) described that the subcellular localisation of the PR proteins depends on the protein isoelectric points. Most extracellularly expressed PR proteins are usually acidic, while basic PR proteins were localised in the vacuole (Jain & Khurana, 2018). It is noteworthy that PR10 proteins are the only PR protein family that is intracellularly expressed (or also known as cytosolic) (Van Loon, 2006) due to the absence of signal peptides in the protein sequence.

2.10 Functional analyses of a gene

Functional genomic is defined by the evolution and application of experimental technique to determine gene functionality by utilising the data obtained from structural genomics (Hieter & Boguski, 1997) such as genome sequencing and mapping. The underlying strategy in functional genomics is to widen the range of biological studies

from emphasising on single gene/protein study to studying all genes/proteins at once in a structured manner (Walker & Rapley, 2009). Initially, this discipline was developed from the suggestion made by Sir Archibald Edward Garrod in early 1900s that genes control metabolic steps (Robinson, 1974). Then, Beadle and Tatum brought forward the "one gene, one enzyme" concept using bread mould, *Neurospora crassa*, where they proved that mutations occurring in the DNA affected the production of specific amino acids (Beadle & Tatum, 1941). This discovery contributed to the foundation of functional genomics. From then on, researchers exploit this concept in characterisation studies of a gene by including the functional identification of the gene (Albert *et al.,* 2002).

Gene functions can be determined as part of biochemical function, cellular function, developmental function, or adaptive function of a gene (Bouchez & Höfte, 1998). In addition, recent advances in functional genomics showed that computational approaches have transcended from identification of DNA or protein sequences similarity to assessments on the phylogenetic profiles of protein families, domain fusions, gene adjacency in genomes, and protein expression patterns to predict or deduce the possible protein functions (Koonin & Gelperin, 2000). Specific motif discovery in the protein sequences has been widely used to identify an enzyme's active sites, ligand-binding sites, cleavage sites, post-translational modification sites, and targeting sites (Mohamed *et al.,* 2016), in which these motifs are associated with specific protein functions. This was observed clearly in PR protein families where each PR family with specific motifs was discovered to encode for specific protein functions e.g., PR2 protein family encoding β-1,3-glucanase possesses specific glucan-binding sites (Xu *et al.,* 2016) and PR3 protein family encoding chitinase possesses specific chitin-binding sites (Hamid *et al.,* 2013). Multiple reports adopted the dinitrosalicylic acid assay (e.g., Zhou *et al.,* 2017; Khan & Umar, 2021) and Nelson-Somogyi assay (De La Cruz *et al.,* 1995; Li *et al.,* 2003) to verify β-1,3-glucanase activity. On the other hand, most reports utilised Schales'

procedure (e.g., Liu *et al.,* 2010; Tran *et al.,* 2018; Okongo *et al.,* 2019) to unravel chitinase activity. In the current study, PR10 protein was subjected to functionality tests based on the presence of specific motifs, i.e., the glycine-rich motif and the glucan-binding motif. The former motif represents a nuclear-binding site for the ribonuclease activity (Wu *et al.,* 2003) while the latter belongs to the glycoside hydrolase family 16 known as a catalytic site for β-1,3-glucanase (Behar *et al.,* 2018).

2.10.1 Dinitrosalicylic acid (DNS) assay

Dinitrosalicylic acid (DNS) assay and Nelson-Somogyi assay are the most common methods used to measure enzymatic activities against polysaccharides (McCleary *et al.,* 2015) e.g., β-1,3-glucanase. Both methods assess the enzymatic activity based on the production of reducing sugar upon enzymatic scissions of the glycosidic bond between two carbohydrates (Gusakov *et al.,* 2011). Glucose polymer, laminarin, is commonly used in these assays since β-1,3-glucanase digests laminarin to produce reducing sugar (Becker *et al.,* 2017). DNS assay was recommended by the International Union of Pure and Applied Chemistry (IUPAC) commission on biotechnology for measuring standard cellulase activities (Ghose *et al.,* 1987), hence widely used in laboratories around the world. On the other hand, Nelson-Somogyi's assay is less favourable because it involves the usage of arsenomolybdate, a carcinogenic compound that is harmful to the environment (Hatanaka & Kobara, 1980). In addition, DNS assay is extensively used worldwide due to its robustness, and simplicity in terms of its biochemistry which enables reactions to be observed colourimetrically and measurable using a spectrophotometer (Luo *et al.,* 2019). The biochemical mechanism of DNS assay is based on the detection of the orange-red solution (3-amino-5-nitro-salicylic acid), from the enzymatic effect of the reducing sugar on 3,5-dinitrosalicylic acid (yellow DNS reagent) under an alkaline condition (Jain *et al.,* 2020). The reduced complex has a maximum light absorbance value at 540 nm, which is measured using a spectrophotometer.

Neucere *et al.* (1995) and Zhang *et al.* (2019) reported a correlation between antifungal properties and the accumulation of β-1,3-glucanase, suggesting the role of β-1,3-glucanase against fungal pathogens. Similarly, a correlation was also observed in microbial growth inhibition and ribonuclease activity of plants (Chadha & Das, 2006; Liu & Ekramoddoullah, 2006; Xu *et al.*, 2014), suggesting a possible antifungal property for the PR10 protein.

2.11 Opportunistic and pathogenic fungi

2.11.1 *Aspergillus fumigatus*

Aspergillus fumigatus is an environmental saprophytic fungus (Barber *et al.,* 2020) which was also reported to be a human opportunistic pathogen causing invasive aspergillosis (Ballard *et al.,* 2020). This ubiquitous saprophytic fungal species releases the spores to the environment. It is estimated that every human being would have breathed in approximately hundreds to thousands of *A. fumigatus'* conidia daily (Pollmächer & Figge, 2014). This event is detrimental to immune-compromised patients, making *A. fumigatus* the most important airborne fungal pathogen to human (Brakhage *et al.,* 2010).

Aspergillosis contributed to a substantial mortality rate of 30 - 50 % in a community with impaired immunity (Latgé & Chamilos, 2019). De Vries & Visser (2001) reviewed that this fungus can also be a threat to plants since *A. fumigatus* was reported to produce a cell wall degradation enzyme. Besides that, the thermotolerance of this fungal species allows them to survive in higher temperatures such as 75 ℃. This is an advantageous trait for pathogenicity (Tekaia & Latgé, 2005). Berger *et al.* in 2017 reported that *A. fumigatus* developed resistance to azole fungicide that is widely used in agriculture. This prompted the Centre of Disease Control and Prevention, USA (CDC, 2019) to monitor the pathogenicity of *A. fumigatus* and azole resistance constantly.

2.11.2 *Aspergillus niger*

Aspergillus niger is a black filamentous mould with an extremely diverse habitat (Lima *et al.,* 2019). This saprophytic pathogenic fungus is known for its ability to produce secondary metabolites such as nonribosomal peptides, polyketides and lipopeptides, that incur pharmacological implications (Richter *et al.,* 2014). This fungus has also been utilized for microbial fermentation of Pu'er tea, Awamori, citric acid, extracellular enzyme, and antioxidant production (Frisvad *et al.,* 2007).

James Currie's discovery on extracting high concentration of citric acid from *A. niger* has developed a multi-billion-dollar industry that utilises this fungus (Cairns *et al.,* 2018) as main biochemical producer of citric acid. However, as a secondary metabolite producer, this fungus is commonly associated with postharvest decay of organic substances by producing a diverse range of hydrolytic and oxidative enzymes that cause significant damage to fruits, cereals, and vegetables (Sharma, 2012). Besides, this fungus is a major concern to the agricultural industry and human lives due to their ability to produce classes of mycotoxins (Palencia *et al.,* 2010) such as ochratoxin A, fumonisin B2, and aflatoxins (Noonim *et al.,* 2009; Al-Abdalall, 2009), which are carcinogenic in nature, therefore, harmful to living things.

The mycotoxin produced could elicit damages specific to human organs (Hope, 2013) such as liver, kidney, nervous system, muscle, skins, and respiratory organs. In plants, this mould causes stem or root rot, thus, it is recognised as an important spoilage fungus (Gautam *et al.,* 2011). Despite being labelled as 'generally recognised as safe' (GRAS) by US Food and Drug Administration (FDA) (Powell *et al.,* 2013), Schuster *et al.* (2002) reported several medical cases on hypersensitive response from patients due to *A. niger* spores suggesting that this fungus remains as a threat to human health.

2.11.3 *Fusarium oxysporum* f. sp. *cubense*

Fusarium oxysporum f. sp. *cubense* is considered as one of the most devastating fungal pathogens worldwide, especially to bananas (Maymon *et al.,* 2020). This fungal species is categorised into four races, depending on its host range (Mostert *et al.,* 2017), but at least 24 vegetative compatibility groups are known within the races thus far (Fourie *et al.,* 2011). Vegetative compatibility is defined as the ability of hyphae to successfully fuse with another hyphae (Read & Roca, 2006), where fungi with similar vegetative compatibility group develop their colony by self-fusing to form complex interconnecting networks of hyphae (Fischer & Glass, 2019).

Ploetz (2005) reported that *F. oxysporum* f. sp. *cubense*: Tropical Race 1 caused the Panama disease that destroyed the well-established banana variety and former export cultivar of trade, Gros Michel (Ploetz, 2015) during mid-20th century. This destruction led to a worldwide growth of another replacement cultivar, Cavendish because this banana variety was resistant to *F. oxysporum* f. sp. *cubense*: Tropical Race 1. However, Ploetz (2015) reviewed that *F. oxysporum* f. sp. *cubense*: Tropical Race 4 is threatening Cavendish production with no effective management method against this fungus established thus far.

This predicament suggests for the usage of a resistant banana line as an alternative practical approach. Although Li *et al.* (2015) reported the sources of resistant to *F. oxysporum* f. sp. *cubense*: Tropical Race 4 in bananas, the introduction of such resistant sources into banana genomes via a breeding programme is a complicated endeavour due to the sterility of polyploid bananas (Ortiz, 2013). Therefore, Costa *et al.* (2019) suggested using antifungal secondary metabolites as control agents to manage fungal infection in plants such as citrus fruit. Ongena and Jacques (2008) reported that secondary metabolites produced by several *Bacillus* species successfully shown antifungal property

against plant pathogens. It is noteworthy that secondary metabolites with antifungal properties from plants and microorganisms have been recognised (Paiva et al., 2010; Coleman et al., 2011) as possible fungal control agents as well.

2.11.4 Antifungal susceptibility test

Certain PR proteins have not only been demonstrated to possess antifungal properties *in vitro*, but also exhibit antifungal activity *in vivo* (Ferreira *et al.,* 2007). PR10 proteins were associated with potential antifungal property in grapevine (Xu *et al.,* 2014), maize (Zandvakili *et al.,* 2017), and soybean (Fan *et al.,* 2015) but this property has yet to be demonstrated *in vitro* for *M. acuminata*. The current study found a sequence motif encoding β-1,3-glucanase activity in the isolated PR10 protein variants. This glucan binding motifs had long been associated with antifungal property (Calderan-Rodrigues *et al.,* 2018), hence, warrants further functional analyses. In this light, an antifungal susceptibility assay was carried out on the isolated protein variants against fungal species since the cell walls of the fungi were made of chitin-glucan complex.

Antifungal susceptibility assay is conducted to detect antifungal resistance against a fungus and to discover the best treatment to limit their growth (Berkow *et al.,* 2020). To date, there were many established methods available for antifungal susceptibility assay published by the Clinical and Laboratory Standards Institute (CLSI), and European Committee on Antimicrobial Susceptibility (EUCAST) to determine the minimum inhibitory concentration (MIC) of the antifungal peptides to impede fungal growth. However, MIC have yet to be established for *Aspergillus* spp. (Lass-Flörl *et al.,* 2006) and *Fusarium* spp. (Alastruey-Izquierdo *et al.,* 2015). Notwithstanding, CLSI has standardised the well diffusion method, an established antifungal susceptibility assay which is commonly used in many laboratories (Magaldi *et al.,* 2004) due to its robustness and reproducibility. Amongst the many successful assays were on *Alternaria alternata*

(Kaur er al., 2017) and selected species of *Aspergillus* spp. (Bocate *et al.,* 2019). Therefore, this method was used in the current study. The diffusion method readily allows the detection of physical changes on the agar such as fungal growth impairment (also known as zone of inhibition) caused by the proteins (Hombach *et al.,* 2013). The formation of this inhibition zone allows manual measurement to be made, allowing data documentation.

CHAPTER 3: METHODOLOGY

3.1 Data mining

A data mining procedure was carried out in the GenBank and Banana Genome Hub for VVPEIVVSGAVLEGDGSVGSVR (ITC1587_Bchr9_P26466_MUSBA) peptide sequence. This peptide was reported to be significantly regulated in *M. incognita*–Grand Naine (ITC 1256) compatible interaction after 30 days of inoculation (Al-Idrus *et al*., 2017) suggesting its importance in banana defence system. The reported peptide sequence was first translated to nucleotide sequence with translated nucleotide Basic Local Alignment Search Tool (tBLASTn) search in the GenBank (https://blast.ncbi.nlm.nih.gov/Blast.cgi) and Banana Genome Hub (https://banana-genome-hub.southgreen.fr/blast) using tBLASTn. From the top query hits in the BLAST results, six reference sequences were chosen from both databases. The six reference sequences (accession numbers of the *Musa* spp. reference sequences from the GenBank database: JK271128.1 and LOC103998084, and from Banana Genome Hub database: Ma03_g08140, Ma03_g0815, Ma03_g08160, and Ma03_g15840) were aligned with ITC1587_Bchr9_P26466_MUSBA transcript sequence using MEGA X (Molecular Evolutionary Genetics Analysis) software to design a degenerate primer pair to isolate the *MaPR1-like* gene from the banana cultivars.

3.2 Plant tissue culture and transplantation

Tissue culture plantlets of two banana varieties namely Berangan and Grand Naine (ITC 1256) were maintained and propagated as described in Jalil *et al.* (2003). The plantlets were subcultured in standard propagation Murashige and Skoog (MS) media supplemented with vitamins [0.4 mg/L thiamine hydrochloride (HCl), 0.5 mg/L pyridoxine HCl, 0.5 mg/L nicotinic acid and 2 mg/L glycine], 30 g/L sucrose, 2 g/L gelrite® and 3.5 mg/L 6-Bensylamunopurine (BAP) with the pH of the media adjusted to 5.75. The MS media were prepared in a 1 L beaker and approximately, seven millilitres

of the MS media were transferred into 15 cm × 2.5 cm test tubes. Then, the tubes were autoclaved at 121 ℃ for 15 min.

Banana tissue culture plantlets were propagated in MS media for three months and then transferred into plant rooting MS media (prepared similarly as the propagation media, except for BAP which was replaced with 0.5 g/L active charcoal) with the pH of the media adjusted to 6.2. Banana plantlets were grown in the media until they reached the four-leave stage. Before transplantation, banana root system was thoroughly washed to ensure all media residues were removed to prevent fungal infections. The plantlets were transplanted into a 12 cm diameter polybag containing autoclaved soils (3 black soil: 1 sand) and left to acclimatise in the soil for eight weeks in the growth room set with 12-h light and 12-h dark photoperiod. Then, the plantlets were transferred to a 1 L plastic pot. Fertilisers were applied to the plants once a week starting from the second week of transplantation. At least three Grand Naine (ITC 1256) cultivars were used as host plants for the plant-parasitic nematodes, *M. incognita*. Soil used in this experiment was first autoclaved at 121 ℃ for 20 min prior to transplantation.

3.3 Propagation of *M. incognita* in plants

Meloidogyne incognita (Malaysian population) 'seed' culture was obtained from the Malaysian Agricultural Research and Development Institute (MARDI), courtesy of Mr. Nazarudin Anuar. This culture was then propagated and maintained in susceptible banana variety, Grande Naine (ITC 1256). To propagate the nematode culture, nematode egg masses were hand-picked from the dissected root fragments under a compound microscope (100× magnification; Olympus, USA) and subsequently placed in a 50 mL beaker containing sterilised distilled water (sdH_2O). The egg masses were hatched as described in Speijer and De Waele (1997) by adding a few drops of 1 % sodium hypochlorite (w/v) to release the nematode juveniles. Nematode juveniles were used as

inoculums with the number of J2 were estimated by averaging the triplicates of nematode juveniles obtained per mL. Then, nematode juveniles were adjusted to 1000 J2 individuals for each treatment on the Grand Naine (ITC 1256) cultivars. The nematode suspension was pipetted into a 3 cm-deep-hole in soil, near the banana root system. Note that the root tissues of the *M. incognita*-infected banana plants were harvested and subjected to mRNA isolation.

3.4 DNA isolation from banana leaf tissues

DNA sample was isolated from 1 g banana leaf tissues of Berangan and Grand Naine (ITC 1256). The leaf tissues were rinsed with tap water and left to dry before placed in an aluminium foil. Subsequently, the wrapped sample was snapped-frozen in liquid nitrogen and stored at –80 ℃ until further use. DNA sample was isolated from the stored leaf tissues using the CTAB method described in Khayat *et al.* (2004) with minor modifications.

Firstly, 1 g of the snap-frozen leaf tissues was ground into fine white powder using a sterile mortar and pestle pair in the presence of liquid nitrogen. Approximately 0.5 g of the fine powder was added into 500 µL of extraction buffer [4 % CTAB, 100 mM Tris-HCl (pH 8.0), 50 mM NaEDTA (pH 8.0), 1 % DTT, and 1.4 M NaCl] in a sterile 1.5 mL microcentrifuge tube. The sample was then incubated at 55 ℃ for 30 min and centrifuged at 2, 655 × *g* for 5 min at room temperature. The resulting supernatant was transferred into a fresh 1.5 mL microcentrifuge tube and incubated at 37 ℃ with RNase A (10 mg/ml) for 3 h. Then, an equal volume of phenol:chloroform:isoamyl-alcohol (PCI; 25:24:1) (Sigma-Aldrich, Germany) was added to the sample, which was then vortexed and centrifuged at 2, 655 × *g* for 5 min at room temperature. The aqueous upper layer of the mixture containing the nucleic acid was transferred into a sterile 1.5 mL microcentrifuge tube. An equal volume of chloroform:isoamyl-alcohol (CI; 24:1) (Sigma-Aldrich,

Germany) was added to the sample, before it was vortexed and centrifuged using parameters as previously stated. Similarly, the aqueous upper layer of the supernatant was transferred into a sterile 1.5 mL microcentrifuge tube. To precipitate the DNA, an equal volume of cold isopropanol was added to the sample, and the solution was mixed well by inverting and incubated at –80 ℃ overnight. Subsequently, the sample was thawed without agitation at 4 ℃ and centrifuged at 7, 674 × *g*, 4 ℃ for 20 min to pellet the DNA. The resulting pellet was washed twice with 1 mL of 70 % ethanol in which each washing step was accompanied by a centrifugation step at 17, 949 × *g* for 5 min at room temperature. The pellet was then vacuum-centrifuged at 25 ℃ for 5 min to remove ethanol residue in the tube. Finally, the pellet was dissolved in 30 µL of sdH_2O and stored in –20 ℃ until further use.

3.5 RNA isolation from plant tissues

3.5.1 Diethylpyrocarbonate (DEPC) treatment on the apparatus used for RNA isolation experiment

Mortars, pestles, and storage boxes used in this experiment were soaked in 3 L distilled water containing 1 % DEPC and left overnight at room temperature. Subsequently, the mortars and pestles were dried and wrapped with aluminium foil while excess water in the storage box was drained out prior to autoclaving at 121 ℃ for 45 minutes. Then, the mortars and pestles were air-dried at 60 ℃ in an oven and stored until future use. On the other hand, the storage boxes, were air-dried and filled with nuclease-free 0.5 mL and 1.5 mL microcentrifuge tubes, and nuclease-free 10 µL, 100 µL, 200 µL and 1000 µL tips in dedicated boxes. The storage boxes containing tubes and tips were autoclaved at 121 ℃ for 45 min and stored for future use.

3.5.2 RNA isolation from *M. incognita*-infected banana root tissues

Total RNA sample was isolated from *M. incognita*-infected root tissues of two banana varieties namely Berangan and Grand Naine (ITC 1256) using lithium chloride (LiCl) precipitation method as described in Kistner and Matamoros (2005). Firstly, 150 mg of root sample was ground into fine powder using a pair of sterile mortar and pestle in the presence of liquid nitrogen. Subsequently, 100 mg of the fine powder was added into a prewarmed (65 °C) RNA extraction buffer [2 % CTAB, 2 % PVP, 100 mM Tris-HCl (pH 8.0), 25 mM NaEDTA (pH 8.0), 2 M NaCl and 2 % β-mercaptoethanol] in a sterile 1.5 mL microcentrifuge tube. An equal volume of phenol:chloroform:isoamyl-alcohol (PCI; 25:24:1) (Sigma-Aldrich, Germany) was immediately added to the tube and it was vortexed for 5 min. Subsequently, the tube was incubated at 55 °C for 10 min. The sample was centrifuged at 17, 949 × *g*, 4 °C for 10 min. The resulting supernatant was then transferred into a sterile 1.5 mL microcentrifuge tube. Similar step was repeated once again by adding an equal volume of PCI (25:24:1) (Sigma-Aldrich, Germany) to the supernatant, but with a 5 min centrifugation step. The aqueous layer containing the nucleic acid was pipetted into a sterile 1.5 mL microcentrifuge tube. To precipitate the RNA, 8 M LiCl was added to the sample to a final concentration of 2 M followed by an overnight incubation at 4 °C. Subsequently, the mixture was centrifuged at 17, 949 × *g*, 4 °C for 10 min. The resulting supernatant was then discarded, and the pellet was washed with 1 mL of 2 M LiCl. The sample was again centrifuged at 17949 × *g*, 4 °C for 10 min. Similarly, the resulting supernatant was discarded, and the pellet was washed twice with 1 mL of cold 80 % ethanol. The pellet was then vacuum-centrifuged at 25 °C for 5 min to remove residual ethanol residue in the tube and dissolved in 30 µL RNAse-free sdH_2O. The sample was stored in –80 °C until further use.

3.5.3 RNA isolation from *A. thaliana* leaf tissues

Total RNA was isolated from the leaf tissues of *A. thaliana* using Nucleospin® RNA Plant Kit (Mackerey-Nagel, Germany) as described in the manufacturer's protocol. Approximately 50 mg of *A. thaliana* leaf tissues was ground into fine powder using a sterile mortar and pestle in the presence of liquid nitrogen. The powder was transferred into a sterile 1.5 mL microcentrifuge tube and 350 µL of Buffer RA1 with 1 % β-mercaptoethanol was added into the tube. The tube was vortexed vigorously and the sample was pipetted into a NucleoSpin® Filter column. The column was subjected to a centrifugation step at 11, 000 × *g* for 1 min at 25 ℃. The collected supernatant was transferred into a fresh sterile 1.5 mL microcentrifuge tube and 350 µL of 70 % ethanol were thoroughly mixed with the sample. The mixture was pipetted into a NucleoSpin® RNA Plant column and centrifuged at 11, 000 × *g* for 30 sec at 25 ℃ to bind RNA in the column. The flow-through was then discarded. The column with RNA sample was later loaded with 350 µL membrane desalting buffer (MDB) to dry the membrane and centrifuged at 11, 000 × *g* for 1 min. Again, the flow-through was discarded. Next, 95 µL of 10 % DNase reaction mixture were loaded into the column and incubated at room temperature for 15 min. After incubation, three washing steps were performed with the flow-through of each washing step was discarded. For the first washing step, the column was pipetted with 300 µL of Buffer RA2 and centrifuged at 11, 000 × *g* for 30 sec. This was followed by addition of 600 µL of Buffer RA3 into the column. The column was then subjected to a centrifugation step using the same parameters as described above. The final washing step was performed by adding another 250 µL of Buffer RA3 into the column prior to centrifugation at 11, 000 × *g* for 2 min. Finally, the column was placed into a sterile 1.5 mL microcentrifuge tube for the elution step. To elute the total RNA sample, 60 µL of RNase-free water were pipetted into the column and centrifuged at 11,

000 × *g* for 1 min at room temperature. The sample was then stored at –80 °C until further use.

3.6 Quantification and quality assessment of nucleic acid samples

The quantity and quality of the isolated nucleic acid samples were estimated using a NanoPhotometer® (Implen Gmbh, Germany). For DNA quantification, sdH_2O was used as the blank sample while nuclease-free water was used for RNA quantification. The purity of DNA and RNA samples was estimated by obtaining the absorbance ratios of A_{260}/A_{280} and A_{260}/A_{230}. On the other hand, the quality of the isolated DNA and RNA samples was determined by subjecting the samples to agarose gel electrophoresis.

3.7 Agarose gel electrophoresis

3.7.1 Gel electrophoresis of DNA sample

The electrophoresis for DNA and PCR samples was carried out using 1 % (w/v) agarose gel in 1X TBE [89 mM tris base, 89 mM boric acid, and 2 mM Ethylenediaminetetraacetic acid (EDTA)] that was pre-stained with 0.1 mg/mL ethidium bromide (EtBr) for a 30 mL-gel volume. The electrophoresis was run using 5 µL of each sample in 1X TBE buffer at 120 V for 25 min. The size of the DNA fragment was estimated using a 100 bp DNA ladder (Thermo Fisher Scientific, USA). The gel was then viewed under 312 nm wavelength UV transilluminator, and the gel image was captured and stored in a gel documentation system (Perkin Elmer, USA).

3.7.2 Gel electrophoresis of RNA sample

The apparatus used to carry out agarose gel electrophoresis of RNA sample were first treated with DEPC as described in Section 3.5.1. In addition, the electrophoresis tank used in RNA sample electrophoresis was DEPC-treated and rinsed with nuclease-free water *a priori*. One microgram of the isolated total RNA sample was mixed with 1 mL of 2X RNA loading dye (Thermo Fisher Scientific, USA) by gentle pipetting. The mixture

was then heated at 65 ℃ for 15 min. This heating process was performed to denature RNA secondary structures present in the sample. The sample was then electrophoresed on a 1 % (w/v) agarose gel that was pre-stained with 0.1 mg/mL EtBr in 1X TBE buffer prepared with nuclease-free water. Agarose gel electrophoresis was performed at 90 V for 45 min in 1X TBE buffer. The gel was then viewed under 312 nm wavelength UV transilluminator and the gel image was captured and stored in a gel documentation system (Perkin Elmer, USA). The size of the RNA fragment was estimated using High Range RNA ladder (200–6000 bases) (Thermo Fisher Scientific, USA).

3.8 Isolation of Musa acuminata pathogenesis-related 1-like (MaPR1-like) gene from banana DNA samples

3.8.1 Primer design for the isolation of *MaPR1-like* gene

Based on data mining in Section 3.1, a pair of degenerate primer was designed to isolate the *MaPR1-like* gene from the two banana cultivars. The suitability of all designed primers for PCR was assessed using an online *in silico* PCR primer stat analysis (https://www.bioinformatics.org/sms2/pcr_primer_stats.html). The expected amplicon size for the genomic *MaPR1-like* was ~550 bp (Figure 3.1).

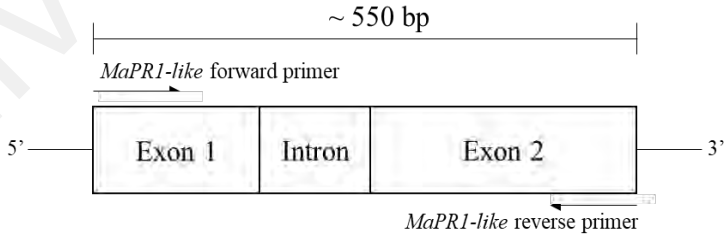

Figure 3.1: Diagram showing the positions of forward and reverse degenerate primers targeting *MaPR1-like* gene.

3.8.2 PCR amplification of *MaPR1-like* gene from banana genomic samples

A degenerate primer pair was designed to target *MaPR1-like* gene that showed sequence similarity with ITC1587_Bchr9_P26466_MUSBA, a banana *PR* sequence described in Section 3.8.1. PCR was performed in a 50 µL-reaction mixture containing 1X PCR Buffer A (EURx, Poland), 200 µM for each dNTP, 1.5 mM $MgCl_2$, 0.4 of µM

each primer, 1 U *Taq* polymerase (EURx, Poland), 50 ng DNA template and sdH_2O. A negative control reaction was included by replacing the DNA template with sdH_2O. PCR was conducted in a thermocycler (peqSTAR, USA) with an amplification profile consisting of an initial denaturation step at 94 ℃, 38 cycles of a denaturation step at 94 ℃ for 1 min, an annealing step at 60.7 ℃ for 1 min, an elongation step at 72 ℃ for 44 sec, and a final extension step at 72 ℃ for 5 min. The PCR product was subjected to agarose gel electrophoresis as described in Section 3.7.1.

3.8.3 DNA purification

The amplified PCR products with an expected size of ~550 bp for genomic sample and ~480 bp for transcript sample were purified using QIAquick gel extraction kit (Qiagen, USA) according to the manufacturer's protocol. Firstly, 90 µL of PCR products were electrophoresed as described in Section 3.7.1 but at 100 V for 40 min. Subsequently, the band of interest was carefully excised under 302 nm UV light using a clean scalpel. To obtain the weight of the excised gel, a sterile and empty 1.5 mL microcentrifuge tube was initially weighed, and the weight was recorded. The excised gel was then placed into the weighed microcentrifuge tube and the weight of the tube containing the gel slice was recorded. The weight of the gel was then obtained by subtracting the weight of the empty tube from the weight of the tube containing the gel slice. Then, 300 µL of buffer QG was added for every 100 mg of excised gel.

The tube containing the excised gel was incubated at 50 °C for 10 min to dissolve the gel. Subsequently, an equal volume of isopropanol was added to the sample once the gel was completely dissolved. The mixture was pipetted into a QIAquick spin column and centrifuged for 1 min at 11, 300 × *g*. The flow-through was then discarded and the column was placed in the collection tube again. Then, 750 µL of PE buffer (150 µL PE buffer mixed thoroughly with 600 µL of 100 % ethanol) was freshly prepared and added into

the column. The column was left to stand at room temperature for 4 min before being centrifuged for 1 min at 11, 300 × *g*. The resulting supernatant was discarded, and the column was vacuum-centrifuged (Cole Palmer, USA) for 1 min at 11, 300 × *g*. The resulting supernatant was discarded. The column was later air-dried for 1 min. Subsequently, 30 µL of sdH_2O were added into the column and left to stand at room temperature for 1 min.

Finally, the column containing sdH_2O was centrifuged for 1 min at 11, 300 × *g* to collect the purified DNA sample. The purified product was subjected to agarose gel electrophoresis as described in Section 3.7.1, with modification on the composition of samples loaded in the well. Each well was loaded with 5 µL of purified DNA sample mixed with 1 µL of DNA loading dye and 1 µL of 30 % glycerol to increase the density of the purified DNA sample. The purified DNA sample was later subjected to a T-A cloning procedure.

3.8.4 Preparation of *Escherichia coli* strain JM109 competent cells using calcium chloride ($CaCl_2$)

Escherichia coli strain JM109 competent cells were prepared using calcium chloride ($CaCl_2$) as described in Sambrook *et al*. (2006). The 'seed' culture was initially purchased from Promega, USA and continuously subcultured then on. A sterile inoculation loop was used to inoculate the cells in 10 mL Luria-Bertani (LB) broth (10 g/L Tryptone, 5 g/L yeast extract, and 10 g/L NaCl) and incubated at 37 ℃ overnight with 220 rpm shaking. Subsequently, 1 mL of culture was inoculated into another 10 mL LB broth using similar condition as previously described, but just for 2 h. The OD_{600} reading of the new culture was monitored using a NanoPhotometer®.

As the OD_{600} reading of culture reaches approximately 0.4, the culture was transferred into a sterile 1.5 mL microcentrifuge tube and chilled in ice for 15 min. The tube was

centrifuged at 3, 300 × *g*, 4 ℃ for 10 min. The resulting supernatant was then discarded. The pellet was dissolved in 500 µL of cold 0.1 M $CaCl_2$ and left in ice for 30 min. The tube was again centrifuged at 3, 300 × *g*, 4 ℃ for 10 min, and the resulting supernatant was discarded. The pelleted cells were resuspended in 100 µL buffer containing 0.1 M $CaCl_2$ and 15 % glycerol. The culture was then snapped-frozen in liquid nitrogen and stored in –80 ℃ until future use.

3.8.5 T-A Cloning

3.8.5.1 DNA Ligation

The purified PCR products obtained from Section 3.8.3 were each ligated into pGEM®-T Easy Vector System I (Promega, USA) as described in the manufacturer's protocol. The ligation reaction was carried out in a 0.5 mL microcentrifuge tube containing 2X rapid ligation buffer, 1 µL of pGEM®-T easy vector, 1 µL of T4 DNA ligase (3 Weiss units/µL), 2 µL of purified DNA sample, and 1 µL of sdH_2O in a final volume of 10 µL. The mixture was thoroughly mixed by gentle pipetting and incubated at 4 ℃ for 16 h prior to transformation procedure.

3.8.5.2 Transformation

Transformation procedure was carried out as described in Sambrook *et al.* (2006). Luria Bertani (LB) bacterial growth agar plate [30.5 g/L LB agar powder, 50 µg/mL of ampicillin, 0.5 mM isopropyl β-d-1-thiogalactopyranoside (IPTG), and 0.08 mg/mL of X-Gal] was first prepared and solidified in a petri dish prior to carrying out the transformation step. Then, the ligation reaction mixture was centrifuged at 11, 300 × *g* for 1 min in order to collect the content at the bottom of the tube. Subsequently, 2 µL of the ligation reaction was pipetted into a 1.5 mL microcentrifuge tube containing 100 µL *E. coli* strain JM109 competent cells that were prepared in Section 3.8.4. The mixture was then gently mixed by flicking and then incubated in ice for 20 min. Later, the

competent cells were subjected to a heat-shock treatment at 42 °C in a water bath for 45 sec and immediately placed in ice for 2 min. Subsequently, 950 µL of LB broth [10 g/L tryptone, 5 g/L yeast extract, and 10 g/L NaCl] was added to the sample and the cells were incubated for 3 h at 37 °C in an incubator (Memmert, Germany). Subsequently, the transformation culture was centrifuged at 3, 000 × *g* for 2 min and 700 µL of the resulting supernatant were discarded. The pellet was then mixed with the remaining supernatant by gentle pipetting. Lastly, 150 µL of the transformation culture was plated on an LB agar plate and incubated at 37 °C for 16 h.

3.8.5.3 Selection of transformants and screening of transformed bacterial colonies

The transformation experiment in Section 3.8.5.2 resulted in the formation of blue and white bacterial colonies. The presence of white colonies indicated the presence of successful ligations of the gene of interest into the plasmids. The formation of white colonies was due to the inactivation of *lacZ* gene in the plasmids by the insert, which disrupted the expression of β-galactosidase. The lack of functioning β-galactosidase left the X-gal in the plate uncleaved, hence the colour of recombinant cells was white. On the other hand, untransformed cells produced functional β-galactosidases, cleaving the X-gal compound into 5-bromo-4-chloro-indoxyl which oxidises spontaneously into a 5, 5'-dibromo-4, 4'-dichloro-indigo, resulting in the formation of blue colonies. The white colonies were picked with a sterile toothpick and transferred into a gridded 6 × 6 LB agar mini library and the remainder of the colony was dipped into a sterile 0.5 mL microcentrifuge tube containing 30 µL of sdH_2O. The tube was then heated at 99 °C for 10 min in a heat block to lyse the bacterial cells and the cell lysate was subsequently subjected to colony PCR to detect the presence of the cloned fragment.

3.8.5.4 Colony PCR

A colony PCR was conducted in a 25 µL reaction mixture containing 1X PCR buffer A (EURx, Poland), 200 µM of each dNTPs, 1.5 mM $MgCl_2$, 0.5 µM of each universal M13 universal primers (M13 Forward primer: 5' GTAAAACGACGGCCAGT 3' and M13 Reverse primer: 5' GCGGATAACAATTTCACACAGG 3'), 1 U *Taq* polymerase (EURx, Poland), 1 µL of lysed bacterial cell sample obtained in Section 3.8.5.3, and sdH_2O in a sterile 0.2 mL microcentrifuge tube. A negative control reaction was included by replacing the DNA template with sdH_2O. PCR was carried out as described in Section 3.8.2, but with the annealing temperature adjusted to 60 °C. The colony PCR product was subjected to agarose gel electrophoresis as described in Section 3.7.1 to confirm the presence of insert in the plasmid. Colonies showing the presence of the cloned fragment were subjected to plasmid isolation.

3.8.6 Plasmid isolation using alkaline lysis with sodium dodecyl sulfate (SDS)

Plasmid isolation was conducted as described in Sambrook *et al.* (2006). A single bacterial colony from the 6 × 6 colony library in Section 3.8.5.3 showing the presence of the fragment of interest was cultured in a universal bottle containing 10 mL LB broth [10 g/L Tryptone, 5 g/L yeast extract, 10 g/L NaCl, and 50 µg/mL ampicillin]. The culture was incubated for 16 h at 37 °C in a shaking incubator at 220 rpm. Subsequently, 850 µL of the incubated colony culture was transferred into a sterile 1.5 mL microcentrifuge tube containing 150 µL of 100 % glycerol and the tube was then stored in –80 °C as a stock. The remainder was transferred into a sterile 15 mL tube and centrifuged at 12, 857 × *g* for 5 min. The resulting supernatant was then discarded, and the pellet was dissolved in 200 µL Solution I [50 mM Glucose, 10 mM EDTA, and 25 mM Tris-Cl] on ice and then transferred into a sterile 1.5 mL microcentrifuge tube. Solution I was added into the tube with pellets to destabilise the bacterial cell membrane and prevent DNA shearing. The mixture was mixed with 200 µL Solution II [10 M NaCl, and 10 % SDS] for 4 min to

lyse the bacterial cell and 200 µL Solution III [5 M potassium acetate, and glacial acetic acid] was added. Solution III was added to induce the SDS-protein complex formation and precipitate high molecular weight RNAs. Subsequently, the mixture was gently mixed for 15 min in ice prior to centrifugation at 11, 300 × *g* for 10 min. The resulting supernatant was transferred into a sterile 1.5 mL microcentrifuge tube and 10 mg/mL of RNase A was added before incubating the sample at 37 ℃ for 3 h. Subsequently, one volume of phenol was mixed to the sample by vortexing for 1 min and the mixture was centrifuged for 5 min at 11, 300 × *g*. The resulting supernatant was then transferred into a sterile 1.5 mL microcentrifuge tube. One volume of chloroform was added to the sample, followed by brief vortex and centrifugation at 11, 300 × *g* for 5 min. The resulting upper layer of the mixture was transferred into a sterile 1.5 mL microcentrifuge tube. Next, 0.1 volume of 5 M NaCl and 2.5 volume of cold isopropanol were added to the mixture to precipitate the plasmid DNA. The tube was incubated in ice for 20 min and centrifuged at 11, 300 × *g* for 15 min. The resulting supernatant was discarded, and the pellet was washed with 70 % ethanol. Finally, 30 µL of sdH_2O was added and the sample was stored at 4 ℃ for future use. The isolated plasmid DNA was subjected to quantification as described in Section 3.6 and quality assessment as described in Section 3.7.1. All centrifugation steps in this study were conducted at room temperature.

3.8.7 Restriction enzyme (RE) digestion assay

The isolated plasmid DNA obtained in Section 3.8.6 was digested with *Eco*RI restriction enzyme (RE) to confirm the presence of the fragment of interest. *Eco*RI RE recognises and cuts G*AATTC sequence sites that were present at both arms of the vector, releasing the cloned fragment. RE digestion reaction was conducted in a final volume of 20 µL containing 10X Buffer (Promega, USA), 10 µg/µL BSA (Promega, USA), 12 U *Eco*RI RE (Promega, USA), 1 µg DNA sample, and sdH_2O in a sterile 0.5 mL microcentrifuge tube. For the negative control, *Eco*RI enzyme was substituted with

sdH_2O. The reaction tube was then incubated at 37 ℃ for 1 h. The reaction was then inactivated by subjecting the sample to 65 ℃ incubation for 10 min. The product was then subjected to agarose gel electrophoresis as described in Section 3.7.1 and the plasmids with the correct insert size were subjected to cycle sequencing.

3.8.8 Cycle sequencing

Plasmids containing cloned fragment obtained in Section 3.8.7 were subjected to cycle sequencing using BigDye® Terminator v3.1 chemistry (Thermo Fisher Scientific, USA) with a slight modification in the amount of DNA and primer concentrations used. Briefly, PCR reactions were performed in a final volume of 20 µL using 1 µL of BigDye® Terminator v3.1 Ready Reaction Mix (Applied Biosystems), 3 µL of sequencing buffer, 3.2 µM M13 primer pair and 300 ng of plasmid DNA in a 0.2 mL microcentrifuge tube. Thermal cycler condition used was as described in the manufacturer's specifications. Amplification profile consisted of an incubation step at 94 ℃ for 1 min, 25 cycles of a denaturation step at 94 ℃ for 10 sec, an annealing step at 50 ℃ for 5 sec, an extension step at 60 ℃ for 4 min, and finally, halted at 4 ℃. The products were purified using ethanol/EDTA precipitation as described in the manufacturer's protocol. The precipitation product was resuspended in 10 µL Hi-Di® Formamide (Thermo Fisher Scientific, USA) and separated on Applied Biosystems 3130XL Genetic Analyser using 50 cm capillaries (Thermo Fisher Scientific, USA). StdSeq50_POP7 module was chosen as the standard run parameters which included the sample injection procedure for 15 sec at 8.5 kV, and electrophoresis performed at 8.5 kV for 120 min at 60 ℃ using POP-7® polymer (Thermo Fisher Scientific, USA).

3.8.9 Sequence and phylogenetics analyses of the isolated genomic clones

Chromatogram analysis of each clone was carried out using Chromas version 4.0 (Technelysium Pty. Ltd.). A full clone sequence was obtained by concatenating the

sequences from forward and reverse sequencing reactions. For the ease of analysis, each sequence was edited to begin with the *MaPR1-like* forward primer sequence and ended with *MaPR1-like* reverse primer sequence. All sequences were subjected to homology comparison with sequences available in the GenBank and Banana Genome Hub (https://banana-genome-hub.southgreen.fr/) databases. Sequences of the target region were aligned using MEGA X software (Kumar *et al.* 2018). To estimate the number of *MaPR-like* sequence group present in the banana genomes studied, a phylogenetic tree was constructed using 44 cloned sequences isolated from both Berangan and Grand Naine (ITC 1256) cultivars, and *Musa acuminata PR1* sequences obtained from the GenBank (JF271128.1 and KF582558.1) and Banana Genome Hub (BGH; Ma09_g15840, Ma03_g08160.1, Ma03_g08150.1 and Ma03_g08140) databases.

A total of 44 nucleotide sequences with 566 nucleotide positions were aligned and subjected to sequence model test function available in the software. A model with the lowest Bayesian Information Criterion (BIC) score was chosen. Then, a maximum likelihood phylogenetic tree was constructed using Kimura-2 parameter model with a bootstrap value of 1000. Non-uniformity of evolutionary rates among sites was modelled using a discrete Gamma distribution (+G) with 5 rate categories and the assumption that a certain fraction of sites was evolutionarily invariable (+I). Two genomic cloned sequences namely gBe-E3 and gGN-C6 were randomly chosen from each banana genomes studied as the probes for Southern blot hybridisation assay.

3.9 Copy number analysis of *MaPR1-like* gene in the two banana genomes

3.9.1 Hybridisation probe design

Based on the phylogenetics analysis in Section 3.8.9, banana cultivar specific primers were designed to isolate the *MaPR1-like* gene in order to prepare the hybridisation probes for Southern blotting assay. Each primer sequence was designed to contain an *Nco*I RE

binding site (CCATG) at the 5' end to facilitate downstream analyses. All designed primers were subjected to an online *in silico* PCR primer stat analysis (https://www.bioinformatics.org/sms2/pcr_primer_stats.html) to assess primer suitability for PCR.

3.9.2 Southern blot assay

Southern blot hybridisation assay was carried out as described in Sambrook *et al.* (2006) to determine the copy number of *MaPR10* gene in both Berangan and Grand Naine (ITC 1256) cultivars. Two probes were used in this assay as stated in Section 3.8.9. For probe preparation, PCR was performed as described in Section 3.8.2 on the plasmids containing genomic cloned fragment gBe-E3 and gGN-C6. The PCR product was purified using QIAquick® gel extraction kit (Qiagen, USA) as described in Section 3.8.3. The purified fragment was then labelled with Digoxygenin-dUTP (DIG) (Roche, USA) as described in the manufacturer's protocol to produce 35 ng/µL probe. The labelled probes were stored at –20 °C. Subsequently, DNA extraction was performed on 7 g of Berangan and Grand Naine (ITC 1256) leaf tissues as described in Section 3.4. The extracted DNA sample was subjected to gel electrophoresis as described in Section 3.7.1 and the DNA sample quality was assessed as described in Section 3.6. Southern blot assay was carried out by digesting 20 µg of banana DNA sample from each cultivar using 20 U of three REs namely *Eco*RI, *Eco*RV and *Dra*I. RE digestion was conducted at 37 °C, overnight, in a water bath (Memmert, Germany). The digested DNA sample was then electrophoresed for two hours in a non-EtBr-stained 0.7 % agarose gel and transferred onto a nylon membrane (Amershan, UK). The membrane was incubated in a hybridisation oven with 5 mL pre-hybridisation buffer [6X saline-sodium citrate (SSC), 5X Denhardt's reagent, 0.5 % (v/v) SDS, 100 mg/ml herring sperm, and 50 % (v/v) formamide] for 4 h at 42 °C. Subsequently, the buffer was discarded, and the membrane was incubated for 16 h at 42 °C with 10 mL hybridisation buffer. The difference between

a pre-hybridisation buffer and a hybridisation buffer was the latter contained 35 ng/µL probes (thawed on ice prior usage) as opposed to the former. Following hybridisation, the membrane was washed with washing buffers in a high stringency condition. First, the membrane was washed with Buffer A [2X SSC, and 0.5 % SDS] for 5 min. This was followed with Buffer B [2X SSC, and 0.1 % SDS] for 5 min, Buffer C [1X SSC, and 0.1 % SDS] at 65 ℃ for 10 min, and finally 0.1 % SSC for 5 min. Then, immunological detection was performed as described in the manufacturer's protocol (Roche, USA). The membrane was washed with a washing buffer [0.1 M Maleic acid, 0.15 M NaCl (pH 7.5), and 0.3 % (v/v) Tween 20 (20 ℃)] and incubated with a blocking reagent (Roche, USA) for 30 min. Subsequently, the blocking reagent was discarded, and the membrane was incubated with an antibody solution containing 750 U/mL anti-Digoxigenin-AP conjugate (Roche, USA) for 30 min. Next, the antibody solution was discarded and washed with a washing buffer twice. The membrane was then equilibrated with a detection buffer [0.1 M Tris-HCl, and 0.1 M NaCl (pH 9.5), 20° C] for 5 min. Lastly, the membrane was incubated with a colour substrate solution [(Nitro blue tetrazolium chloride (NBT)/5-Bromo-4-chloro-3-indolyl phosphate (BCIP)] (Roche, USA) in the dark for 16 h. Bands observed on the membrane were photographed.

3.10 Isolation of *MaPR1-like* transcript from RNA samples

3.10.1 Reverse transcriptase-PCR of *MaPR1-like* transcript and cloning of the isolated fragment

cDNA sample was synthesised from the total RNA of Berangan and Grand Naine (ITC 1256) root tissues was done using Omniscript Reverse Transcription Kit (Qiagen, USA) following the manufacturer's protocol. Briefly, cDNA synthesis was performed in a 20 µL reaction mixture containing 0.3 µg total RNA sample, 1X Buffer RT, dNTP mix (0.5 mM each), 1 µM Oligo-dT primer, 4 U Omniscript RTase, and RNase-free sdH_2O in a 0.2 mL microcentrifuge tube. *MaPR1-like* transcript was then isolated using the primers

designed in Section 3.9.1. The expected amplicon size for the *MaPR1-like* transcript was ~480 bp (Figure 3.3). PCR was performed in a 50 µL reaction mixture containing 1X PCR Buffer A (EURx, Poland), 200 µM for each dNTP, 1.5 mM $MgCl_2$, 0.4 of µM each primer, 1 U *Taq* polymerase (EURx, Poland), 50 ng cDNA template, and sdH_2O. A negative control reaction was included by replacing the DNA template with sdH_2O. PCR was conducted in a thermocycler (peqSTAR, USA) with the similar amplification profile described in Section 3.8.2 except for the annealing temperature being adjusted to 56.3 °C. PCR product obtained was subjected to agarose gel electrophoresis as described in Section 3.7.1 and subjected to T-A Cloning following the procedures described from Section 3.8.3–3.8.8.

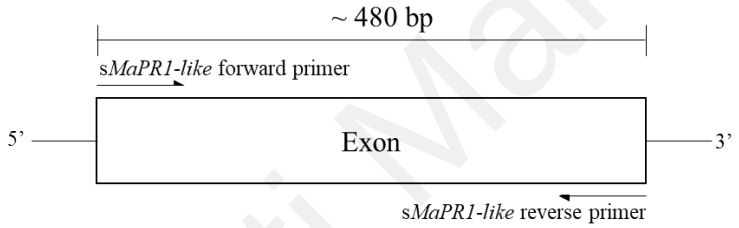

Figure 3.2: Diagram showing the positions of forward and reverse specific primers targeting *MaPR1-like* transcript.

3.10.2 Sequence analysis of putative *MaPR1-like* transcript clones using deduced amino acid sequences

Similar to what was done on the genomic cloned sequences, the forward and reverse sequences of each *MaPR1-like* transcript clone were concatenated from the two single strand chromatograms using Chromas version 4.0 (Technelysium Pty. Ltd). All sequences were subjected to homology comparison with sequences available in the GenBank and Banana Genome Hub. These sequences were then translated into amino acid sequences using the 'translate' option available in an online tool, Sequence Manipulation Suite software (https://www.bioinformatics.org/sms2). Since the top 100 sequences listed in the GenBank's BLASTn hit result included *PR10* gene sequences from other plants, two randomly chosen *MaPR-like* deduced amino acid cloned sequences

namely BeB5 and GNA5 were aligned with expressed plant PR1 and PR10 amino acid sequences available in the GenBank. To further confirm the identity of the isolated clones, the two chosen *MaPR-like* deduced amino acid cloned sequences (BeB5 and GNA5) were subjected to conserved domain search option using Conserved Domain Database (CDD) available in the GenBank (https://www.ncbi.nlm.nih.gov/Structure/cdd/wrpsb.cgi). Then, the deduced amino acid sequences of the two *MaPR-like* clonal variants were aligned with other plant PR10 amino acid sequences using EMBI-EBI Clustal Omega's multiple sequence alignment tool (https://www.ebi.ac.uk/Tools/msa/clustalo/) to highlight the conserved regions of these sequences across five plant species. There are three signature motifs that characterise the PR10 protein family namely glycine-rich loop domain (GXGGXGXXK), Bet v 1 motif (with three conserved amino acid residues E96, E148 and Y150), and a PR10 specific domain (KAXEXYL) (Jain and Kumar, 2015). The reference sequences used were *Lilium regale* (AHG94650.1), *Oryza sativa* (AAL74406.1), *Sorghum bicolor* (AAW83209.1) and *Zea mays* (ADA68331.1).

3.10.3 Phylogenetic analysis of the deduced amino acid cloned sequences of MaPR10

A total of 44 genomic (excluding the intronic region) and 25 transcript sequences of the isolated clones were translated into amino acid sequences (N = 69). The deduced amino acid sequences were then aligned with translated *PR10* reference sequences obtained from the GenBank i.e., *L. regale* (KF746437), *O. sativa* (AF395880), *S. bicolor* (AY751553), *Z. mays* (FJ897503), and *M. acuminata* (JF271128.1, KF582558.1, LOC103977652, LOC103998084, LOC103977651, LOC103977653) and translated *M. acuminata PR1* reference transcript sequences obtained from Banana Genome Hub database i.e., Ma09_g15840, Ma03_t08160.1, Ma03_t08150.1, Ma03_t08140.1 using MEGA X software (Kumar *et al.,* 2018). A total of 83 amino acid sequences with 169

positions were aligned and subjected to sequence model test function available in the software. The evolution model with the lowest Bayesian Information Criterion (BIC) score was chosen. The evolutionary history was inferred using the Maximum Likelihood method and Jones-Taylor-Thornton (JTT) matrix-based model (Jones *et al.,* 1992) with 1000 bootstrap replicates. A discrete Gamma distribution was used to model evolutionary rate differences among sites [5 categories (+G, parameter = 0.9230)]. Two clonal variants, each representing Berangan and Grand Naine (ITC 1256) cultivars that clustered together with ITC1587_Bchr9_P26466_MUSBA reference sequence group were chosen for subcellular localisation study and protein functional analyses.

3.11 *Agrobacterium tumefaciens*-based infiltration study using inner epidermal onion cells

This infiltration study was conducted to identify the localisation of the isolated MaPR10 protein variants. The subcellular localisation of the deduced amino acid of MaPR10-BeB5 and MaPR10-GNA5 variants were initially predicted using Plant-mPLoc online software (http://www.csbio.sjtu.edu.cn/bioinf/plant-multi/). Subsequently, *in vivo* subcellular localisation experiment was then conducted as described in Sun *et al.* (2007) using the inner epidermal layer of onion (*Allium cepa)* cells to verify the computational prediction.

3.11.1 Propagation and cloning of *MaPR10-BeB5* and MaPR10-*GNA5* transcript fragments into pCAMBIA1304 expression vector

To carry out subcellular localisation study on the chosen protein variants, *MaPR10-BeB5* and *MaPR10-GNA5* transcript fragments were cloned into pCAMBIA1304 expression vector using directional cloning method (Green & Sambrook, 2020) where both plasmid and DNA fragment were cleaved with *Nco*I restriction enzyme and then propagated in *E. coli* strain JM109 cells.

3.11.2 Amplification and purification of *MaPR10-BeB5* and *MaPR10-GNA5* transcript fragments

MaPR10-BeB5 and *MaPR10-GNA5* transcript fragments were isolated from the plasmid stock in Section 3.10.1 using the gene-specific primer pair designed in Section 3.9.1. In this experiment, PCR was conducted using High-fidelity Kod-Neo-Plus polymerase (Toyobo, Japan). PCR was performed in a 50 µL reaction mixture containing 1X KOD-Plus-Neo buffer (Toyobo, Japan), 0.2 mM of each dNTP, 1.5 mM $MgSO_4$, 0.4 µM of each primer, 1 U Kod-Plus-Neo Polymerase (Toyobo, Japan), 50 ng DNA sample, and sdH_2O. A negative control reaction was included by replacing DNA template with sdH_2O. PCR was conducted in a thermocycler (peqSTAR, USA) with an amplification profile consisting of an initial denaturation step at 94 ℃ for 3 min, 35 cycles of a denaturation step at 94 ℃ for 1 min, an annealing step at 56.3 ℃ for 1 min, an elongation step at 72 ℃ for 44 sec, and a final extension step at 72 ℃ for 5 min. The PCR product was subjected to agarose gel electrophoresis as described in Section 3.7.1 and the amplicon was subjected for gel-purification procedure as described in Section 3.8.3.

3.11.3 Purification of the *Nco*I-digested *MaPR10* transcript fragments and *Nco*I-digested pCAMBIA1304 vector

*Nco*I restriction enzyme was used to produce sticky ends on both *MaPR10* transcript fragments and pCAMBIA1304 vector. *Nco*I enzyme recognised and cleaved *Nco*I sequence sites (CCATG) present in the transcript, producing a ~480 bp long fragment with sticky ends. Similarly, the circular vector was cleaved upon recognition of the digestion sites, producing a linearised vector. The RE digestion reaction was conducted in a final volume of 20 µL containing 10X Buffer (Promega, USA), 10 µg/µL bovine serum albumin (Promega, USA), 1 U *Nco*I restriction enzyme (Promega, USA), 1 µg of DNA or vector sample, and sdH_2O, in a sterile 0.5 mL microcentrifuge tube. For the negative control, *Nco*I enzyme was substituted with sdH_2O. The reaction tube was

incubated at 37 ℃ for 3 h. The reaction was then inactivated at 65°C for 10 min. The product was then subjected to agarose gel electrophoresis as described in Section 3.7.1. Then, the RE digestion product was subjected for gel-purification procedure using QIAquick Gel Extraction kit (Qiagen, Germany) as described in Section 3.8.3.

3.11.4 Directional cloning

Directional cloning is an efficient approach to insert a clonal fragment into a vector in a specific orientation assisted by the restriction enzyme. In this study, *MaPR10-BeB5* and *MaPR10-GNA5* transcript fragments were cleaved with *Nco*I and cloned into the pCAMBIA1304 expression vector (Appendix A-1). The plasmid was then propagated in *E. coli* strain JM109 cells.

3.11.4.1 DNA ligation

The digested *MaPR10-BeB5* and *MaPR10-GNA5* transcript fragments were each ligated into the linearised pCAMBIA1304 vector using T4 DNA ligase (NEB, United Kingdom) as described in the manufacturer's protocol to produce pCAMBIA1304::CaMV35S::*MaPR10-BeB5*::*mgfp5*::*GUS*::6xHis and pCAMBIA1304::CaMV35S::*MaPR10-GNA5*::*mgfp5*::*GUS*::6xHis expression cassettes (Figure 3.3). The ligation reaction was carried out in a 0.5 mL microcentrifuge tube containing 2 µL of 10X T4 DNA ligase buffer, 300 ng of vector, 1 µL T4 DNA ligase (1 cohesive end unit/µL), 35 ng purified DNA sample and sdH_20 in a final volume of 20 µL. Note that the amount of purified DNA sample for ligation was estimated based on NEB ligase online calculator software (https://nebiocalculator.neb.com/#!/ligation) using the ratio of DNA inserts to vector pre-set at 3:1. The mixture was thoroughly mixed by gentle pipetting and incubated at 4 ℃ for 16 h prior transformation.

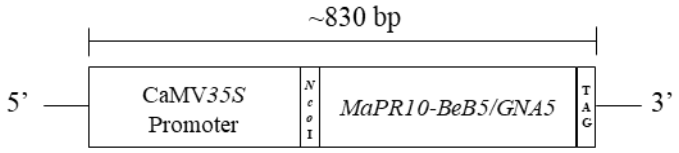

Figure 3.3: pCAMBIA1304 expression cassettes harbouring *MaPR10-BeB5/GNA5* transcripts. The expected amplification size of pCAMBIA1304::CaMV35S::*MaPR10-BeB5/GNA5*::*mgfp5*::*GUS*::6xHis expression cassettes was ~830 bp.

3.11.4.2 Transformation and screening of bacterial colonies via colony PCR

To propagate the clones in bacterial cell, approximately 2 µL of the ligation product was transformed into *E. coli* strain JM109 cells as described in Section 3.8.5.2. Note that as opposed that described in Section 3.8.5.2, the agar plate used for this transformation procedure contained 30.5 g/L LB agar powder with 50 µg/mL Kanamycin instead of Ampicillin and only white colonies were expected to be observed on the plates. The white colonies were picked using a sterile toothpick and transferred into a gridded 6 × 6 LB agar mini library and the remainder was dipped into a sterile 0.5 mL microcentrifuge tube containing 30 µL of sdH_2O. The tube was heated at 99 °C for 10 min in a heat block to lyse the bacterial cells and the lysates were subjected to colony PCR. PCR was conducted as described in Section 3.8.5.4, except for the universal CaMV35S promoter forward primer (5' CTATCCTTCGCAAGACCCTTC 3') and the s*MaPR1-like*(R) primer (Section 3.9.1) were used instead to detect the presence of the cloned fragment. The amplification profile used for the PCR was described in Section 3.8.2 with the annealing temperature adjusted to 58 °C. The colony PCR product was subjected to agarose gel electrophoresis as described in Section 3.7.1 to confirm the presence of inserts in the plasmid. Colonies showing the presence of the cloned fragment were subjected to plasmid isolation.

3.11.5 Plasmid isolation and restriction enzyme digestion assay

Plasmid isolation was conducted on the bacterial colonies containing positive transformants as described in Section 3.8.6. Subsequently, to further confirm the presence

of the cloned fragment in the isolated plasmids, the plasmid DNA was digested with *Nco*I restriction enzyme. *Nco*I enzyme recognises and cut CCATG restriction sites (Appendix A-1) that were present at the arms of the vector, releasing the ~480 bp cloned fragment from its respective plasmid. The RE digestion product was then subjected to agarose gel electrophoresis as described in Section 3.7.1 and the plasmids with the correct insert size were subjected to cycle sequencing as described in Section 3.8.8.

3.11.6 Sequence analysis on the cloned fragment

Chromatogram analysis of each cloned fragment was carried out using Chromas version 4.0 (Technelysium Pty. Ltd.) as described in Section 3.8.9. A full sequence of the cloned fragment was obtained by concatenating the forward and reverse sequences of a sample. For the ease of analysis, each sequence was edited to begin with the universal CaMV35S promoter forward primer sequence and end with the s*MaPR1-like*(R) primer sequence (Section 3.9.1). From the sequence analysis, plasmids containing only cloned fragments that were verified to share 100 % homology with *MaPR10-BeB5* and *MaPR10-GNA5* sequences were chosen for transformation into *A. tumefaciens* strain LB4404.

3.11.7 Propagation of pCAMBIA1304::CaMV35S::*MaPR10-BeB5/GNA5*:: *mgfp5*::*GUS*::6xHis vector into *A. tumefaciens* strain LB4404

Plasmids with the cloned fragment that were verified to share 100 % homology with *MaPR10-BeB5* and *MaPR10-GNA5* sequences were transformed into LB4404 strain *A. tumefaciens* cells as described in Wise *et al.* (2006). Competent *A. tumefaciens* strain LB4404 cells were prepared (similar to the *E. coli* competent cells) as described in Section 3.8.4. Briefly, 2 µL of the isolated plasmid were pipetted into 1.5 mL microcentrifuge tube containing 100 µL competent *A. tumefaciens* strain LB4404 cells. The mixture was then gently mixed by flicking and placed in ice for 30 min. Later, the competent cells were freeze-thawed by placing the tube in liquid nitrogen for 45 sec and

immediately placed in 37 ℃ in an incubator (Memmert, Germany) for 4 min. Then, 950 µL of LB broth medium (10 g/L tryptone, 5 g/L yeast extract, and 10 g/L NaCl) was added to the sample and the mixture was incubated for 4 h at 28 ℃ in an incubator (Memmert, Germany). Subsequently, the transformation culture was centrifuged at 3, 300 × *g* for 2 min and 700 µL of the resulting supernatant was discarded. The pelleted cells were then mixed with the remaining supernatant in the tube by gentle pipetting. Lastly, 150 µL of the transformation culture was plated on an LB agar plate (30.5 g/L LB agar powder, and 50 µg/mL Kanamycin) and incubated at 28°C for 2 days. Transformants were screened for colonies with Kanamycin resistance. An LB agar mini library of 6 × 6 grid was prepared, and a single white colony was transferred onto it using a sterile toothpick with the remainder dipped into a sterile 0.5 mL microcentrifuge tube containing 30 µL of sdH_2O. The tube was then heated at 99°C for 10 min in a heat block to lyse the bacterial cells. Colony PCR was conducted as described in Section 3.8.5.4. The PCR product was then subjected to agarose gel electrophoresis as described in Section 3.7.1 to confirm the presence of pCAMBIA1304::CaMV35S::*MaPR10-BeB5*::*mgfp5*::*GUS*::6xHis or pCAMBIA1304::CaMV35S::*MaPR10-GNA5*::*mgfp5*::*GUS*::6xHis vector in each of the isolated *A. tumefaciens* strain LB4404 colonies.

3.11.8 β-glucuronidase (GUS) histochemical assay on transformed *A. tumefaciens* cells

To confirm the expression of pCAMBIA1304::CaMV35S::*MaPR10-BeB5*::*mgfp5*::*GUS*::6xHis and pCAMBIA1304::CaMV35S::*MaPR10-GNA5*::*mgfp5*::*GUS*::6xHis cassettes in the transformed *A. tumefaciens* cells, GUS histochemical assay was performed as described in Nelson-Vasilchik *et al.* (2016). The bacterial cells were first cultured in 10 mL LB Broth [10 g/L tryptone, 5 g/L yeast extract, 10 g/L NaCl, and 50 mg/mL Kanamycin] for two days. Subsequently, 1 mL of the culture

was pipetted into a sterile 1.5 mL microcentrifuge tube and centrifuged at 3, 300 × *g* for 2 min. The resulting supernatant was then discarded, leaving the pelleted cells in the tube. Subsequently, the bacterial cells were incubated with 1 mL GUS solution [0.1 M $NaPO_4$, 10 mM NaEDTA (pH 8.0), 0.1 % Triton X-100, 1 mM $K_3Fe(CN)_6$, and 2 mM X-glucuronide] at 37 ℃ for 16 h. Since *GUS* gene expressing β-Glucuronidase (GUS) enzyme hydrolyses X-Glucuronide substrate at 37 ℃, the hydrolysation product i.e., glucuronide was dimerised in the presence of oxygen to form an insoluble chloro-bromo-indigo precipitant. This chemical reaction resulted in the production of blue bacterial cells, visible to the naked eye, indicating successful expression of the cloned gene.

3.11.9 *In vivo* subcellular localisation of MaPR10-BeB5 and MaPR10-GNA5 protein variants in inner epidermal onion cells

In vivo subcellular localisation experiment was conducted as described in Sun *et al.* (2007) using the inner epidermal layer of onion cell. *A. tumefaciens* cells were transformed with either one of the three constructs: (i) pCAMBIA1304::CaMV35S::*MaPR10-BeB5*::*mgfp5*::*GUS*::6xHis, (ii) pCAMBIA1304::CaMV35S::*MaPR10-GNA5*::*mgfp5*::*GUS*::6xHis, and (iii) pCAMBIA1304::CaMV35S::*mgfp5*::*GUS*::6xHis that served as a positive control to indicate successful infiltration procedure. An untransformed onion cell was prepared for this assay as a negative control sample. The bacterial cells were incubated in a 1.5 mL microcentrifuge tube at 28 ℃ for 24 h until the OD_{600} reading reached 1.0. Next, the cells were centrifuged at 4, 000 × *g* for 10 min and the resulting supernatant was discarded. The pellet was then resuspended with 6 mL of a freshly prepared infiltration medium (5 % sucrose, 100 mg/L acetosyringone, and 0.02 % silwet-77). A healthy fresh onion inner epidermal cell (1 – 1.5 cm × 1cm) was immersed in the infiltration medium for 12 h at 28 ℃ with 80 rpm shaking in a petri dish covered with a piece of aluminium foil. Then, the onion cells were transferred to a petri dish containing a half-MS medium [2.2 g/L MS

powder, 20 g/L sucrose, and 1 % gelrite (pH 5.7)] in a laminar flow cabinet and co-cultivated at 28 ℃ (120 rpm shaking) with *A. tumefaciens* cells for 2 days. After 48 h, the onion cells were observed using an inverted microscope (Olympus, USA) equipped with 100 W mercury lamp. The localisation of the recombinant protein in onion cells was indicated by the detection of green fluorescent protein (GFP) expressed by the constructs. Images were taken under the dark and bright fields to capture GFP signals and display cell morphology, respectively.

3.12 Overexpression of *MaPR10-BeB5* and *MaPR10-GNA5* transcripts in *Escherichia coli* strain BL21 cells

To carry out functional analyses on the chosen protein variants, *MaPR10-BeB5* and *MaPR10-GNA5* transcript fragments were cloned into pET30a(+) expression vector (Appendix A-2) using directional cloning method (Green & Sambrook, 2020) where both plasmid and DNA fragment were cleaved with the restriction enzyme *Nco*I and then propagated in *E. coli* strain JM109 cells.

3.12.1 Amplification and fragment purification of *Nco*I-digested *MaPR10-BeB5* and *MaPR10-GNA5* transcript fragments and pET30a(+) expression vector

MaPR10-BeB5 and MaPR10-GNA5 transcript fragments were PCR-amplified from the stored bacterial colonies using High-fidelity Kod-Neo-Plus Polymerase (Toyobo, Japan) as stated in Section 3.11.2. The PCR product obtained was then purified as described in Section 3.8.3. Next, the transcript fragments and pET30a(+) vector (Novagen, USA) were digested with *Nco*I and gel-purified as described in Section 3.11.3 to produce a ~480 bp long *MaPR10* transcript fragments with *Nco*I sticky ends and a linearised pET30a(+) vector.

3.12.2 DNA ligation, transformation, and bacterial screening of transformed *E. coli* strain JM109 cells via colony PCR

The purified *Nco*I-digested *MaPR10* transcript fragments were ligated into the linearised pET30a(+) vector using T4 DNA ligase (NEB, United Kingdom) to produce the expression cassettes pET30a(+)::T7promoter::6xHis::*MaPR10-BeB5* and pET30a(+)::T7promoter::6xHis::*MaPR10-GNA5* (Figure 3.4). The ligation reaction was carried out as described in Section 3.11.4.1, with the amount of purified DNA adjusted to 33 ng for the reaction. The screening of transformed *E. coli* strain JM109 colonies via colony PCR was carried out as described in Section 3.11.4.2, using universal T7 promoter primer pair to detect the presence of cloned fragment with the annealing temperature for PCR adjusted to 53 ℃. The colony PCR product was subjected to agarose gel electrophoresis as described in Section 3.7.1 to confirm the presence of insert in the plasmid. Plasmid isolation was conducted on the bacterial colonies showing the presence of the cloned fragment and subsequently, the presence of the cloned fragment in the isolated plasmid was verified by subjecting the plasmids to restriction enzyme assay as described in Section 3.11.5. Finally, the plasmids with the correct insert size were subjected for cycle sequencing as described in Section 3.8.8. Sequence analysis on the cloned fragments was carried out as described in Section 3.11.6 but using a universal T7 promoter primer pair (T7 forward primer: 5' TAATACGACTCACTATAGGG 3' and T7 reverse primer: GCTAGTTATTGCTCAGCGG) instead. Cloned fragments verified to share 100 % homology with that of *MaPR10-BeB5* and *MaPR10-GNA5* sequences were chosen for transformation into *E. coli* strain BL21(E3).

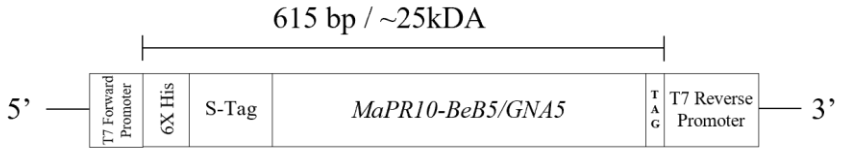

Figure 3.4: pET30a(+) expression cassette harbouring *MaPR10-BeB5/GNA5* transcript. pET30a(+)::T7promoter::6xHis::*MaPR10-BeB5*/*GNA5* expression cassettes with an expected amplicon size of 615 bp and an expected protein size of ~25 kDa.

3.12.3 Propagation of pET30a(+)::T7promoter::6xHis::*MaPR10*-BeB5*/GNA5* vector in *Escherichia coli* strain BL21(E3) cells

Isolated plasmids with cloned fragments verified to have 100 % homology with *MaPR10-BeB5* and *MaPR10-GNA5* transcript sequences were transformed into *E. coli* strain BL21(E3) cells following the manufacturer's protocol (Novagen, USA). First, *E. coli* strain BL21(E3) competent cells were prepared as described in Section 3.8.4. Transformation and bacterial screening via colony PCR were carried out as described in Section 3.12.2, using the universal T7 promoter primer pair for the detection of the presence of cloned fragment and the annealing temperature for the PCR reaction was adjusted to 53 ℃. Finally, the PCR product was subjected to agarose gel electrophoresis as described in Section 3.7.1 to confirm the presence of pET30a(+)::T7promoter::6xHis::*MaPR10-BeB5* & *-GNA5* vectors in *E. coli* strain BL21(E3) cells. Once verified, one bacterial colony from each variant was chosen for protein isolation.

3.12.4 Induction of heterologous gene expression in *E. coli* strain BL21(E3) cells

Heterologous gene expression in *E. coli* strain BL21(E3) cells and crude protein isolation were carried out as described in the manufacturer's protocol (Novagen, USA). Bacterial cells containing the cloned fragments that were verified to share 100 % homology with *MaPR10-BeB5* and *MaPR10-GNA5* transcripts were chosen from Section 3.12.3. Briefly, the chosen bacterial cells were incubated in 10 mL LB broth (10 g/L tryptone, 5 g/L yeast extract, 10 g/L NaCl, and 50 mg/mL Kanamycin) at 37 ℃ for 16 h with 220 rpm shaking. Then, 3 mL of the culture was added into a sterile 1 L conical flask containing 250 mL LB broth. The flask was then incubated at 37 ℃ for 2 h with 220 rpm shaking until the OD_{600} value reached 1.0. Subsequently, the expression of *MaPR10-BeB5* and *MaPR10-GNA5* heterologous genes were induced by adding 0.1 mM Isopropyl ß-D-1-thiogalactopyranoside (ITPG) and followed by an incubation step at 14 ℃ for 16

h in the incubator (N-Biotek, Korea). It is noteworthy that, uninduced cells were included as the negative control sample of this experiment. The sample was then subjected to a centrifugation step at 3, 824 × *g*, 4 ℃ for 15 min to pellet the cells. The pellet was later freeze-thawed as described in Sambrook *et al.* (2006) by placing the pellet alternately in –80 ℃ for 10 min and 0 ℃ (in ice) for 20 min. This process was carried out three times and then the pellet was resuspended in 20 mM Tris-HCl (pH 8.0). Subsequently, the cell lysates were subjected to a centrifugation step at 17, 949 × *g*, 4 ℃ for 15 min to isolate both the soluble and insoluble proteins. The resulting supernatant (soluble proteins) and pellet (insoluble proteins) were stored in –80 ℃. Since PR10 proteins were described as ubiquitous and soluble (McBride *et al.,* 2019), only the soluble protein fraction was subjected to protein purification step using nickel His Gravitrap™ affinity column (GE Healthcare, USA).

3.12.5 Purification of MaPR10-BeB5 and MaPR10-GNA5 protein variants using nickel His Gravitrap™ affinity column

The expression cassettes, pET30a(+)::T7promoter::6xHis::*MaPR10-BeB5* and pET30a(+)::T7promoter::6xHis::*MaPR10-GNA5* (Figure 3.4) were designed to contain a 6xHis tag (six consecutive histidine residues, HHHHHH) at the upstream of the target gene so that the overexpressed protein could be purified using nickel His Gravitrap™ affinity column (GE Healthcare, USA) following the manufacturer's protocol. Briefly, the flow column with resin was firstly recharged with 10 mL of 50 mM EDTA (pH 7.4), and then with 10 mL of 5 mg/mL nickel chloride. The flow-through was then discarded. Later, the column was loaded with 10 mL phosphate buffer [20 mM Na_3PO_4 (pH 7.4) and 500 mM NaCl] to equilibrate the column and prevent it from drying, and the flow-through was discarded. Next, 4 mL of soluble protein sample was loaded into the column and the flow-through was collected. Later, the column was washed with 10 mL binding buffer [20 mM Na_3PO_4 (pH 7.4), 500 mM NaCl, and 20 mM imidazole] with the flow-through

collected. Finally, the purified protein was eluted in an elution buffer [20 mM NaOAc (pH 7.4), 500 mM NaCl, and 500 mM imidazole].

3.12.6 Precipitation of the purified MaPR10-BeB5 and MaPR10-GNA5 protein variants

The purified MaPR10-BeB5 and MaPR10-GNA5 protein variants were precipitated using chloroform-methanol-water method as described in Wessel and Flügge (1984). Firstly, 100 µL of the purified protein was added into four equal volume of 100 % methanol in a sterile 1.5 mL microcentrifuge tube. The mixture was vortexed for a short while. Then, an equal volume of chloroform was added to the mixture and the mixture was vortexed. The tube was centrifuged at 15, 000 × *g* for 2 min and the upper layer of the supernatant was discarded. The remaining lower layer of the supernatant was added with four equal volume of 100 % methanol and the sample was vortexed. The tube was centrifuged at 15, 000 × *g* for 2 min and the resulting supernatant was then discarded leaving only the pelleted proteins in the tube. The pellet was air-dried for 5 min at room temperature and dissolved in 0.1 M NaOAc (pH 5.0). Subsequently, the purified protein was quantified using Bradford assay, and subjected to SDS-PAGE and western blot analysis.

3.12.7 Bradford assay

Bradford assay was carried out to determine the concentration of crude proteins samples and the purified MaPR10-BeB5 and MaPR10-GNA5 protein variants isolated in this study using Coomassie Brilliant Blue G-250 (Coomassie G-250) dye (Bio Rad, USA) as described in the manufacturer's protocol. The change in Coomassie G-250 colour from red to blue upon binding to protein was measured spectroscopically. Since the amount of the blue anionic complex formed as a result of the formation of a complex after protein binding is proportional to the amount of protein in the sample, the quantity of protein in

the sample was estimated by measuring UV absorption at 595 nm wavelength using a NanoPhotometer®. Briefly, one part of Coomassie G-250 dye was diluted with four parts of ionised water and the diluted dye was then filtered with a piece of Whatman #1 filter paper. Subsequently, 1000 µL of dye were mixed with 50 µL of protein sample in a 1.5 mL cuvette. The UV absorbance value of the protein sample at 595 nm wavelength was recorded. A standard curve was generated (Appendix A-3) using serial dilutions of a standard protein i.e., bovine serum albumin (BSA) with a linear concentration range of 0, 0.1, 0.2, 0.3, 0.4, and 0.5 µg/µL, as suggested by the manufacturer.

3.12.8 SDS-PAGE and western blot analysis

3.12.8.1 Sodium dodecyl sulfate-polyacrylamide gel electrophoresis (SDS-PAGE)

The purified MaPR10-BeB5 and MaPR10-GNA5 protein variants were separated by SDS-PAGE (Bio-Rad, USA) as described in the manufacturer's protocol. The Mini-Protean 3 casting tray and glass plates were set up based on the manufacturer's protocol (Mini-Protean®3 System, Bio-Rad, USA). A 12.5 % resolving gel [1.5 M Tris-HCl (pH 8.8), 30 % acrylamide/ 0.8 % bis-acrylamide (Bio-Rad, USA), 10 % SDS, 10 % ammonium persulfate (APS), and 10 µL tetramethyl ethylenediamine (TEMED; AMRESCO, USA)] and 4.5 % stacking gel [0.5 M Tris-HCl (pH 6.8), 30 % acrylamide/ 0.8 % bis-acrylamide (Bio-Rad, USA), 10 % SDS, 10 % ammonium persulfate (APS), and 10 µL TEMED (AMRESCO, USA)] were prepared. The resolving gel was first prepared and pipetted into the stacked glass plates leaving a 1-cm gap from the edge of the glass. Next, 100 % butanol was pipetted into the glass plates, filling the gap to flatten the gel. The gel was left to solidify for approximately 45 min. The butanol was then removed using C-fold tissues and the stacking gel mixture was pipetted into the glass plates to fill up the gap left above the resolving gel. A ten-well comb was immediately placed at the top edge of the glass plates to produce wells in the gel. Again, the gel was left to solidify for ~45 min. Next, the glass plates were placed into the electrode assembly

and later placed inside an electrophoresis mini tank. The tank was filled with 1X electrophoresis buffer [25 mM Tris (pH 8.3), 192 mM glycine, and 0.1 % SDS]. The sample was mixed with 2X SDS-PAGE sample buffer [125 mM Tris-Cl (pH 6.8), 20 % glycerol, 4 % SDS, 0.05 % bromophenol blue, and 10 % β-mercaptoethanol] and incubated in a dry bath at 99 ℃ for 4 min. Next, the tube was centrifuged at 17, 949 × *g* for 5 min at room temperature, and 3 µg protein were loaded into the well. BLUltra Prestained Protein Ladder (Genedirex, UK) was used to estimate the molecular weight of the analysed protein. Electrophoresis was carried out at 180 V for 60 min at room temperature prior to Coomassie blue staining.

3.12.8.2 Coomassie blue staining

SDS-PAGE gel was subjected to Coomassie blue staining once electrophoresis ended as described in the manufacturers' manual (Bio-Rad, USA). Firstly, fixing solution (40 % methanol and 10 % acetic acid) was added into a container containing the electrophoresed SDS-PAGE gel for 30 min with 60 rpm shaking. The solution was then discarded, and the gel was stained with Coomassie blue solution [50 % (v/v) methanol, 0.05 % (v/v) Coomassie Brilliant Blue R250, and 10 % (v/v) acetic acid] for 1 h with 60 rpm shaking. The solution was discarded, and the gel was finally washed with a de-staining solution (20 % ethanol, and 7 % acetic acid) for 10 min or until protein bands were clearly observed. The developed gel was photographed.

3.12.8.3 Western blot assay

Western blot assay was carried out using Mini-Protean®3 system as described in the manufacturer's manual (Bio-Rad, USA). Firstly, the purified protein samples were electrophoresed with a pre-stained protein marker (BLUltra Prestained Protein Ladder, Genedirex, UK) in SDS-PAGE gel as described in Section 3.12.8.1. Subsequently, the gel was blotted onto a nitrocellulose membrane (Amersham Biosciences, USA). The

assembly of western blot apparatus was prepared as described in the manufacturer's manual (Mini-Protean®3 System, Bio-Rad). Briefly, the nitrocellulose membrane, sponges, and the filter papers (cut according to the gel size) were blotted in a transfer buffer (25 mM tris, 192 mM glycine, and 10 % methanol) at 4 ℃. Once completed, the gel was rinsed with distilled water; both the gel and the nitrocellulose membrane were then assembled into a sandwich clamp in the order of sponge-filter paper-gel-membrane-filter paper-sponge. The sandwich cassette was then placed in a mini gel tank (Mini-Protean®3 System, Bio Rad, USA) along with ice blocks and magnetic bar at the bottom. The tank was placed on a magnetic plate (BS Technology, India) and filled with the transfer buffer. Electrophoresis was carried out at 100 V for 60 min. Once electrophoresis completed, the membrane was transferred into an aluminium-covered container where it was soaked with a blocking buffer [5 % of skim milk (non-fat or low-fat) in 1X Tris-buffered Saline (TBS)] at 4 ℃, overnight. Next, the membrane was swirled in blocking buffer with 2 µg anti-His primary antibody (ID# ab188492; Abcam, USA) for 2 h at room temperature with 60 rpm shaking. Later, the membrane was rinsed with 1X TBS and washed three times with washing buffer (1X TBS with 0.1 % Tween-20) for 5 min. The membrane was then rinsed again with 1X TBS before being swirled in blocking buffer with 2 µg anti-mouse IgG-alkaline phosphatase, produced in goat secondary antibody (Cat. #SLBB9232, Sigma-Aldrich, USA) for 1 h at room temperature with 60 rpm shaking. Later, the membrane was rinsed with 1X TBS and washed three times with the washing buffer (1X TBS, and 0.1 % Tween-20) for 5 min. The membrane was then rinsed again with 1X TBS and incubated with Western Blue® stabilised substrate for alkaline phosphate (Promega, USA) in the dark at room temperature until protein band(s) observed. The development reaction was halted by adding sdH_2O to the membrane and the result obtained was photographed. Heterologous protein with its presence confirmed in the western blot assay was subjected to functional analyses.

3.13 Functional analyses of MaPR10-BeB5 and MaPR10-GNA5 protein variants

3.13.1 Ribonuclease activity assay

Ribonuclease activity assay was performed as described in Zhou *et al.* (2002) with a minor modification. Instead of yeast total RNA, this assay was conducted on *Arabidopsis thaliana* total RNA. This assay was conducted in a final volume of 0.5 mL RNase enzymatic reaction mixture which consists of 5 µg purified proteins (MaPR10-BeB5 or MaPR10-GNA5), 2 µg *A. thaliana* total RNA obtained from Section 3.5.3, and 50 mM NaOAc (pH 5.0) in a sterile 1.5 mL microcentrifuge tube. The mixture was incubated at 56 ℃ for 30 min and the enzymatic reaction was terminated by adding one volume of 4 M LiCl into the mixture prior to incubation at 4 ℃ for 3 h. Subsequently, the sample was centrifuged at 15, 294 × *g*, 4 ℃ for 5 min. The resultant supernatant was diluted twice and the UV absorbance value at A_{260} was recorded using a NanoPhotometer®. One unit (U) of enzyme activity was defined as an increase in absorption of 0.001A caused by the amount of protein after 30 min incubation. Triplicate of absorbance values were obtained for each treatment. The mean of absorbance values of a treated sample was normalised by subtracting the mean of absorbance value of a negative control reaction from the mean of absorbance of each sample. The mean of absorbance values for each treatment after normalisation will be the total RNAse activity for 5 µg purified proteins. Specific activity of an enzyme is defined by the number of enzyme units per reaction volume, further divided by the concentration of the protein. Therefore, in this study, the total RNAse activity was divided by 5 µg to calculate the specific RNAse activity of each 1 µg of MaPR10 protein variants. Nucleic acid degradation was further confirmed qualitatively by subjecting the treated and control samples to agarose gel electrophoresis as described in Section 3.7.2.

3.13.2 Laminarin-dinitrosalicylic acid assay of purified MaPR10-BeB5 and MaPR10-GNA5 protein variants

Laminarin-dinitrosalicylic acid assay was conducted on purified MaPR10-BeB5 and MaPR10-GNA5 protein variants as described in Zhang *et al.* (2019) with minor modifications, i.e., the potassium acetate buffer was replaced with sodium acetate buffer. Laminarin was used as a substrate because it will be converted into reducing sugar upon interaction with β-1,3-glucanase. If either of the purified MaPR10 protein variants was to function as β-1,3-glucanase, it will convert laminarin into reducing sugar. The presence of reducing sugar can then be colorimetrically observed using dinitrosalicylic (DNS) reagent (3,5-dinitrosalicyclic). A standard curve of the assay was plotted as described in Bailey (1992) using glucose (Sigma, Germany) as the reference reducing sugar. Briefly, a reducing sugar stock solution was prepared at the concentration of 0.01 M by dissolving the reducing sugar in 0.1 M NaOAc (pH 5.0). Subsequently, serial dilutions of the glucose stock solution were prepared at 5 mM, 2.5 mM, and 1.25 mM concentrations. UV absorbance value for each glucose concentration was measured at 540 nm to prepare the standard curve. Each protein variant namely MaPR10-BeB5 and MaPR10-GNA5 was assayed at two concentrations i.e., 3.5 µg and 10 µg. The assay was conducted by incubating each protein variant with 10 mg/ml laminarin (Sigma, Germany) and 0.1 M NaOAc (pH 5.0) in a sterile 1.5 mL centrifuge tube at 50 ℃ for 15 min. Later, the mixture was transferred into a sterile test tube. Subsequently, 3 mL of DNS (Sigma, Germany) was added into the reaction and the tube was boiled for 10 min. The amount of reducing sugar released was determined as described in Bailey (1992). A total of 200 µL of each reaction was transferred into a 96-well plate and photographed. The conversion of DNS reagent colour from yellow to reddish-brown indicated the presence of reducing sugar. Next, 1 mL of reaction sample was boiled at 99 ℃ for 10 min and transferred into a 1.5

mL cuvette. The presence of reducing sugar in the reaction was measured by obtaining the absorbance value at 540 nm wavelength using a NanoPhotometer®.

3.14 Antifungal susceptibility assay of MaPR10-BeB5 and MaPR10-GNA5 protein variants against *Aspergillus fumigatus*, *Aspergillus niger* and *Fusarium oxysporum* f. sp. *cubense*: Tropical Race 4

3.14.1 Fungal culture growth

Three fungal cultures were used in this study. *A. fumigatus* and *A. niger* cultures were obtained from Programme of Microbiology, Institute of Biological Sciences, Universiti Malaya, courtesy of Dr. Khanom Simarani, while the *F. oxysporum* f. sp. *cubense*: TR4 (henceforth will be referred to as *F. oxysporum*) culture was obtained from the same programme courtesy of Prof. Dr. Rofina Yasmin Othman. The fungal cultures were provided in potato-dextrose agar (PDA) plates. To subculture each fungal sample, a sterile inoculation loop was used to scrub the surface of the agar plate to collect fungal mycelia. The mycelia were then transferred onto a freshly prepared PDA plate. Then, the culture was incubated at 28 °C for 7 days and subjected to morphological- and molecular-based identification procedures.

3.14.2 Morphological-based identification of *A. fumigatus*, *A. niger* and *F. oxysporum*

Morphological-based identification procedure was performed on *Aspergillus* spp., and *F. oxysporum* as described in Nithiyaa *et al.* (2012), and Leslie *&* Summerell (2008), respectively. After seven days of incubation, the culture was placed on a black surface to observe the macroscopic characteristics of the colonies i.e., colony colour and hyphae surface. Later, a sterile inoculation loop was used to scrub the surface of the PDA plate to collect and transfer fungal mycelia to a microscope slide. Next, a single drop of 100 % lactophenol blue solution (Sigma-Aldrich, Germany) was added onto the mycelia and the

sample was immediately covered with a cover slip. The microscopic characteristics of the fungus i.e., hyphae structure and shape of spores were observed using a compound microscope (Leica Microsystems GmbH, Germany) at 10X and 40X magnification levels.

3.14.3 Molecular-based identification of *A. fumigatus*, *A. niger* and *F. oxysporum*

Molecular-based identification for the two *Aspergillus* spp. and *F. oxysporum* was carried out to further confirm the morphological-based characterisation result.

3.14.3.1 DNA isolation of A. fumigatus, A. niger and F. oxysporum

DNA isolation procedure was carried out as described in González-Mendoza *et al.* (2010) from the three fungal species studied in an aseptic condition. Fungal DNA was isolated from seven-day-old fungal culture on PDA. Mycelia were collected by adding sterile distilled water containing 0.01 % Tween 80 to the surface of the culture and gently scrubbing it with a sterile spatula. The mycelial suspension was then transferred into a sterile 1.5 mL microcentrifuge tube and centrifuged at 3, 000 × *g*, 4 °C for 5 min. The resulting supernatant was then discarded and the pellet containing approximately 100 mg mycelia was snapped-frozen in liquid nitrogen for a few seconds. Subsequently, 200 µL extraction buffer [1 M Tris-HCl (pH 8.0), 3 % SDS, 0.5 mM EDTA, and 1 M NaCl] was added into the tube containing the pelleted mycelia and vigorously vortexed for 15 sec. Then, 200 µL phenol:chloroform solution (1:1) were added to the tube and vigorously vortexed for 15 sec before being incubated for 5 min at 65 °C. Subsequently, the tube was centrifuged at 10, 000 × *g*, 4 °C for 4 min. The upper layer of the resulting supernatant was transferred into a fresh sterile 1.5 mL microcentrifuge tube and an equal volume of ice-cold isopropanol was added into the tube. The mixture was thoroughly mixed by gentle pipetting and incubated for 20 min at –20 °C. The tube was centrifuged at 10, 000 × *g* for 10 min at room temperature. The resulting supernatant was then discarded, and

the pellet was washed with 1 mL 75 % ethanol. The tube was centrifuged at 10, 000 × *g*, 4 ℃ for 5 min and the resulting supernatant discarded. The pellet was air-dried at room temperature and dissolved in 30 µL sdH_2O. DNA sample was stored at –20 ℃ till further use.

3.14.3.2 PCR amplification of the internal transcribed spacer 1 (ITS1)-*5.8S* rRNA fragment of *A. fumigatus* and *A. niger,* and *28S*-intergenic spacer (IGS)-*18S* ribosomal RNA fragment of *F. oxysporum*

Internal transcribed spacer (ITS) region 1-*5.8S* gene of ribosomal DNA (rDNA) fragment was isolated from *A. fumigatus* and *A. niger* as described in Norlia *et al.* (2019) using ITS(F) 5' TCC GTA GGT GAA CCT GCG G 3' and *5.8S*(R) 5' TCC GCT TAT TGA TAT GC 3' primer pair. On the other hand, *Foc*TR4(F) 5' CAC GTT TAA GGT GCC ATG AGA G 3' and *Foc*TR4(R) 5' GCC AGG ACT GCC TCG TGA 3' primer pair published in Dita *et al.* (2010) was used to isolate the *28S*- intergenic spacer (IGS)-*18S* ribosomal DNA fragment from *F. oxysporum*. PCR was carried out as described in Section 3.11.4 using the designated primer pair for each fungal species. The PCR amplification profile used was similar to that of described in Section 3.8.2 but the annealing time for *Aspergillus* spp. specific primer pair was adjusted to 55 ℃ and 60 ℃ for *F. oxysporum*. The PCR products obtained were subjected to agarose gel electrophoresis as described in Section 3.7.1. Subsequently, the PCR products were gel-purified as described in Section 3.8.3 and subjected to cycle sequencing as described in Section 3.8.8.

3.14.3.3 Sequence analyses of the isolated gene fragments from *A. fumigatus*, *A. niger* and *F. oxysporum*

Chromatogram analysis of fragment sequence was carried out using Chromas version 4.0 (Technelysium Pty. Ltd.) as described in Section 3.8.9. A fragment sequence was

obtained by concatenating the sequences from forward and reverse sequencing reactions. For the ease of analysis, the ITS1-*5.8S* DNA fragment isolated from *Aspergillus* spp. was edited to begin with the ITS1(F) primer sequence and ended with *5.8S*(R) primer sequence. Similarly, for *28S*- IGS-*18S* DNA fragments isolated from *F. oxysporum* was edited to begin with the *Foc*TR4(F) primer sequence and ended with *Foc*TR4(R) primer sequence. All three fungal sequences were subjected to BLASTn analysis in the GenBank.

3.14.4 Well-diffusion method for antifungal susceptibility assay of MaPR10-BeB5 and MaPR10-GNA5 protein variants against *A. fumigatus, A.* niger and *F. oxysporum*

Antifungal susceptibility assay of *A. fumigatus*, *A. niger* and *F. oxysporum* towards MaPR10-BeB5 and MaPR10-GNA5 protein variants was conducted as described in Rodriguez-Tudela *et al.* (2008) using well-diffusion method. A sterile inoculation loop was used to scrape the surface of the agar plate to collect fungal mycelia. The mycelia were then transferred to a freshly prepared PDA plate and subjected to a seven-day incubation period in the dark at 28 ℃. Subsequently, a fungal spore suspension was prepared by pouring 7 mL sterile water containing 0.01 % Tween 80 on a fungal-sporulating plate. Then, the mycelia and spores formed on the surface of the agar were scraped using a sterile spatula forming a mycelia-spore mixed solution in the plate. Next, the solution was filtered with a sterile mesh cloth to remove the mycelia, leaving only the spore suspension that was later collected in a 15 mL falcon tube. Then, one millilitre of the spore suspension was pipetted onto a haemocytometer and observed under a compound microscope (Olympus, USA) at 40X magnification level to obtain the viable fungal spore count. The spore suspension was added with 100 % glycerol under sterile condition and subsequently stored at –20 ℃ till further use. To carry out the well-diffusion assay, the concentration of the fungal spore suspension was adjusted to 2 x 10^5

CFU/mL. The spore was inoculated on a PDA plate by swabbing the suspension using a sterile cotton. The plate was left to dry for approximately 4 min in an aseptic condition. An autoclaved straw was used to prepare the well in the PDA plate and the well was later filled with 1 mg/mL of each MaPR10 protein variant as a treatment. A no treatment plate was prepared as a positive control reaction to the experiment. The plates were incubated for 4 days at 28 ℃ and observed for the formation of a clear halo region surrounding the well. This experiment was conducted in triplicates, where 1 mg/ml purified protein were filled into each of the three wells made in each PDA plate treated with fungi. On the other hand, the media was only swapped with the spore suspension for the positive control sample. A halo region was defined as the region/zone surrounding the well exhibiting the inhibited growth of the fungus due to the presence of the protein. The diameter of the halo region was measured using a ruler and subjected to statistical analysis. Results observed on plates were photographed. Note that the whole experiment was conducted in triplicates in a sterile condition, in a laminar flow cabinet.

3.14.5 Statistical analysis

Statistical analysis was performed on the quantitative results obtained from the antifungal susceptibility test of MaPR10-BeB5 and MaPR10-GNA5 protein variants against *A. fumigatus* using STATISTICA 13.0 (TIBCO Software Inc, 2018). The results were expressed as mean ± standard deviation (SD). A graph of zone of inhibition on PDA (cm) against the protein variants was plotted. The standard error bar was calculated based on the least squares mean method. One-way analysis of variance (ANOVA) and significant difference (Tukey) post-hoc test were used to determine the level of significance with $p < 0.05$ was defined as significant and $p < 0.01$ was defined as highly significant.

CHAPTER 4: RESULTS

4.1 Isolation of putative *Musa acuminata Pathogenesis-related 1-like* gene

4.1.1 Data mining and primer design for the isolation of *MaPR1-like* gene from Berangan and Grand Naine (ITC 1256) cultivars

From the tBLASTn analysis conducted in the GenBank and Banana Genome Hub databases (Appendix B-1) using ITC1587_Bchr9_P26466_MUSBA peptide sequence (VVPEIVVSGAVLEGDGSVGSVR), two *Pathogenesis-related 1* gene sequences from the GenBank (Accession numbers: JK271128.1, and XM_009419475.2) showed 100% similarity with the query sequence, with an E-value of 0.003. On the other hand, similar analysis conducted in Banana Genome Hub hit four *Pathogenesis-related 1* gene sequences (Accession numbers: Ma03_t08140, Ma03_t0815, Ma03_t08160, and Ma03_t15840) showing 100% similarity with the query sequence, with an E-value ranging between 0.001 to 8 x 10^{-05}.

An alignment of the deduced amino acid sequence of the six reference sequences (Appendix B-2) verified that all sequences shared a conserved PR1-like motif VVPEIVVSGAVLEGDGSVGSVR that was detected in a proteomics study of banana-*M. incognita* interaction reported by Al-Idrus *et al*. (2017). However, a degenerate primer pair needed to be designed due to the high heterogeneity level observed at both C- and N-termini of the aligned transcript sequences (Appendix B-3). The designed primer pair denoted as *MaPR1-like*_F: 5' ATGGCTTCYGGWTCTTGGAC 3' and *MaPR1-like*_R: 5' CTACRSRTAGGCDKMWGGRTKGGC 3' was subjected to a PCR primer stats analysis using Sequence Manipulation Suite software (Stothard, 2000). Primer stats analysis revealed that both forward (20-mer) and reverse (24-mer) primers met all the requirements listed in the PCR suitability test except for the melting temperature (T_m) in which the values are higher than 58 °C for both primers (Figure 4.1).

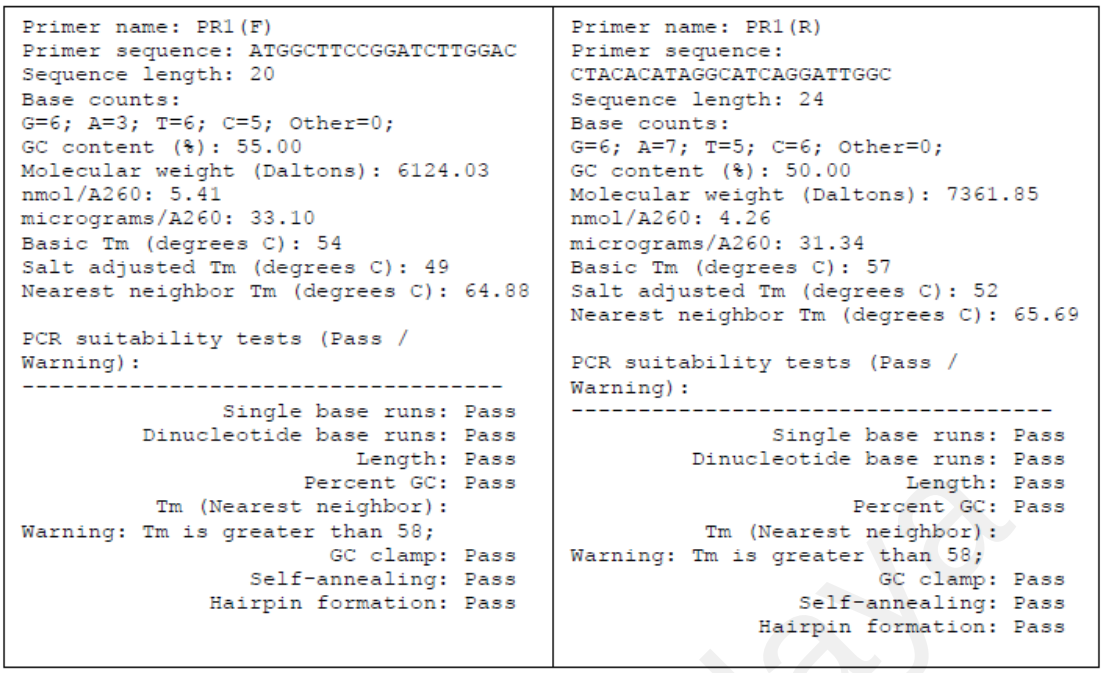

```
Primer name: PR1(F)
Primer sequence: ATGGCTTCCGGATCTTGGAC
Sequence length: 20
Base counts:
G=6; A=3; T=6; C=5; Other=0;
GC content (%): 55.00
Molecular weight (Daltons): 6124.03
nmol/A260: 5.41
micrograms/A260: 33.10
Basic Tm (degrees C): 54
Salt adjusted Tm (degrees C): 49
Nearest neighbor Tm (degrees C): 64.88

PCR suitability tests (Pass /
Warning):
-----------------------------------
               Single base runs: Pass
         Dinucleotide base runs: Pass
                        Length: Pass
                    Percent GC: Pass
          Tm (Nearest neighbor):
Warning: Tm is greater than 58;
                       GC clamp: Pass
                  Self-annealing: Pass
              Hairpin formation: Pass
```

```
Primer name: PR1(R)
Primer sequence:
CTACACATAGGCATCAGGATTGGC
Sequence length: 24
Base counts:
G=6; A=7; T=5; C=6; Other=0;
GC content (%): 50.00
Molecular weight (Daltons): 7361.85
nmol/A260: 4.26
micrograms/A260: 31.34
Basic Tm (degrees C): 57
Salt adjusted Tm (degrees C): 52
Nearest neighbor Tm (degrees C): 65.69

PCR suitability tests (Pass /
Warning):
-----------------------------------
               Single base runs: Pass
         Dinucleotide base runs: Pass
                        Length: Pass
                    Percent GC: Pass
          Tm (Nearest neighbor):
Warning: Tm is greater than 58;
                       GC clamp: Pass
                  Self-annealing: Pass
              Hairpin formation: Pass
```

(a) (b)

Figure 4.1: PCR primer stats result. This figure shows the properties of the designed (a) *MaPR1-like* forward primer and (b) *MaPR1-like* reverse primer. The parameters assessed include primer melting temperature, the percentage of GC content, and the molecular weight of each primer. Both forward and reverse primers passed all the requirements listed in the PCR suitability test except for the melting temperature (T_m) parameter, of which, both primers did not meet the par due to the T_m values being higher than 58 °C.

4.1.2 DNA isolation from Berangan and Grand Naine (ITC 1256) cultivars

Total genomic DNA sample was successfully isolated from the leaf tissues of two banana cultivars namely Berangan and Grand Naine (ITC 1256). Agarose gel electrophoresis analysis revealed that a band of high molecular weight was obtained for each banana cultivar (Figure 4.2) indicating the presence of DNA. Each band was accompanied with a smear along the lane indicating DNA degradation. In addition, EtBr fluorescence signal was also observed in the well of the gel indicating either the presence of high molecular weight DNA molecules or too high a concentration of a DNA sample being loaded. DNA quantification (Appendix B-4) result supported the latter assumption showing that both samples were of high concentration values ranging from 0.1–0.2 µg/µL with an average $A_{260/280}$ value of 1.95. On the other hand, the $A_{260/230}$ values for both samples were 1.26 and 2.26 for Berangan and Grand Naine, respectively. The low $A_{260/230}$ value for Berangan indicated phenolic contamination in the isolated DNA sample.

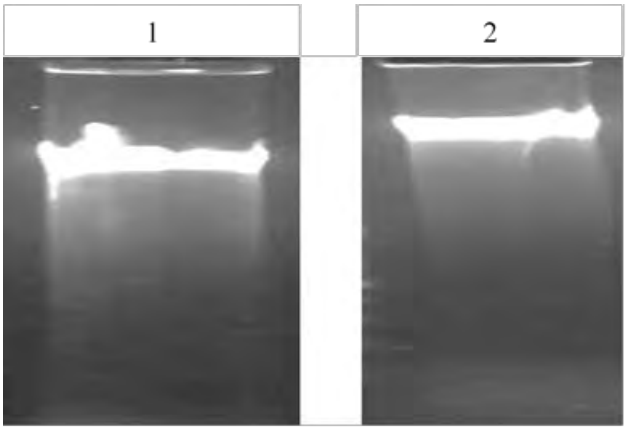

Figure 4.2: DNA extraction result from banana cultivars. Agarose gel electrophoresis result of total DNA sample isolated from Berangan (Lane 1) and Grand Naine (ITC 1256; Lane 2) leaf tissues showing successful isolation of high molecular weight DNA. Smearing observed in both lanes indicated DNA degradation or due to too high a concentration of DNA sample being loaded into each lane.

4.1.3 Isolation and purification of *MaPR1-like* gene from Berangan and Grand Naine (ITC 1256) cultivars

PCR was carried out using the designed primers in Figure 4.1 to isolate *MaPR1-like* gene from the genomic sample of Berangan and Grand Naine (ITC 1256) cultivars. Agarose gel electrophoresis analysis showed the successful amplification of a distinct band of ~550 bp from the genomic sample of the two banana cultivars studied (Figure 4.3a). In addition, a faint band of ~800 bp was observed in both samples, indicating unspecific binding of the primers. Note that no amplification was obtained in the negative control reaction. To eliminate the unspecific bands, both PCR products were purified using QIAquick Gel Extraction kit (Qiagen, Germany) for cloning purposes. The purification resulted in an isolation of a distinct ~550 bp single band (Figure 4.3b) that was later cloned into pGEM-T Easy Vector.

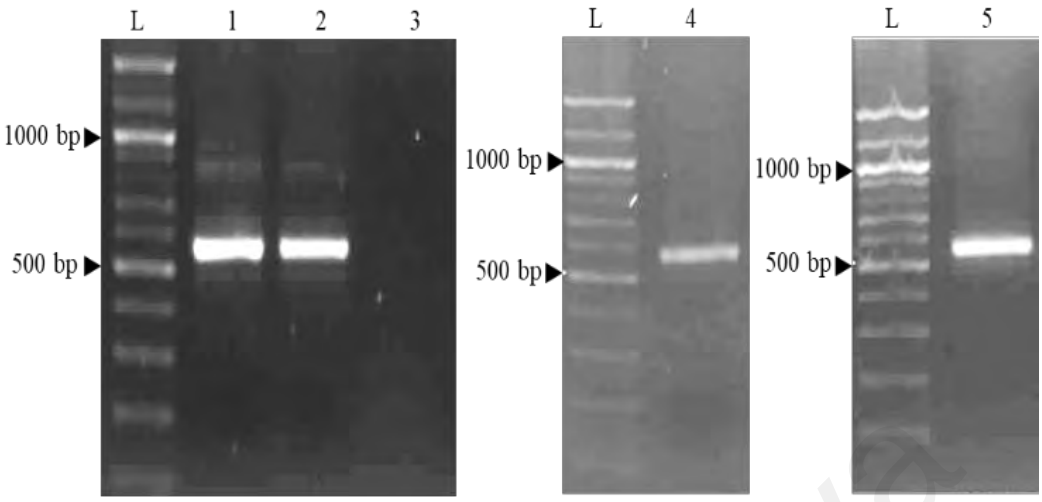

Figure 4.3: PCR amplification of *MaPR1-like* gene fragment from banana cultivars. (a) Agarose gel electrophoresis analysis showing the amplification of ~550 bp band from total DNA sample of Berangan (Lane 1) and Grand Naine (ITC 1256; Lane 2). No amplification was obtained in the negative control reaction (Lane 3). (b) Agarose gel electrophoresis result for the purification of ~550 bp long putative *MaPR1-like* gene amplified from sample of Berangan (Lane 4) and Grand Naine (ITC 1256; Lane 5). A 100 bp DNA ladder (Thermo Fisher Scientific, USA) was used to estimate the size of the purified DNA (Lane L).

4.1.4 T-A cloning: Colony screening for the cloned *MaPR1-like* gene fragment

The purified PCR products were ligated into pGEM®-T Easy Vector System I and transformed into *E. coli* strain JM109 cells. Colony PCR was performed using M13 universal primer pair to screen for positive *E. coli* strain JM109 transformants. From a total of 184 bacterial colonies picked for colony PCR, only 77 contained the cloned fragment. The presence of cloned fragment in the transformants was confirmed by the detection of an ~800 bp band, amplified from the cell lysate (Figure 4.4). In this experiment, all negative control reactions showed no amplifications. Smearing was observed in each lane containing the amplification products perhaps due to a surplus amount of DNA template in each reaction. The empty lanes (Lane 11, 22 and 23) signify no amplification of insert.

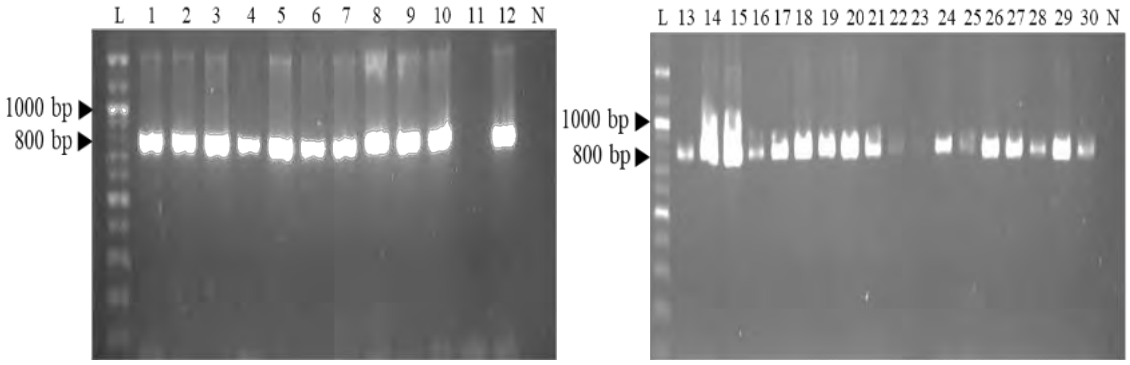

Figure 4.4: Detection of the presence of cloned *MaPR1-like* gene fragment in *E. coli* strain JM109 transformed cells by colony PCR. Agarose gel electrophoresis of colony PCR using universal M13 primer pair showing the detection of positive transformants with an amplification of an 800 bp band in each colony transformed with pGEM®-T Easy Vector System I plasmid containing the cloned *MaPR1-like* DNA fragment isolated from Berangan (Lanes 1–12) and Grand Naine (ITC 1256; Lanes 13–30) cultivars. Negative control reactions yielded no PCR products (Lane N). The size of amplicons was estimated using a 100 bp DNA ladder (Thermo Fisher Scientific, USA;(Lane L).

4.1.5 Isolation of pGEM-T Easy plasmids containing the cloned *MaPR1-like* DNA fragment

A total of 77 plasmids were isolated from positive transformants screened in Section 4.1.4. However, only 65 *MaPR1-like* clones showed high plasmid DNA purity and were subjected to further analyses. From the 65 clones, 35 clones containing *MaPR1-like* genomic fragment were isolated from Berangan while the remainder was from Grand Naine (ITC 1256). Agarose gel electrophoresis analysis revealed the presence of high molecular weight plasmid bands in three different conformations (Figure 4.5). DNA quantification result (Appendix B-5) revealed that A_{260}/A_{280} purity values of all isolated plasmids ranged from 1.8 to 2.0 while A_{260}/A_{230} values were more than 2.0. The concentrations of the isolated plasmids ranged from 1.0 to 4.5 µg/µL.

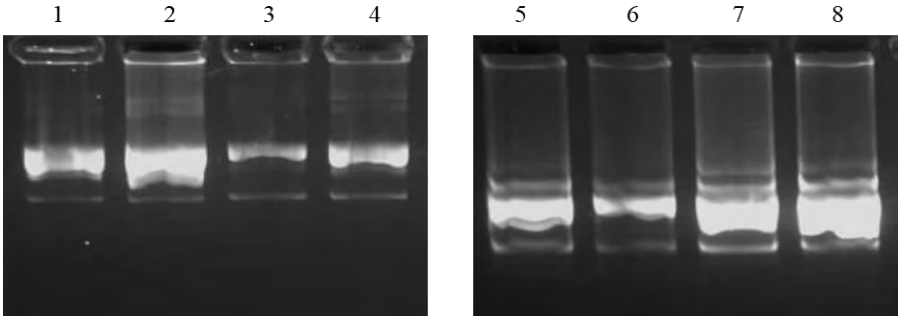

Figure 4.5: Plasmid isolation from bacterial colonies containing clones of *MaPR1-like* gene fragment. Agarose gel electrophoresis result showing the detection of high molecular weight plasmid DNA bands in three different conformations, indicating successful isolation of plasmids from the selected *E. coli* JM109 colonies. The figure shows examples of *MaPR1* clones isolated from Berangan (Lanes 1–4) and Grand Naine (ITC 1256; Lanes 5–8).

4.1.6 Restriction enzyme digestion of pGEM-T Easy vector harbouring *MaPR1-like* DNA fragment

The presence of the cloned *MaPR1-like* DNA fragment in the colony was validated using restriction enzyme (RE) digestion assay. In this assay, the vector was digested with *Eco*RI restriction enzyme, of which its two sites flanked the cloned DNA fragment. This digestion assay resulted in the release of a ~550 bp cloned fragment from the vector, observed in the agarose gel electrophoresis result (Figure 4.6). Note that the presence of a higher molecular weight band in Lanes 1–8 is the linearised plasmid. Out of 65 plasmids, only 44 have the cloned fragment and were then subjected to DNA sequencing procedure.

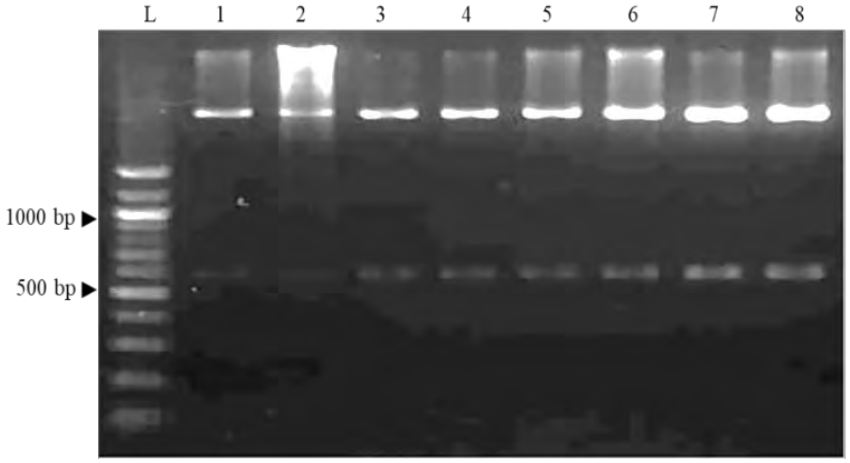

Figure 4.6: Restriction enzyme digestion assay on the isolated plasmids to verify the presence of cloned *MaPR1-like* gene fragment in the plasmids. Agarose gel electrophoresis of the product of *Eco*RI restriction enzyme digestion assay showing the presence of a distinct ~550 bp band of the cloned *MaPR1-like* gene fragment isolated from Berangan (Lanes 1–4) and Grand Naine (ITC1256) (Lanes 5–8). DNA band size was estimated using a 100 bp ladder (Thermo Fisher Scientific, USA).

4.1.7 Sequence analyses of the isolated *MaPR1-like* gene fragment

4.1.7.1 Sequence chromatogram analysis

A total of 44 plasmids were subjected to sequencing and 44 *MaPR1-like* gene sequences were successfully obtained. All chromatograms obtained showed single peaks, indicating the presence of a single DNA template in each reaction (Figure 4.7). The total length of the 44 cloned sequences were obtained in the range of ~900 bp, inclusive of the vector arm sequence. The cloned sequences were identified by the presence of a start (ATG) and a stop (TAG) codons, with a total length of 566 bp.

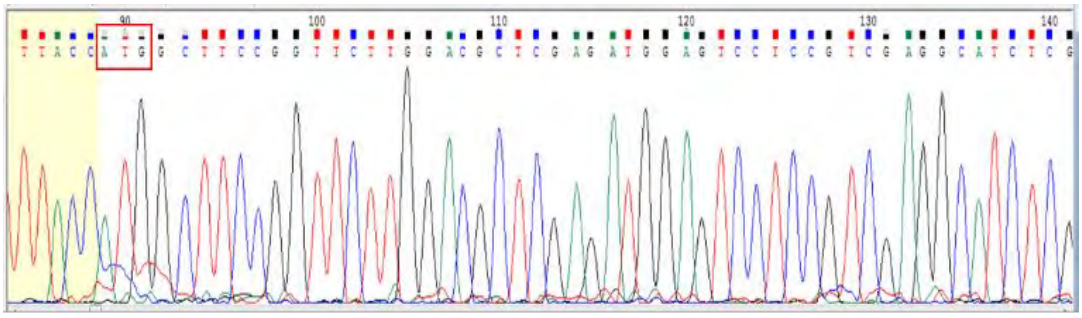

(a)

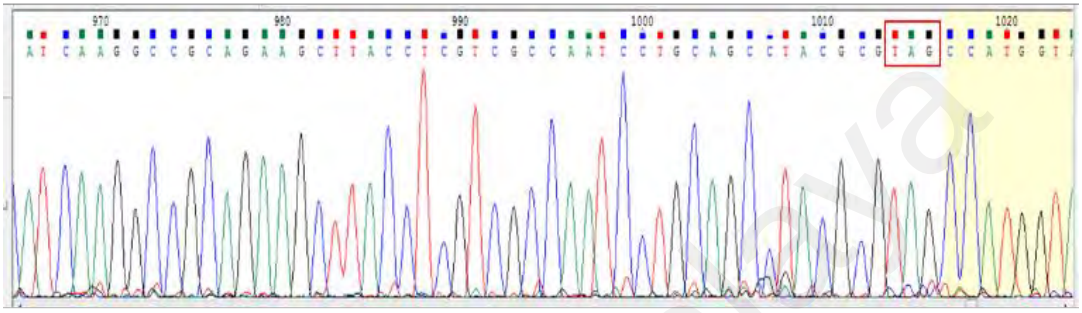

(b)

Figure 4.7: Sequence verification of *MaPR1-like* gene fragment. An example of chromatograms obtained after sequencing one of the plasmid DNA samples harbouring *MaPR1-like* gene using (a) a universal M13 forward primer showing the presence of a start codon (red box), and (b) a universal M13 reverse primer showing the presence of a stop codon (red box) of the gene.

4.1.7.2 BLAST analysis of *MaPR1-like* gene sequences in the GenBank

A total of 44 *MaPR1-like* cloned sequences that were subjected to BLASTn analysis showed 81-97 % similarity with *MaPR1-like* mRNA sequences in the GenBank (Figures 4.8a and 4.8b). Based on the alignment score analysis (Figure 4.8a), the gap in the alignment suggested the possible presence of an intronic region in the gene structure. The E-value obtained for each hit was an average of 2 x 10^{-239} with 84-86% query coverage. On the other hand, BLASTn results conducted in Banana Genome Hub database revealed that the isolated clones showed an exact hit with *PR1-like* gene from chromosomes 3 and 9 of *M. acuminata* with an E-value of 0.0 (Figure 4.8c).

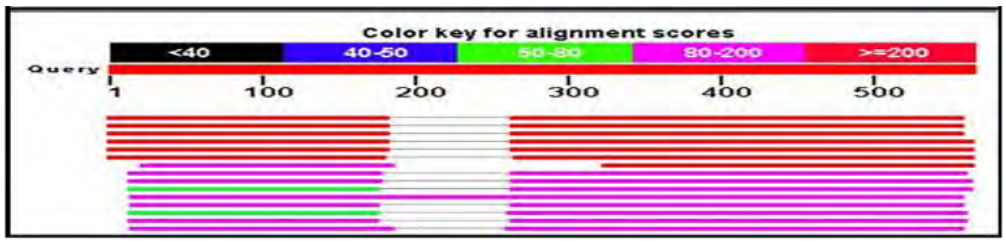

(a)

Description	Max Score	Total Score	Query Cover	E value	Per. Ident	Accession
PREDICTED: Musa acuminata subsp. malaccensis pathogenesis-related protein 1-like (LOC103977653), mRNA	516	831	87%	1e-141	97.08%	XM_009393226.2
PREDICTED: Musa acuminata subsp. malaccensis pathogenesis-related protein 1-like (LOC103977651), mRNA	340	575	87%	5e-89	84.42%	XM_009393223.2
Musa acuminata AAA Group cultivar Cavendish pathogenesis-related protein 1 (PR1-3) mRNA, complete cds	340	584	87%	5e-89	84.42%	KF582558.1
PREDICTED: Musa acuminata subsp. malaccensis pathogenesis-related protein 1-like (LOC103977652), mRNA	335	575	87%	2e-87	84.09%	XM_009393224.2
Musa acuminata AAA Group pathogenesis-related protein mRNA, complete cds	304	539	87%	3e-78	81.82%	JF271128.1
PREDICTED: Musa acuminata subsp. malaccensis pathogenesis-related protein 1-like (LOC103998084), mRNA	299	539	87%	1e-76	81.49%	XM_009419475.2

(b)

```
Length=564

                                                          Score     E
Sequences producing significant alignments:               (Bits)  Value

  Ma03_g08140 Pathogenesis-related protein 1               994     0.0
  Ma03_g08150 Pathogenesis-related protein 1               946     0.0
  Ma03_g08160 Pathogenesis-related protein 1               544     1e-153
  Ma09_g15840 Pathogenesis-related protein 1               531     9e-150
```

(c)

Figure 4.8: BLASTn analysis of *MaPR1-like* gene fragment in sequence databases. An example of a BLASTn result showing (a) a colour key alignment score of more than 200 for the 566 bp query sequence with the presence of a gap in the alignment indicating the presence of an intronic region in the query sequence, and (b) the top six BLASTn hit result with 81–97 % identity between the query sequence and *PR1-like* mRNA and transcript sequences available in the GenBank, while (c) is an example of BLASTn result of one of the cloned sequences that showed an exact hit with *PR1* gene sequences in chromosomes 3 and 9 of *M. acuminata* with an E-value of 0.0 in Banana Genome Hub database.

4.1.8 Phylogenetic analysis of *MaPR1-like* cloned sequences

A maximum likelihood phylogenetic tree (bootstrap value = 1000) was constructed (Figure 4.9) using the genomic clones (N = 44) of *MaPR1-like* gene isolated from Berangan and Grand Naine (ITC 1256) banana cultivars to estimate sequence relationship amongst the cloned sequences. *MaPR1-like* clone sequences clustered into three phylogenetic groups suggesting the presence of at least three types of clonal variants in the two banana genomes studied. It was noted that sequence clustering was at random i.e., not tied down to the cultivar that the clones were isolated from. However, it was observed that the majority of *PR1-like* clone sequences in Group 1 was from Berangan

cultivar as opposed to Group 2 and 3, where a mixture of clones from both cultivars were found.

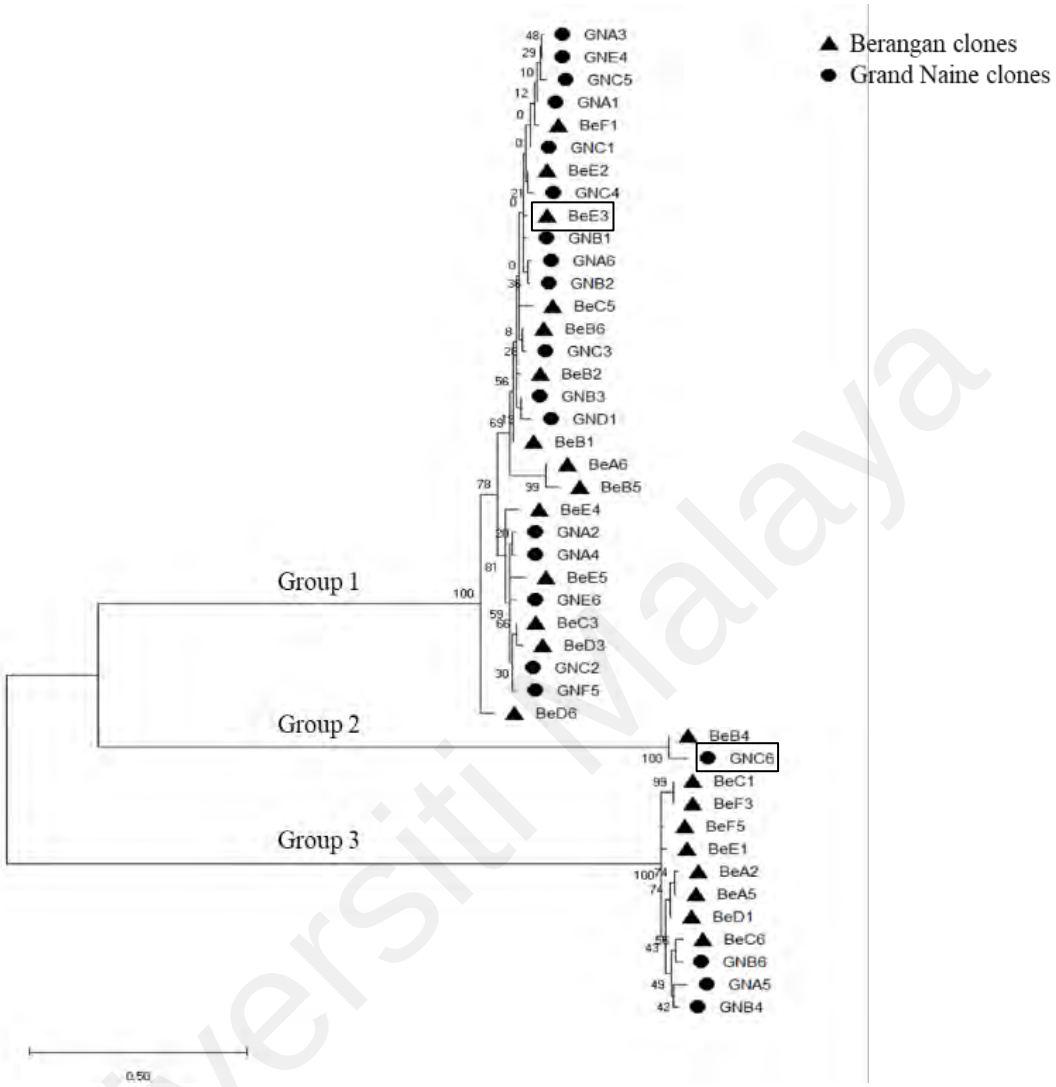

Figure 4.9: Phylogenetic analysis of the clones of *MaPR1-like* gene fragment. Maximum likelihood phylogenetics tree (bootstrap value = 1000) constructed using 44 genomic *PR1-like* clone sequences isolated from Berangan and Grand Naine (ITC 1256) cultivars showing the clustering of the cloned sequences into three groups, indicating the presence of at least three *PR1-like* clonal variant types in the two banana genomes studied. Two *MaPR1-like* cloned sequences, gBeE3 and gGNC6 (boxed), representing each banana cultivar were randomly chosen for copy number analyses. A discrete gamma distribution was used to model evolutionary rate differences among sites (five categories (+*G* parameter = 0.2164)). The rate variation model allowed for some sites to be evolutionarily invariable ([+*I*], 41.29 % sites). The tree was drawn to scale, with branch lengths measured in the number of substitutions per site. There was a total of 566 positions in the final dataset.

4.1.9 Southern blotting analysis

4.1.9.1 Primer design for the Southern blotting hybridisation probes

Two genomic *MaPR1-like* cloned sequences namely, gBeE3 and gGNC6 were randomly chosen from the result obtained in phylogenetic analysis (Figure 4.9) to represent the genome of the two cultivars, i.e., Berangan and Grand Naine (ITC 1256), respectively. These sequences were used to design the specific primers for Southern blot assay. Since the upstream sequences of *MaPR1-like* gene for both banana cultivars were the same, a single forward primer (20-mer) was designed while two reverse primers (20-mer and 24-mer) were designed based on the specific downstream sequences of the chosen *MaPR1-like* gene variants isolated from the two cultivars. An *Nco*I recognition site CCATG was added to the primer sequence to introduce the RE recognition site to the amplified *MaPR1-like* gene to facilitate downstream analyses. The primer pair s*MaPR1-like*(F) 5' TACCATGGCTTCCGGTTCTT 3' / s*MaPR1-like*Be(R) 5' TACCATGGCTACGCGTAGGCTGCT 3' was used to amplify *MaPR-1 like* gene from Berangan cDNA while another pair using the same forward primer s*MaPR1-like*(F) / s*MaPR1-like*GN(R) 5' TACCATGGCTACGGATAGGC 3' was used to amplify *MaPR1- like* gene from Grand Naine cDNA sample to produce the probes. *In silico* result using PCR Primer Stats showed both forward and reverse primers passed all parameters in the PCR suitability tests (Appendix B-6).

4.1.9.2 Analysis of *MaPR10* gene copy number in Berangan and Grand Naine (ITC 1256) genomes by Southern blot assay

Southern blot assays on 20 µg DNA extract of Grand Naine (ITC 1256) and Berangan cultivars showed the development of two to four DNA bands (asterisks) on the blotted nitrocellulose membrane which indicate the number of *MaPR10* gene copy present in the two banana genomes studied (Figure 4.10). This result corroborated the result obtained

in phylogenetic analysis with genomic clones (Section 4.1.8) justifying that there were at least three *MaPR10* clonal variants present in the two banana genomes studied.

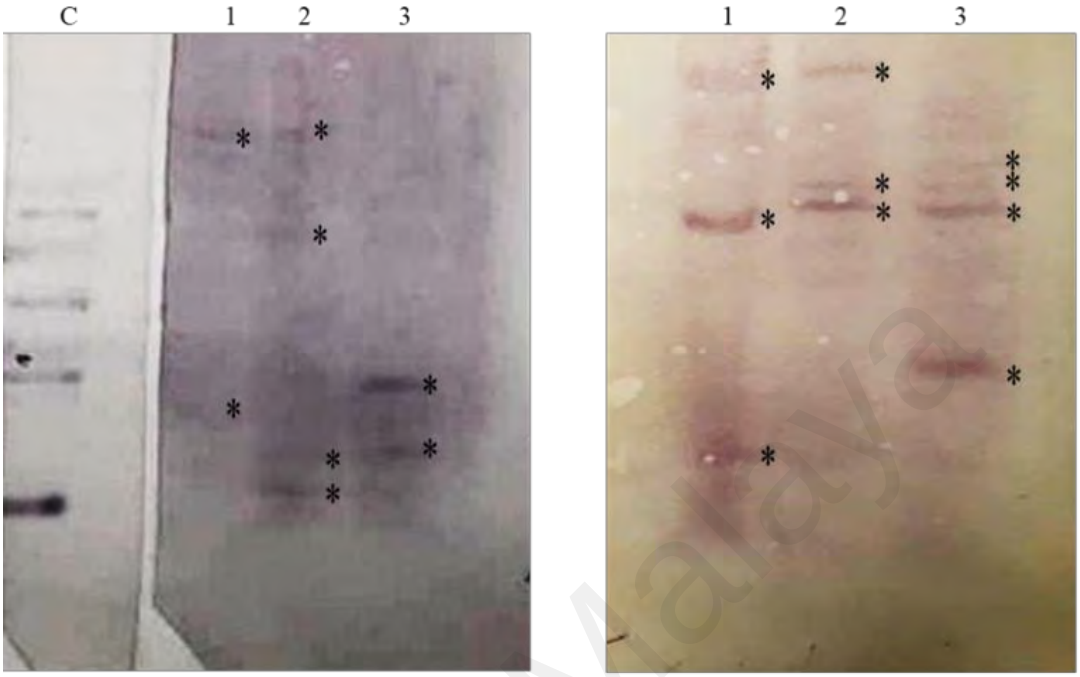

(a) (b)

Figure 4.10: Estimation of the copy number of *MaPR10* gene via Southern blot assay. Southern blotting of the digested 20 µg of total DNA extract for (a) Berangan and (b) Grand Naine (ITC 1256) on the nitrocellulose membrane resulted in the development of two to four bands indicating the copy number of *MaPR10* sequence variants in the banana genomes studied. The total genomic DNA sample of each banana cultivar was digested with *Eco*RI (Lane 1), *Eco*RV (Lane 2) and *Dra*I (Lane 3) restriction enzymes (RE). Two specific sequence probes were used in this assay, representing each banana cultivar studied. Both probes namely BeE3 and GNC6 were randomly chosen from the pool of cloned sequences obtained from this study. *Eco*RI digested-total DNA isolated from the plasmid containing the cloned *MaPR10* fragment was used as a positive control reaction for the assay (Lane C). * DNA bands detected on the blotted nitrocellulose membrane.

4.2 Isolation of *MaPR1-like* transcript fragment

4.2.1 RNA isolation of total RNA sample from the banana root tissues infected with *M. incognita*

Total RNA sample was successfully isolated from the root tissues of Berangan and Grand Naine (ITC 1256) cultivars that served as the hosts for the root-knot nematodes (RKN), *M. incognita*. Agarose gel electrophoresis result showed the presence of *28S* and *18S* bands, albeit faintly, in Berangan sample while only RNA smear was observed for Grand Naine (ITC 1256) sample (Figure 4.11), indicating RNA degradation. However,

no DNA contaminations were observed in both samples, hence DNase treatment was not performed to the two samples. RNA quantification analysis revealed that the average concentration of both RNA samples was 0.1 µg/µL (Appendix B-7). The average $A_{260/280}$ purity value was 2.03, indicating high portion of ribonucleic acids were obtained in the two samples. On the other hand, $A_{260/230}$ purity value for both RNA samples were above 2.0, indicating low phenolic contaminations. Both samples were subjected to cDNA conversion for subsequent analyses.

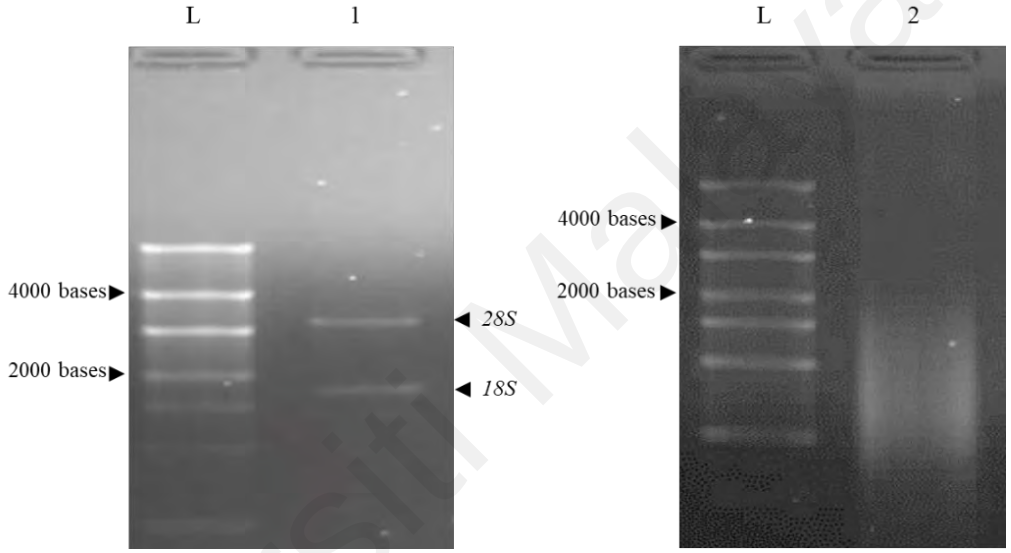

Figure 4.11: RNA extraction from Berangan and Grand Naine (ITC1256). Agarose gel electrophoresis result of the total RNA sample isolated from *M. incognita*-infected root tissues of Berangan (Lane 1) showing *28S* band estimated at 3200 bases and *18S* band estimated at 1800 bases length. However, the total RNA sample isolated from Grand Naine (Lane 2) was only present as a smear. The size of RNA band was estimated using High Range RNA Riboruler (Thermo Fisher Scientific, USA; Lane L).

4.2.2 Reverse transcription-PCR and purification of *MaPR1-like* transcript

cDNA sample was synthesised from 0.3 µg of the total RNA extract of Berangan and Grand Naine (ITC 1256) root tissues using Omniscript Reverse Transcription Kit (Qiagen, USA). Gene specific primers designed in Section 4.1.9.1 were used to amplify *MaPR1-like* transcript fragments from these total RNA samples. Agarose gel electrophoresis results revealed that an expected band of ~480 bp was amplified from both Berangan and Grand Naine (ITC 1256) root samples (Figure 4.12) that were used as hosts to *M. incognita*. The negative control reaction showed no amplification. Despite a

gene specific primer pair being used in this amplification procedure, unspecific bands were still visible in both sample lanes, albeit faintly. Purification procedure resulted in a distinct single band of ~480 bp for both banana cultivars studied, signifying successful purification step. The purified fragments were subjected to cloning into pGEM®-T Easy Vector plasmids.

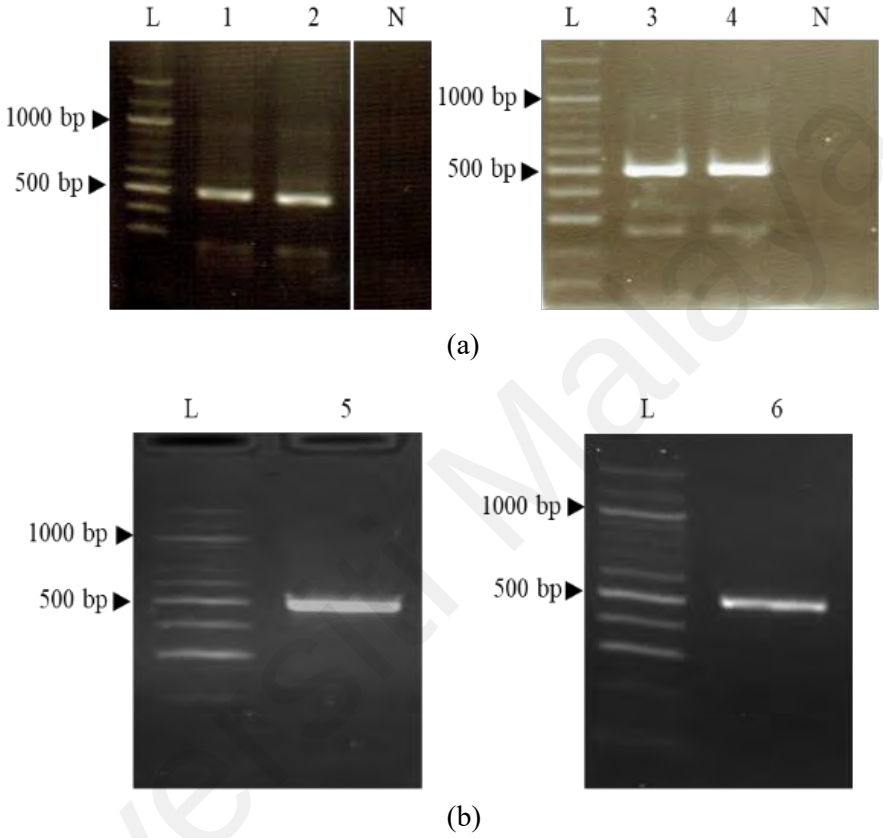

Figure 4.12: PCR amplification and purification of *MaPR1-like* transcript fragment. (a) Agarose gel electrophoresis result showing the amplification of a distinct ~480 bp *MaPR1-like* transcript fragments from Berangan (Lanes 1 and 2) and Grand Naine (ITC 1256; Lanes 3 and 4). No amplification obtained in all negative control reactions (Lane N). (b) Agarose gel electrophoresis result showing successful purification of ~480 bp long *MaPR1-like* transcript fragments isolated from Berangan (Lane 5) and Grand Naine (ITC 1256; Lane 6). These banana plants were used as hosts for *M. incognita* culture. The size of amplicon was estimated using a 100 bp ladder (Thermo Fisher Scientific, USA; Lane L).

4.2.3 Colony PCR for the detection of cloned *MaPR1-like* transcript fragment in the transformed JM109 *Escherichia coli* cells

From a total of 154 transformed JM109 *E. coli* colonies, only 44 contained the cloned fragment. Colony PCR resulted in the amplification of a ~700 bp product indicating the presence of ~490 bp *MaPR1-like* transcript fragments in the transformed colonies (Figure

4.13). All negative control reactions showed no amplification. An unspecific band of ~1200 bp was also observed in some of the samples which could be the result of unspecific primer binding or surplus amount of template used in the PCR reactions. In addition, an unspecific band of ~50 bp observed in lane 48 was most probably a primer dimer. The empty lanes 7, 18, 32, 35, 36, and 38 signify no amplification of insert.

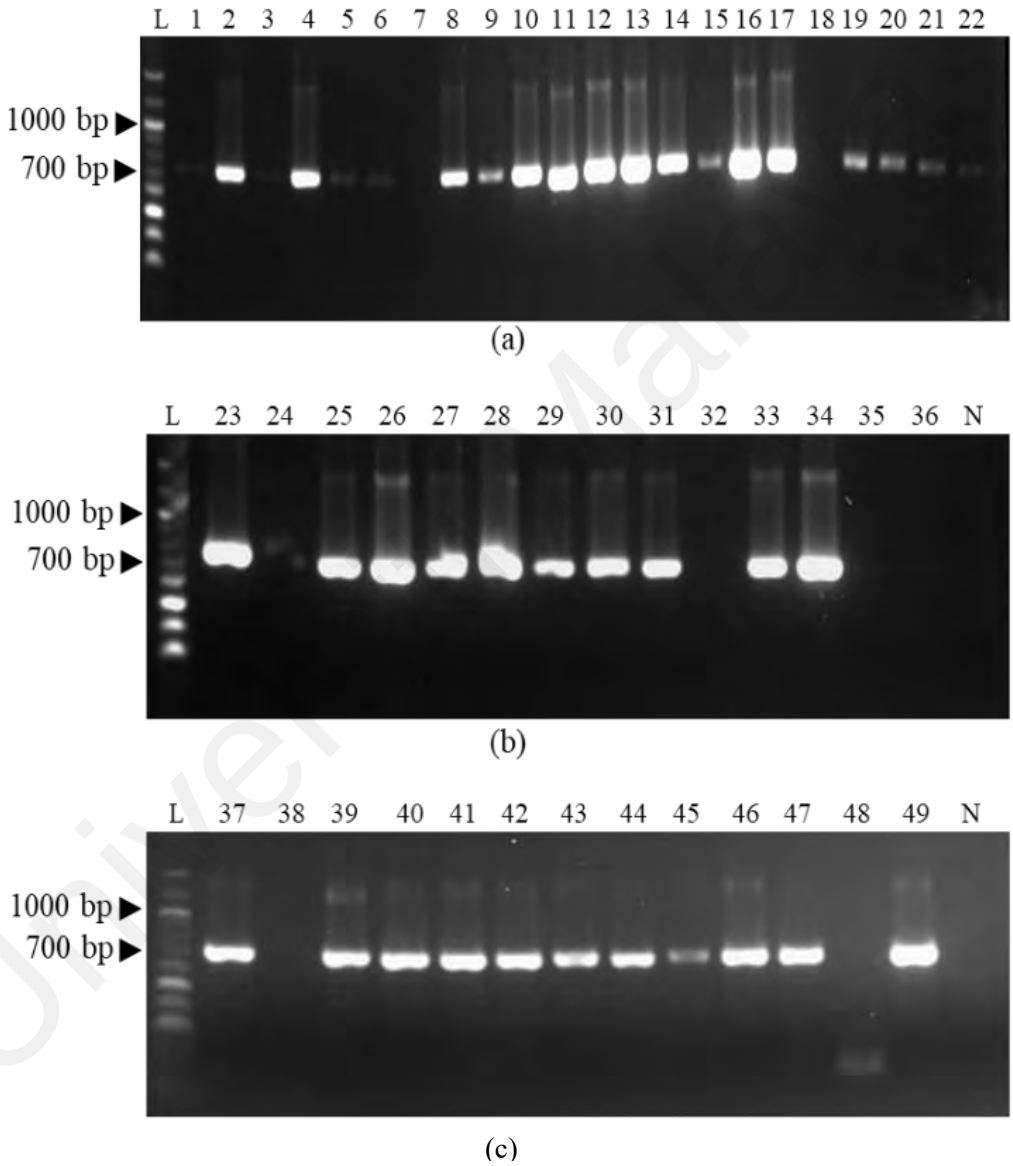

Figure 4.13: Detection of the presence of the cloned *MaPR1-like* transcript fragment in the *E. coli* strain JM109 cells by colony PCR. Agarose gel electrophoresis result showing PCR amplification from the transformed *E. coli* strain JM109 cells yielded a high intensity band of ~700 bp long indicating the presence of cloned fragment. These *MaPR1-like* clones were isolated from Berangan (Lanes 1–36) and Grand Naine (ITC 1256; Lanes 37–49). No amplification observed in Lanes 7, 18, 32, 35, 36, and 38. Negative control reactions yielded no PCR products (Lane N). The size of amplicon was estimated using a 100 bp DNA ladder (Thermo Fisher Scientific, USA; Lane L).

4.2.4 Isolation of pGEM-T Easy Vector plasmids harbouring *MaPR1-like* transcript fragment

Fourty-four plasmids containing *MaPR1-like* transcript fragment were isolated from the bacterial colonies chosen based on the colony PCR result obtained in Section 4.2.3. Qualitative analysis using agarose gel electrophoresis revealed the isolation of high molecular weight plasmids (Figure 4.14). Quantitative analysis showed that the A_{260}/A_{280} purity value of all isolated plasmids ranged between 1.8 to 2.3, while the A_{260}/A_{230} value was more than 2.0 (Appendix B-8). In addition, the concentration of all plasmids obtained ranged from 2.0 to 4.5 μg/μL. Out of the total plasmids, only 25 plasmids have high DNA purity and were subjected to further analyses.

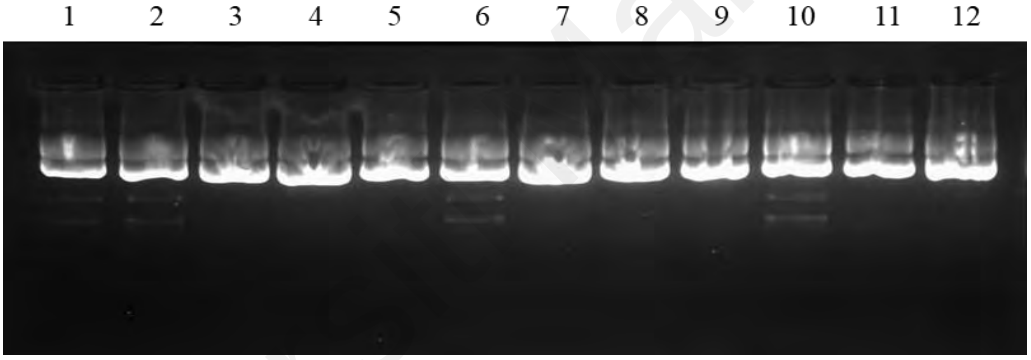

Figure 4.14: Isolation of the plasmids containing the cloned *MaPR1-like* transcript fragment. Agarose gel electrophoresis result showing the presence of high molecular weight band indicating a successful isolation of the desired plasmid from the selected colonies for Berangan (Lanes 1-6) and Grand Naine (ITC 1256; Lanes 7-12) containing cloned *MaPR1-like* gene fragment.

4.2.5 Restriction enzyme digestion of pGEM-T Easy Vector plasmids harbouring *MaPR1-like* transcript fragment

The isolated plasmids were digested with *Eco*RI restriction enzyme to verify the presence of *MaPR1-like* transcript fragment in the plasmid prior to sequencing. The digestion reaction yielded three bands, with one distinct band at ~500 bp (Figure 4.15) indicating the presence of *MaPR1-like* transcript fragment isolated from both banana cultivars. The other two bands of high molecular weight DNA were the linearised plasmids and partially digested plasmids.

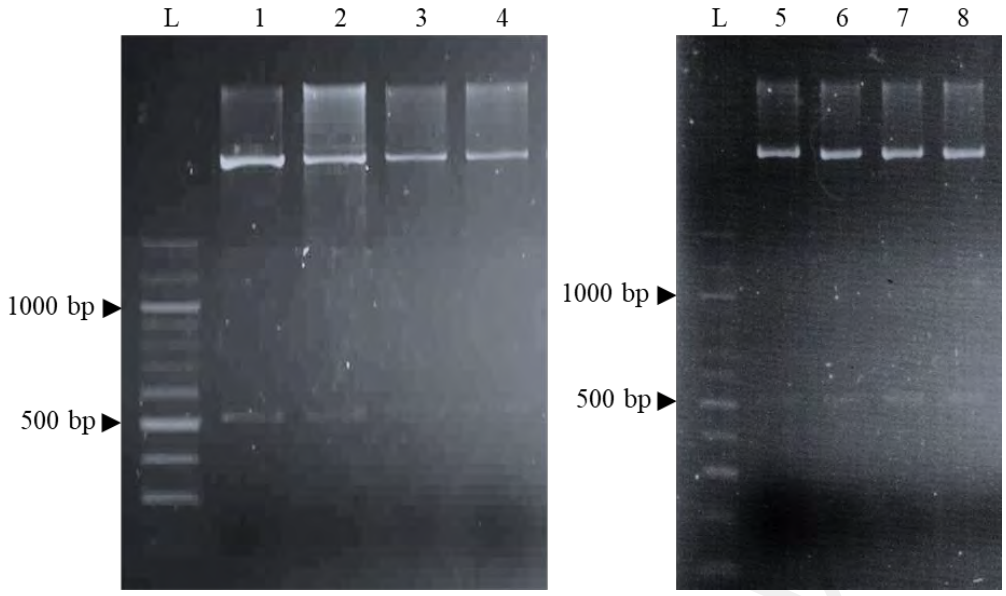

Figure 4.15: Restriction digestion assay to verify the presence of cloned *MaPR1-like* transcript fragment in plasmid. Agarose gel electrophoresis of *Eco*RI restriction digestion assay showing the release of a ~500 bp band of interest indicating the successful cloning of *MaPR1-like* transcript fragment isolated from Berangan (Lanes 1–4) and Grand Naine (ITC 1256; Lanes 5–8) *M. incognita*-infected root tissues into the plasmids. The size of amplicon was estimated using a 100 bp DNA ladder (Thermo Fisher Scientific, USA; Lane L).

4.2.6 Sequence analysis of the putative *MaPR1-like* transcript fragments

Sequence chromatograms were analysed and edited using Chromas version 2.6 software. All 50 chromatograms for 25 plasmids obtained in Section 4.2.5 showed single peaks indicating the presence of single DNA template (Figure 4.16). The length of all cloned transcript fragment obtained was 483 bp. The total sequence length obtained was within the range of 850–900 bp for all 25 cloned sequences. The clone sequences of 483 bp were identified by the presence of a start codon (ATG) right after the vector arm sequence of the forward primer reaction and a stop codon (TAG) right before the vector arm sequence of the reverse primer reaction.

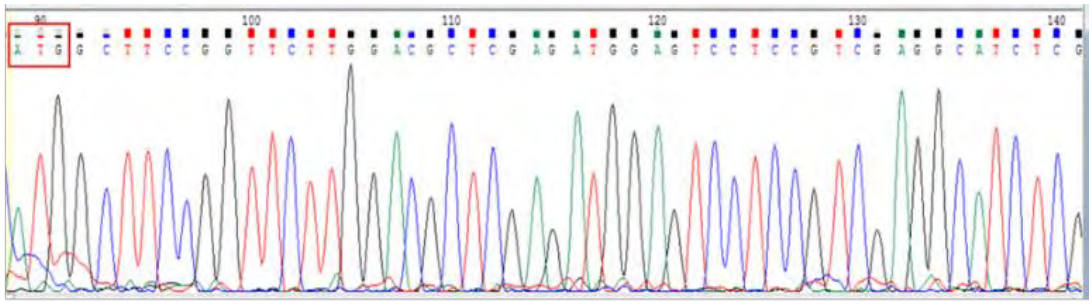

(a)

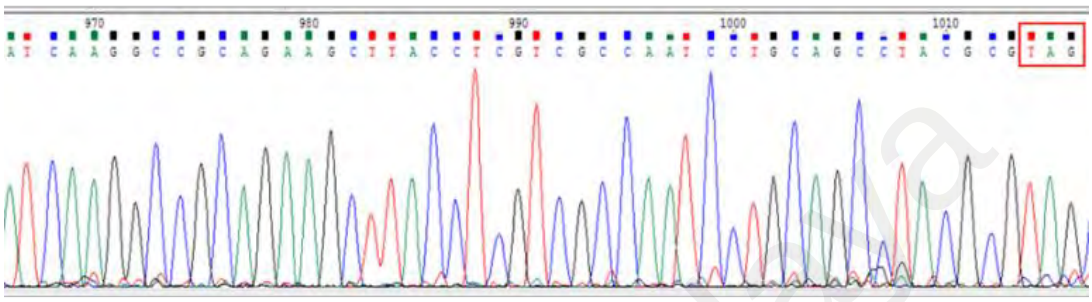

(b)

Figure 4.16: Sequence verification of *MaPR1-like* transcript fragment. An example of chromatograms obtained after sequencing one of the plasmid DNA samples harbouring *MaPR1-like* gene using (a) an M13 forward primer showing the presence of a start codon (boxed) and (b) an M13 reverse primer showing the presence of a stop codon (boxed) of the gene.

4.2.7 BLAST analysis of *MaPR1-like* transcript fragment in the GenBank and Banana Genome Hub database

BLASTn analysis conducted in the GenBank revealed that the isolated transcript fragments showed 86–99 % similarity with the complete coding sequences of *MaPR1-like* mRNA (Figure 4.17a and 4.17b). An average E-value of 2 x 10^{-239} was obtained at the E-value of each hit in the database with 100 % query coverages. On the other hand, BLASTn results conducted in Banana Genome Hub revealed that the isolated clones showed an exact hit with *PR1-like* transcript at a locus in chromosomes 3 and 9 of *M. acuminata* DH Pahang (E-value = 0.0) (Figure 4.17c). This analysis verified the presence of an intronic region in the isolated gene where no gap was observed in the alignment (Figure 4.17a), as opposed to the results obtained in Figure 4.8a. In addition, this analysis also suggested that the *MaPR1-like* transcript fragment belongs to the *PR1* gene family. However, the top 100 BLASTn result from the GenBank (Figure 4.17d) revealed that the query sequence also matched *PR10* gene sequences from other plant species such as

Elaeis guineensis PR10 (HQ436525.1), *L., regale PR10* (KF690636.1) and *Triticum aestivum PR10* (EU908212.1), albeit sharing only at least 68.52 % sequence similarity. This result prompted further analyses conducted to confirm the identity of the isolated *PR* gene on whether to group it in Group 10 or Group 1. To meet this goal, two transcript clonal sequences i.e., BeB5 and GNA5, representing Berangan and Grand Naine (ITC 1256) cultivars, respectively, were randomly chosen for conserved domain analysis in the GenBank.

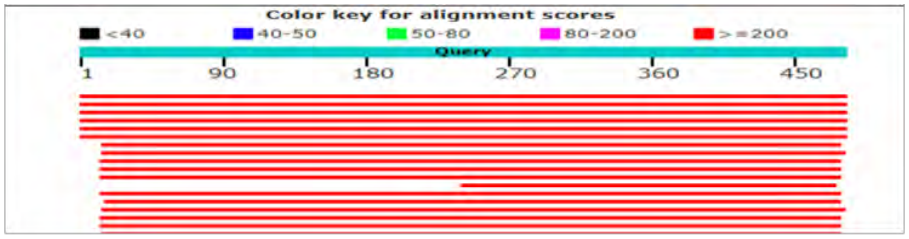

(a)

Description	Max Score	Total Score	Query Cover	E value	Per. Ident	Accession
Musa acuminata AAA Group pathogenesis-related protein mRNA, complete cds	845	845	100%	0.0	98.76%	JF271128.1
PREDICTED: Musa acuminata subsp. malaccensis pathogenesis-related protein 1-like (LOC103988084), mRNA	836	836	100%	0.0	98.34%	XM_009419475.2
PREDICTED: Musa acuminata subsp. malaccensis pathogenesis-related protein 1-like (LOC103977652), mRNA	592	592	100%	4e-165	87.16%	XM_009393224.2
Musa acuminata AAA Group cultivar Cavendish pathogenesis-related protein 1 (PR1-3) mRNA, complete cds	574	574	100%	1e-159	86.34%	KF582558.1
PREDICTED: Musa acuminata subsp. malaccensis pathogenesis-related protein 1-like (LOC103977651), mRNA	565	565	100%	6e-157	85.92%	XM_009393223.2
PREDICTED: Musa acuminata subsp. malaccensis pathogenesis-related protein 1-like (LOC103977653), mRNA	565	565	100%	6e-157	85.92%	XM_009393226.2

(b)

```
Length=483

                                                                 Score     E
Sequences producing significant alignments:                      (Bits)  Value

  Ma09_t15840.1 Pathogenesis-related protein 1                    836     0.0
  Ma03_t08150.1 Pathogenesis-related protein 1                    592     9e-169
  Ma03_t08160.1 Pathogenesis-related protein 1                    565     1e-160
  Ma03_t08140.1 Pathogenesis-related protein 1                    565     1e-160
```

(c)

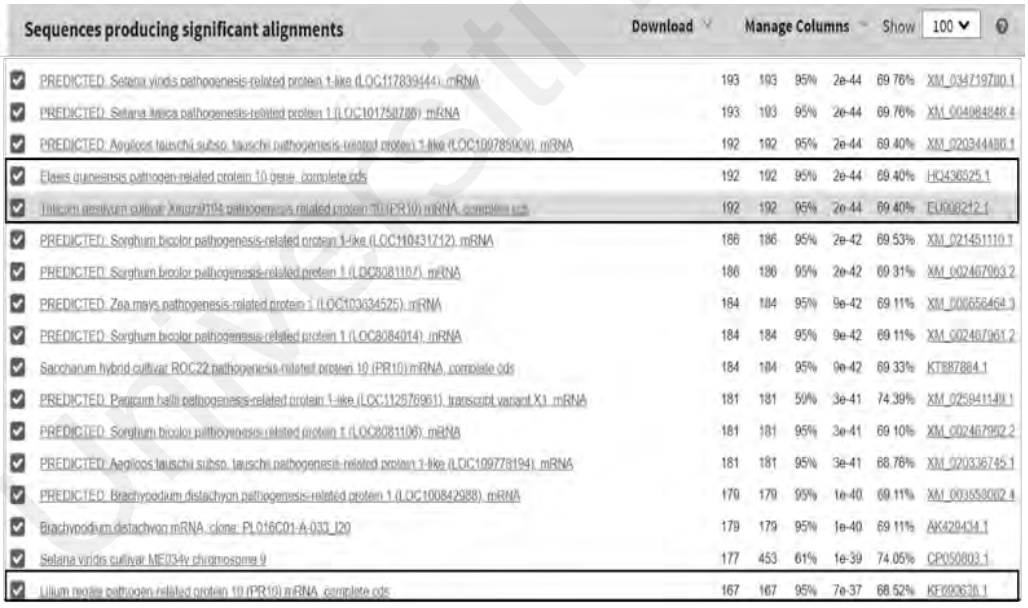

(d)

Figure 4.17: BLAST analysis of *MaPR1-like* transcript fragment in sequence databases. An example of a BLASTn result showing (a) the colour key alignment score of more than 200 for the 483 bp query sequence, and (b) the top six BLAST hit result of *MaPR1-like* mRNA sequences in the database showing 86–99 % identity with the query sequence. (c) An example of a BLASTn result of one of the cloned sequences showing an exact hit (E-value = 0.0) with *PR1* sequence in the Banana Genome Hub database. (d) The top 20 hit of BLASTn analysis showing that the query sequence, *MaPR1-like* transcript, shared at least 69.4 % similarity with *PR10* gene from different plant species namely *E. guineensis PR10* (HQ436525.1), *L. regale PR10* (KF690636.1) and *T. aestivum PR10* (EU908212.1).

4.2.8 Conserved domain analysis on the deduced MaPR1-like amino acid cloned sequences

Two randomly chosen deduced amino acid sequences of *MaPR1-like* gene i.e., BeB5 and GNA5 were subjected to conserved domain analysis using Conserved Domain Database (CDD). The search result (Figure 4.18) revealed that both sequences belong to START/RHO alpha C/PITP/Bet v 1/CoxG/CalC (SRPBCC) ligand-binding domain superfamily. SRPBCC superfamily houses Bet v 1 protein family that is generally associated with PR10 protein family suggesting that *MaPR1-like* cloned sequences isolated in this study belong to *PR10* gene family.

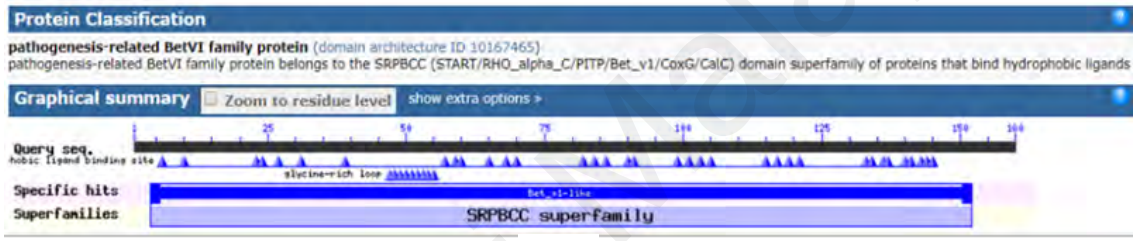

(a)

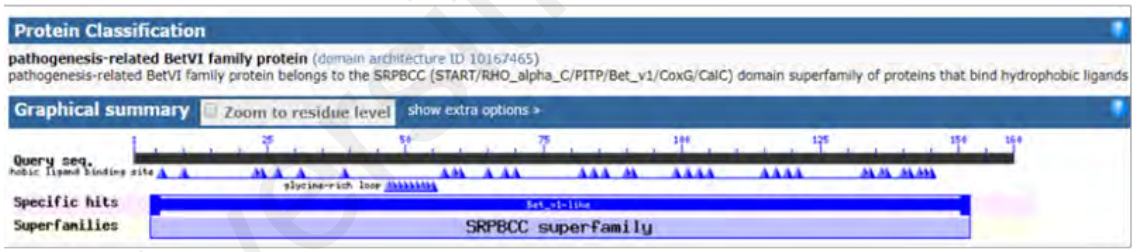

(b)

Figure 4.18: Conserved domain analysis of the deduced amino acid sequences of MaPR10 protein variants. The deduced amino acid sequences of (a) *MaPR1-like* BeB5, and (b) *MaPR1-like* GNA5 analysed in Conserved Domain Database (CDD) showed the presence of Bet v 1 protein domain, a signature domain for PR10 gene family. This analysis suggested that the identity of the isolated *MaPR1-like* clones was supposedly grouped in *PR10* gene family.

4.2.9 Sequence alignment of the deduced amino acid MaPR1-like clonal variants with plant PR10 amino acid sequences

To further investigate the identity of the isolated *MaPR1-like* clonal variants, the deduced amino acid sequences of these clonal variants were aligned with the deduced amino acid sequences of other expressed plant PR1 and PR10 sequences using EMBI-EBI Clustal Omega's online multiple sequence alignment tool. The preliminary amino

acid alignment analysis showed that the isolated banana PR sequences aligned better with plant PR10 amino acid sequences instead of PR1 sequences (Appendix B-9). When the isolated cloned sequences were further aligned with plant PR10 reference sequences from *L. regale* (AHG94650.1), *O. sativa* (AAL74406.1), *S. bicolor* (AAW83209.1) and *Z. mays* (ADA68331.1), it was found that all aligned amino acid sequences shared three conserved signature domains of PR10 protein group (boxed in Figure 4.19) namely the P-loop (GxGxxGxxK) motif, the Bet v I signature motif, and the PR10 specific domain (KAXEXYL). The presence of these three signature domains of PR10 protein family confirmed that the PR clones isolated from both Berangan and Grand Naine (ITC 1256) cultivars were indeed belonged to the *PR10* gene group, henceforth denoted as *MaPR10*. Along with the common PR10 domains, this analysis also resulted in the discovery of the glycoside hydrolase group 16 (GH 16) domain, a novel catalytic domain (bold and underlined in Figure 4.19) found in the selected MaPR10-BeB5 and MaPR10-GNA5 protein sequences, unique only to PR10 sequences isolated from banana cultivars studied. To the best of the author's knowledge, this unique domain for PR10 protein is yet to be reported in any member of PR10 protein group thus far.

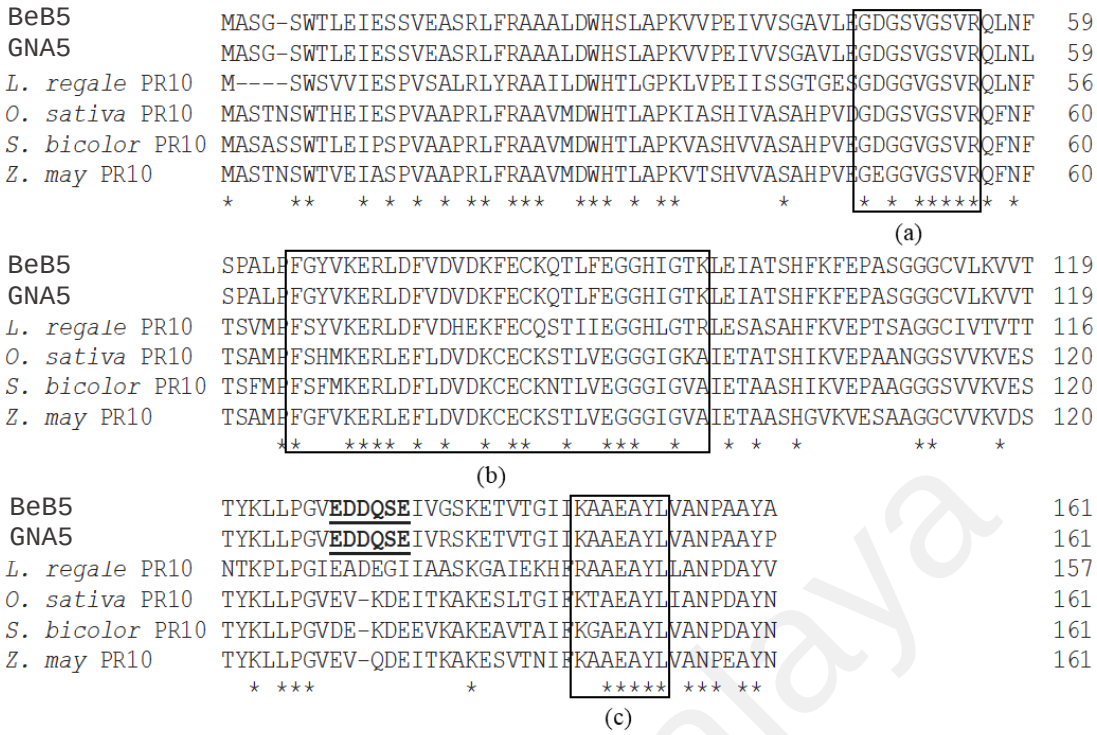

Figure 4.19: Alignment of the deduced amino acid sequences of *MaPR1-like* gene (BeB5 and GNA5), representing Berangan and Grand Naine (ITC 1256) genomes, respectively, with representative PR10 amino acid sequences from four other plant species. The amino acid alignment shows that all PR10 signature motifs were detected in BeB5 and GNA5 amino acid sequences. The PR10 protein signature motifs boxed in the alignment are (a) the P-loop (GxGxxGxxK) motif, (b) the Bet v I signature motif, and (c) PR10 specific domain (KAXEXYL). The novel catalytic motif (EXDXXE) which belongs to glycoside hydrolase group 16 domain was written in bold and underlined in the alignment. Reference sequences obtained from the GenBank were used in this alignment namely *L. regale* (AHG94650.1), *O. sativa* (AAL74406.1), *S. bicolor* (AAW83209.1), and *Z. mays* (ADA68331.1). The number at the end of each sequence is the length of the amino acid sequence. * Conserved amino acid site.

4.2.10 Phylogenetic analysis of the deduced amino acid sequences of MaPR10, banana PR1 reference sequences, and plant PR10 reference sequences

Eighty-four deduced amino acid sequences of *MaPR10* genomic and transcript clones isolated from Berangan and Grand Naine (ITC 1256) banana cultivars, banana PR1 reference sequences obtained from the GenBank and Banana Genome Hub databases, and other plant PR10 reference sequences obtained from the GenBank were aligned and subjected to phylogenetic analysis. A maximum likelihood phylogenetic tree using Jones-Taylor-Thornton (JTT) model with 1000 bootstrap value was constructed to estimate the relationship amongst these sequences (Figure 4.20). It was found that all deduced MaPR10 amino acid sequence clustered into three phylogenetic groups. From the

phylogenetic tree, Groups 1 and 2 housed almost all genomic clones except for the four reference sequences i.e., Ma03_t08150.1, Ma03_t08140.1, Ma03_t08160.1, and KF582558.1, while most MaPR10 transcript clones were clustered in Group 3. On the other hand, PR10 reference sequences from *O. sativa* (AAL74406.1), *S. bicolor* (AAW83209.1), and *Z. mays* (ADA68331.1) were clustered into Group 4. In Group 3, two sequence variants namely MaPR10-BeB5 and MaPR10-GNA5 clustered together with ITC1587_Bchr9_P26466_MUSBA reference sequence, the PR protein found to be differentially regulated by *M. incognita* infection in the susceptible banana variety, Grand Naine (ITC 1256). These two sequences were then chosen for further functional analyses, representing each banana cultivar studied.

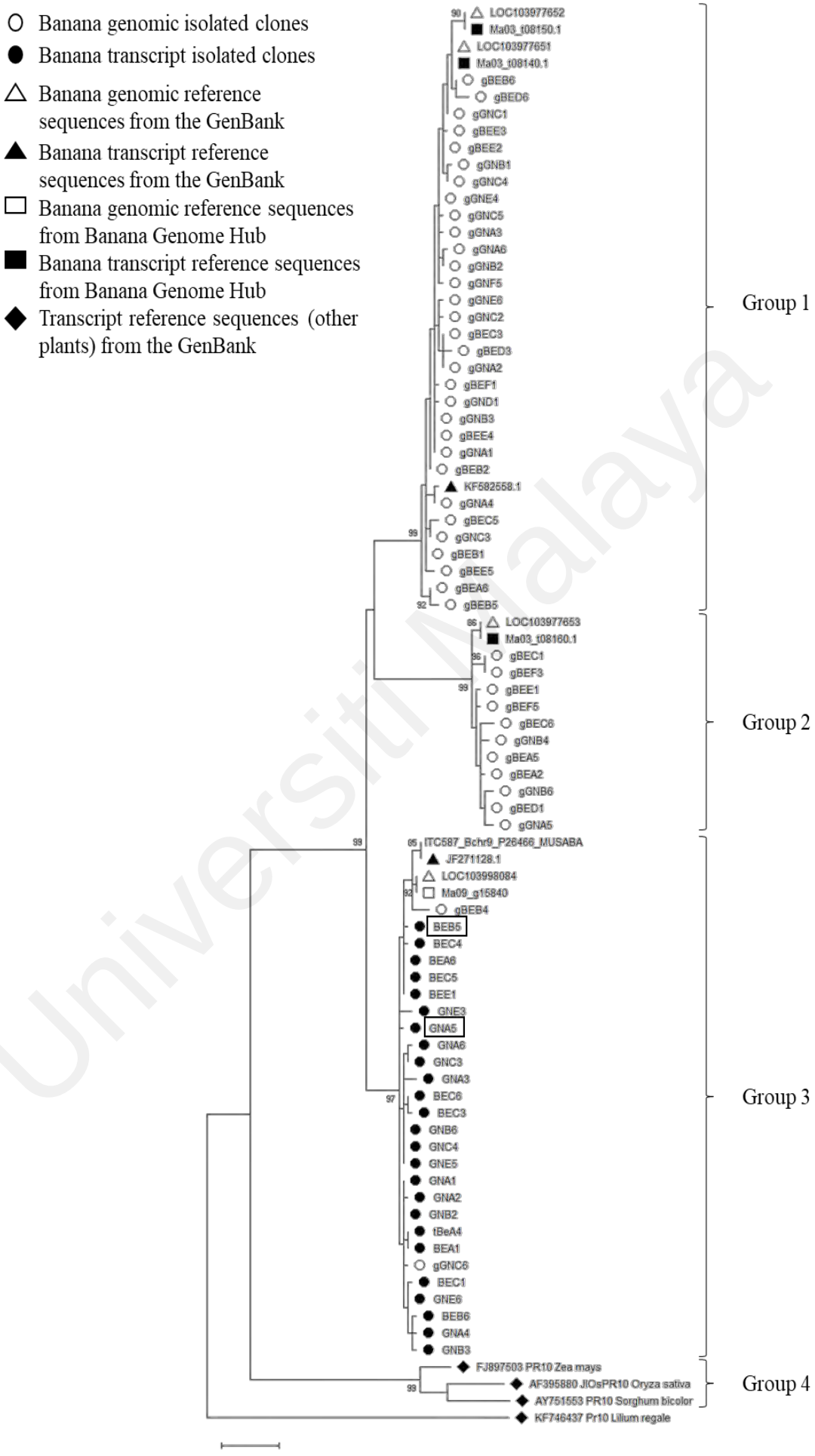

Figure 4.20 (see pp 91): Phylogenetic analysis of the deduced amino acid sequences from the transcript and genomic clones of *MaPR10* fragment, banana PR1 reference sequences and plant PR10 reference sequences. A maximum likelihood phylogenetics tree was constructed using Jones-Taylor-Thornton (JTT) model (Bootstrap value = 1000) to estimate the relationship amongst 84 deduced amino acid sequences of *MaPR10* gene and transcript sequences isolated from Berangan and Grand Naine (ITC 1256) banana cultivars. All MaPR10 peptide sequences isolated in this study clustered into three phylogenetic groups. From the tree, all genomic MaPR10 clones were clustered into Group 1 and 2 with the reference sequences, Ma03_t08150.1, Ma03_t08140.1, Ma03_t08160.1, and KF582558.1. The majority of MaPR10 transcript clones were clustered into Group 3 with ITC1587_Bchr9_P26466_MUSBA reference sequence. On the other hand, PR10 reference sequences from *O. sativa* (AAL74406.1), *S. bicolor* (AAW83209.1), and *Z. mays* (ADA68331.1) were clustered into Group 4. PR10 reference sequence from *L. regale* (KF746437) was sued as outlier. Two peptide sequences, MaPR10-BeB5 and MaPR10-GNA5 (boxed) from Group 3 were chosen for further analyses. A discrete Gamma distribution was used to model evolutionary rate differences among sites (5 categories (+G, parameter = 0.9230)). The rate variation model allowed for some sites to be evolutionarily invariable ([+I], 0 % sites). The tree was drawn to scale, with branch lengths measured in the number of substitutions per site. There was a total of 162 positions in the final dataset.

4.3 Subcellular localisation of MaPR10 protein in *A. cepa* inner epidermal cell

4.3.1 *In silico* subcellular localisation of MaPR10 protein variants

In silico analysis using Plant-mPLoc software predicted MaPR10 proteins to localise in the cytoplasm of the cell (Figure 4.21). This suggested that this protein is an intracellular protein, a common feature of PR10 protein family.

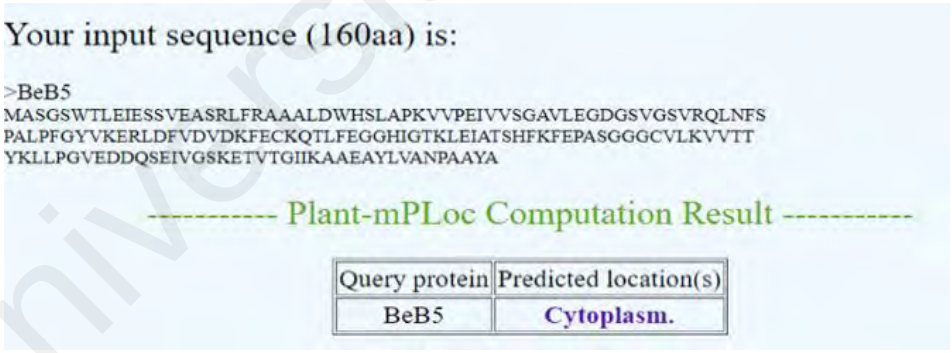
Your input sequence (160aa) is:

>BeB5
MASGSWTLEIESSVEASRLFRAAALDWHSLAPKVVPEIVVSGAVLEGDGSVGSVRQLNFS
PALPFGYVKERLDFVDVDKFECKQTLFEGGHIGTKLEIATSHFKFEPASGGGCVLKVVTT
YKLLPGVEDDQSEIVGSKETVTGIIKAAEAYLVANPAAYA

---------- Plant-mPLoc Computation Result ----------

Query protein	Predicted location(s)
BeB5	Cytoplasm.

(a)

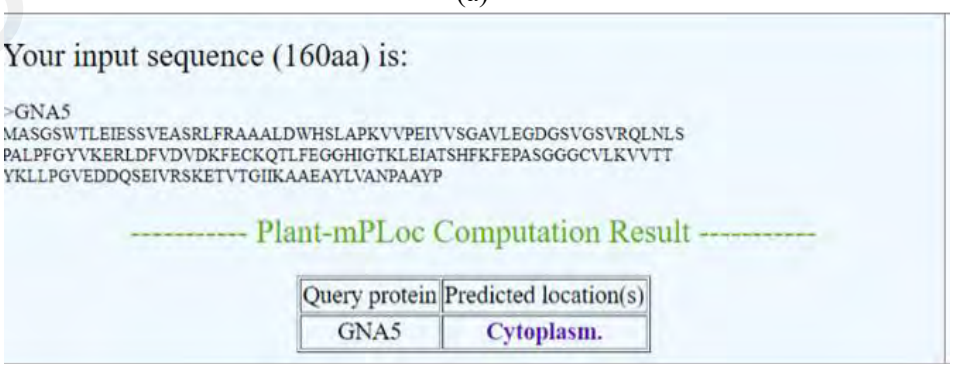
Your input sequence (160aa) is:

>GNA5
MASGSWTLEIESSVEASRLFRAAALDWHSLAPKVVPEIVVSGAVLEGDGSVGSVRQLNLS
PALPFGYVKERLDFVDVDKFECKQTLFEGGHIGTKLEIATSHFKFEPASGGGCVLKVVTT
YKLLPGVEDDQSEIVRSKETVTGIIKAAEAYLVANPAAYP

---------- Plant-mPLoc Computation Result ----------

Query protein	Predicted location(s)
GNA5	Cytoplasm.

(b)

Figure 4.21: *In silico* analysis of protein subcellular localisation prediction using the deduced amino acid sequences. This prediction suggested that both protein variants (a) MaPR10-BeB5, and (b) MaPR10-GNA5 were localised in the cytoplasm i.e., intracellular type.

4.3.2 *In vivo* subcellular localisation of MaPR10 protein variants in the inner epidermal cell of *A. cepa*

4.3.2.1 Propagation and cloning of *MaPR10-BeB5* and *MaPR10*-GNA5 transcript fragments into the pCAMBIA1304 expression vector

MaPR10-BeB5 and *MaPR10-GNA5* transcript fragments were cloned into pCAMBIA 1304 vector to produce pCAMBIA1304::CaMV35S::*MaPR10-BeB5/GNA5*::*mgfp5*::*GUS*::6xHis expression cassette for subcellular localisation study and protein functional analyses. PCR amplification result using the primers designed in Section 4.1.9.1 revealed an expected band size of ~480 bp from pGEM-T Easy vector containing the *MaPR10-BeB5* and *MaPR10-GNA5* transcript fragments (Figure 4.22a). The negative control reactions showed no amplification. Despite gene specific primers were used, unspecific amplifications were visible in the gel, albeit faintly, hence, PCR products were purified using QIAquick Gel Extraction kit (Qiagen, USA). The purification resulted in the isolation of a distinct band of ~480 bp (Figure 4.22b) corresponding to *MaPR10-BeB5* and *MaPR10-GNA5* transcript fragments.

The digestion products of the purified *MaPR10-BeB5* and *MaPR10-GNA5* transcript fragments together with pCAMBIA1304 expression vector with *Nco*I restriction enzyme (RE) yielded a single distinct band of ~480 bp for the transcript fragments, and a single distinct band at the upper part of the gel indicating that the vector has been linearised (Figure 4.22c). These *Nco*I-digested products were gel-purified again and resulted in the recovery of a single distinct band of ~480 bp as observed in agarose gel electrophoresis (Figure 4.22d).

The cloning of purified product to the linearised pCAMBIA1304 vector was conducted to produce pCAMBIA1304::CaMV35S::*MaPR10-BeB5/GNA5*::*mgfp*::*GUS*::6xHis expression construct. Colony PCR was carried on JM109 *E. coli* cells using universal

CaMV35S promoter forward primer and *MaPR10* gene specific reverse primer pair (as mentioned in Section 4.1.9.1) to select for pCAMBIA1304::CaMV35S::*MaPR10-BeB5/GNA5*::*mgfp*::*GUS*::6xHis vector. From a total of 36 colonies screened, only three colonies contained the cloned fragments. Colony PCR resulted in the amplification of a ~700 bp product, indicating the presence of ~480 bp *MaPR10-BeB5* and *MaPR10-GNA5* transcript fragment in the transformed colonies (Appendix B-10). The plasmids from these three colonies were isolated and subjected to sequencing analysis.

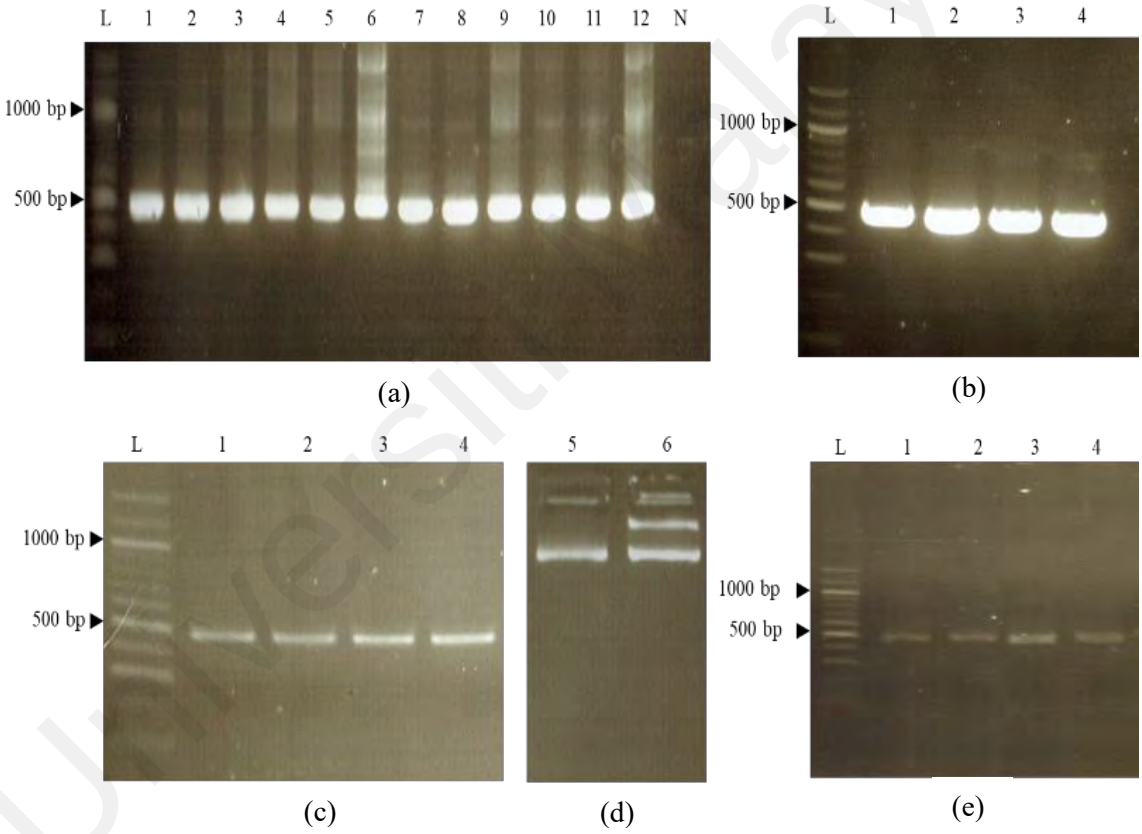

Figure 4.22: PCR amplification, restriction enzyme digestion assay, and purification of *MaPR10-BeB5* and *MaPR10-GNA5* transcript fragments. Agarose gel electrophoresis showing (a) PCR amplification of a distinct, high intensity band of ~480 bp for *MaPR10-BeB5* (Lanes 1–6) and *MaPR10-GNA5* (Lanes 7–12) transcript fragments. No amplification obtained in the negative control reactions (Lane N). (b) Purification yielded in a single, distinct band of ~480 bp for *MaPR10-BeB5* (Lanes 1 and 2) and *MaPR10-GNA5* (Lanes 3 and 4) fragments. Agarose gel electrophoresis showing the (c) *Nco*I-digested DNA fragments at ~480 bp for *MaPR10-BeB5* (Lanes 1 and 2) and *MaPR10-GNA5* (Lanes 3 and 4) transcript fragments, and (d) a single distinct band for *Nco*I-digested pCAMBIA vector (Lane 5), and undigested pCAMBIA1304 vector (Lane 6). (d) DNA Purification yielded a single distinct band of ~480 bp for *MaPR10-BeB5* (Lanes 1 and 2) and *MaPR10-GNA5* (Lanes 3 and 4) transcript fragments. The size of amplicon was estimated using a 100 bp DNA ladder (Thermo Fisher Scientific, USA; Lane L).

4.3.2.2 Isolation of pCAMBIA1304::CaMV35S::*MaPR10-BeB5/GNA5*::*mgfp5*::*GUS*::6xHis expression vector from *Escherichia coli* strain JM109 and sequence characterisation of the isolated plasmids

The three transformed colonies obtained in Appendix B-10 were isolated. One colony contained pCAMBIA1304 plasmid harbouring *MaPR10-BeB5* transcript fragment while the rest contained the same plasmid harbouring *MaPR10-GNA5* transcript fragment. Agarose gel electrophoresis analysis revealed the presence of high molecular weight plasmid bands (Figure 4.23) accompanied by DNA smear. DNA quantification result revealed that A_{260}/A_{280} purity value for all isolated plasmids ranged from 1.8 to 2.0 while A_{260}/A_{230} values were more than 2.0. The concentrations of the isolated plasmids ranged from 1.5 to 2.5 µg/µL (Appendix B-11) These plasmids were subjected to sequencing.

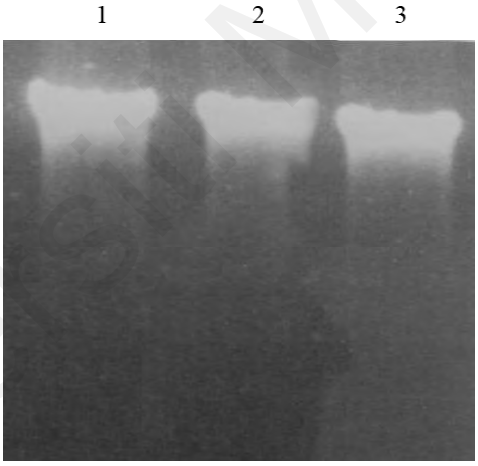

Figure 4.23: Plasmid isolation of pCAMBIA1304 expression vector harbouring the *MaPR10-BeB5/GNA5* transcript. Agarose gel electrophoresis showing the detection of high molecular weight band indicating the successful isolation of pCAMBIA1304::CaMV35S::*MaPR10-BeB5*::*mgfp5*::*GUS*::6xHis (Lane 1) and pCAMBIA1304::CaMV35S::*MaPR10-GNA5*::*mgfp5*::*GUS*::6xHis (Lanes 2 and 3) expression vectors.

Six chromatograms obtained for the three clones showed single peaks, indicating the presence of single DNA template (Figure 4.24) in each clone. The length of all cloned fragments obtained were ~850 bp. All cloned fragment sequences were aligned with *MaPR10-BeB5/GNA5* transcript sequences obtained in Appendix B-11 to verify the sequence of each cloned plasmid. Sequence alignment revealed that the cloned fragments

shared 100 % homology with *MaPR10-BeB5* and *MaPR10-GNA5* sequences (Appendix B-12). Verified plasmids for each sequence variant were then transformed in *A. tumefaciens* for expression analyses.

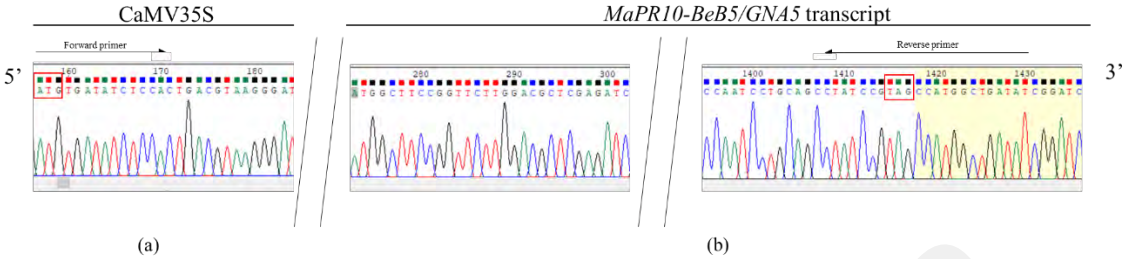

Figure 4.24: Sequence verification of *MaPR1-like* transcript fragment. An example of chromatograms obtained after sequencing one of the pCAMBIA1304::CaMV35S::*MaPR10-BeB5/GNA5*::*mgfp5*::*GUS*::6xHis vectors using (a) a universal CaMV35S promoter forward primer showing the presence of a start codon (boxed), and (b) an *MaPR10* gene specific reverse primer showing the presence of a stop codon (boxed) of the gene. The presence of the CaMV35S promoter sequences was identified in the upstream region from the cloned fragment.

4.3.2.3 Detection of pCAMBIA1304::CaMV35S::*MaPR10-BeB5/GNA5*::*mgfp5*::*GUS*::6xHis vector in *A. tumefaciens* strain LB4404 colonies via colony PCR

The verified plasmids, pCAMBIA1304::CaMV35S::*MaPR10-BeB5/GNA5*::*mgfp5*::*GUS*::6xHis were transformed into *A. tumefaciens* strain LB4404 cells. Colony PCR using universal CaMV35S promoter forward primer and *MaPR10* gene specific reverse primer (Section 4.1.9.1) revealed the amplification of a ~800 bp amplicon in all 12 transformed colonies confirming the presence of the cloned *MaPR10* fragment (Figure 4.25). The negative control reaction showed no amplification.

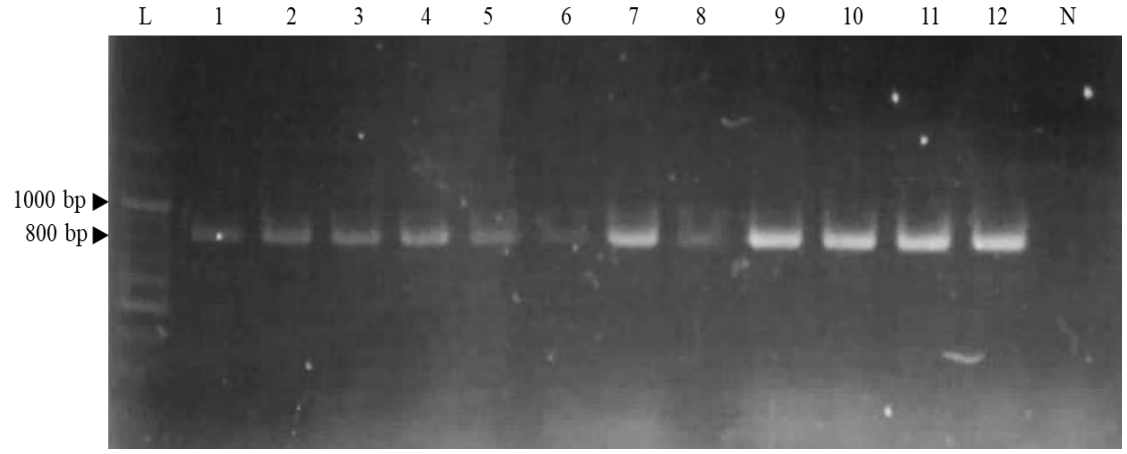

Figure 4.25: Detection of pCAMBIA1304::CaMV35S::*MaPR10-BeB5/GNA5*::*mgfp5*::*GUS*::6xHis plasmids in *A. tumefaciens* strain LB4404 via colony PCR. PCR amplification yielded a specific band of ~800 bp indicating the presence of the cloned fragment in the transformed *A. tumefaciens* strain LB4404 cells. These clones contain *MaPR10-BeB5* (Lanes 1–6) and *MaPR10-GNA5* (Lanes 7–12) sequence variants. Negative control reactions yielded no PCR products (Lane N). The size of amplicon was estimated using a 100 bp DNA ladder (Thermo Fisher Scientific, USA; Lane L).

4.3.2.4 Expression of MaPR10-BeB5 and MaPR10-GNA5 protein variants in transformed *A. tumefaciens* strain LB4404 cells

The transformed *A. tumefaciens* strain LB4404 cells obtained in Section 4.3.2.3 were subjected to GUS assay to verify the expression of the recombinant proteins. This assay resulted in the formation of a clear blue solution for both proteins variants MaPR10-BeB5 and MaPR10-GNA5 indicating the hydrolysis of 5-bromo-4-chloro-3-indolyl glucuronide (X-gluc) into 5,5'-dibromo-4,4'-dichloro-indigo by the GUS protein (Figure 4.26). Since *GUS* gene is located downstream of the cloned fragment, this result showed that both gene variants were also expressed in the transformed cells.

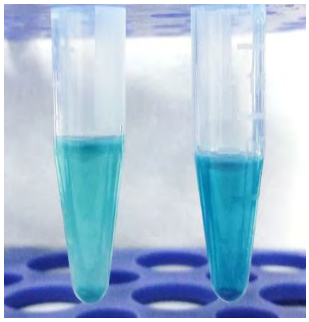

1 2

Figure 4.26: GUS assay on the transformed *A. tumefaciens* strain LB4404. GUS-treated bacterial colonies containing (1) pCAMBIA1304::CaMV35S::*MaPR10-BeB5*::*mgfp5*::*GUS*:: 6xHis, and (2) pCAMBIA1304::CaMV35S::*MaPR10-GNA5*::*mgfp5*::*GUS*::6xHis vectors resulted in the formation of a clear blue solution indicating the presence of GUS protein hydrolysing the 5-bromo-4-chloro-3-indolyl glucuronide (X-gluc) into 5,5'-dibromo-4,4'-dichloro-indigo. Since *GUS* gene is located downstream of the cloned fragment, this result showed that both gene variants were also expressed in the transformed cells.

4.3.2.5 *In vivo* subcellular localisation of MaPR10 protein variants in inner epidermal cells of *A. cepa*

Agrobacterium tumefaciens strain LB4404 cells harbouring recombinant MaPR10-BeB5 and MaPR10-GNA5 was agroinfiltrated separately into *A. cepa* epidermal cells to study the subcellular localisation of the proteins. In this study, MaPR10-(BeB5/GNA5)::GFP signals were observed throughout the cytoplasm of the onion cells indicating the localisation of the two protein variants (Figure 4.27a and b). This observation corroborated the *in silico* prediction conducted in Section 4.3.1. On the other hand, the GFP signals were also observed throughout the cytoplasm in the native vector (pCAMBIA1304::CaMV35::*mgfp5*::*GUS*::6xHis) that serve as positive controls to indicate the successful infiltration of the vector (Figure 4.27c) while no GFP signal was detected in the untransformed cells (Figure 4.27d).

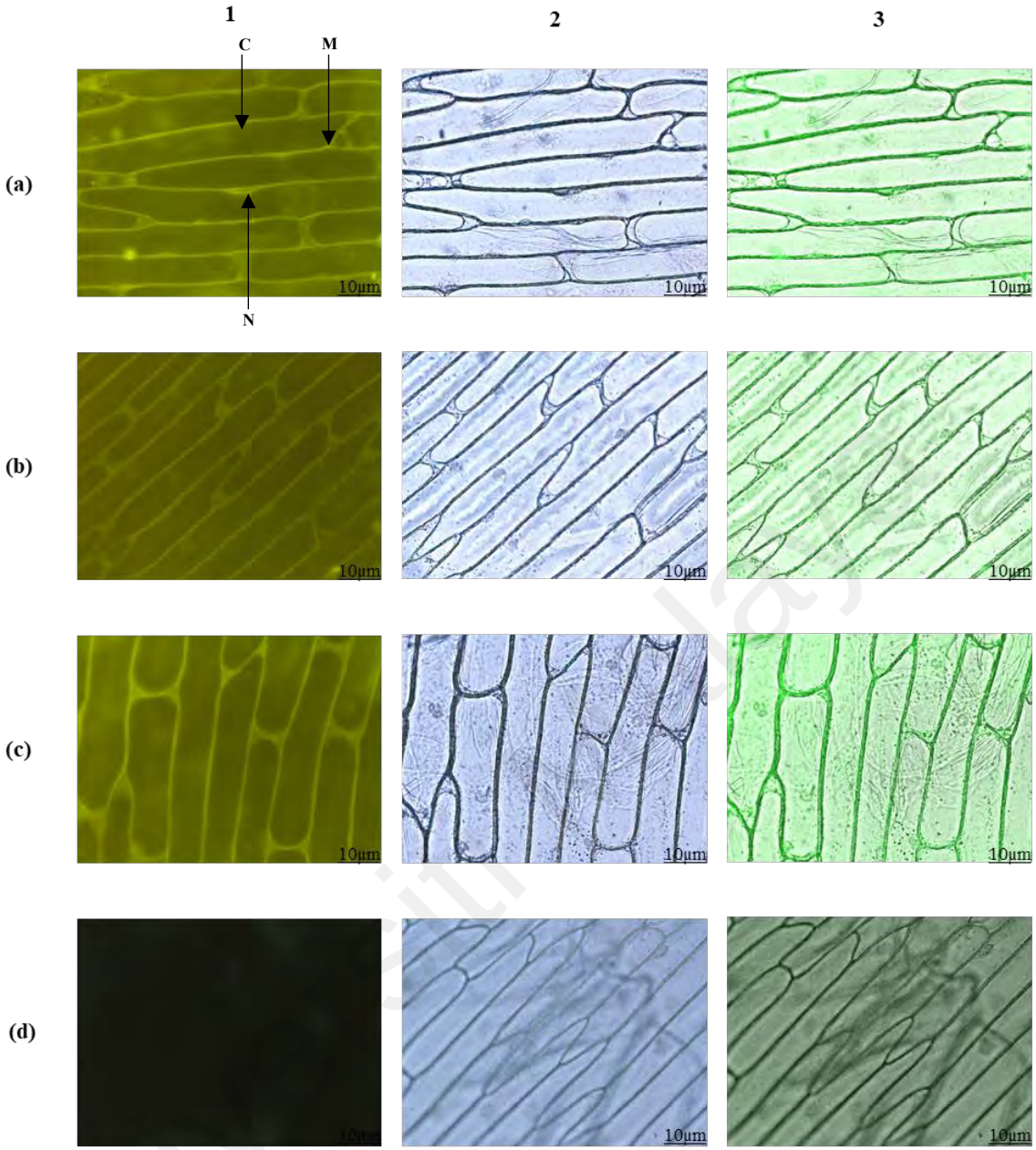

Figure 4.27: Subcellular localisation analysis of MaPR10 protein variants in the inner epidermal onion cell. The result shows that MaPR10 protein variants were present ubiquitously in the cytoplasmic region of the cell. This was observed in onion cells infiltrated by (a) pCAMBIA1304::CaMV35S::*MaPR10-BeB5*::*mgfp5*::*GUS*::6xHis fusion proteins, and (b) pCAMBIA1304::CaMV35S::*MaPR10-GNA5*::*mgfp5*::*GUS*::6xHis fusion proteins, where the GFP signals were scattered throughout the cytoplasm. As a positive control to indicate that infiltration method was successful, onion cell that was infiltrated by (c) pCAMBIA1304::CaMV35::*mgfp5*::*GUS*::6xHis (without *MaPR10* gene) showed that the GFP signal was localised in the cell cytoplasm (C), nucleus (N), and membrane (M). No GFP signal was detected in (d) the negative control sample. The images of the cells were captured with three frames: (1) Green florescence protein (GFP) frame, (2) bright-field (BF) frame, and (3) merged frame (GFP and BF). The bar size for each image was set at 10 µm.

4.4 Purification of MaPR10-BeB5 and MaPR10-GNA5 protein variants from *Escherichia coli* strain BL21 cells

4.4.1 Propagation and cloning of *MaPR10-BeB5* and *MaPR10-GNA5* transcript into pET30a(+) expression vector

Purified *Nco*I-digested *MaPR10-BeB5* and *MaPR10-GNA5* gene fragments (Figure 4.28a) obtained in Section 4.3.2.1 were cloned into pET30(a)+ expression vector. *Nco*I-digested plasmid showed a linearised conformation with a slightly lower molecular weight as compared to the undigested pET30(a)+ vector (Figure 4.28b). The undigested vector was observed to have three bands reflecting the presence of three different plasmid conformations in the sample. Colony PCR using universal T7 promoter forward and reverse primer pair on 65 transformed JM109 *E. coli* cells showed that only five colonies were transformed with the cloned fragments. This was evident in the amplification of a ~800 bp product indicating the presence of ~480 bp *MaPR10-BeB5* and *MaPR10-GNA5* transcript fragments in the transformed colonies (Figure 4.28c and 4.28d) at Lanes 1, 13, 22, 36 and 39. The empty lanes (Lanes 2–12, 14–20, 21, 23–35, 37, 38 and 40) signify no amplification of insert.

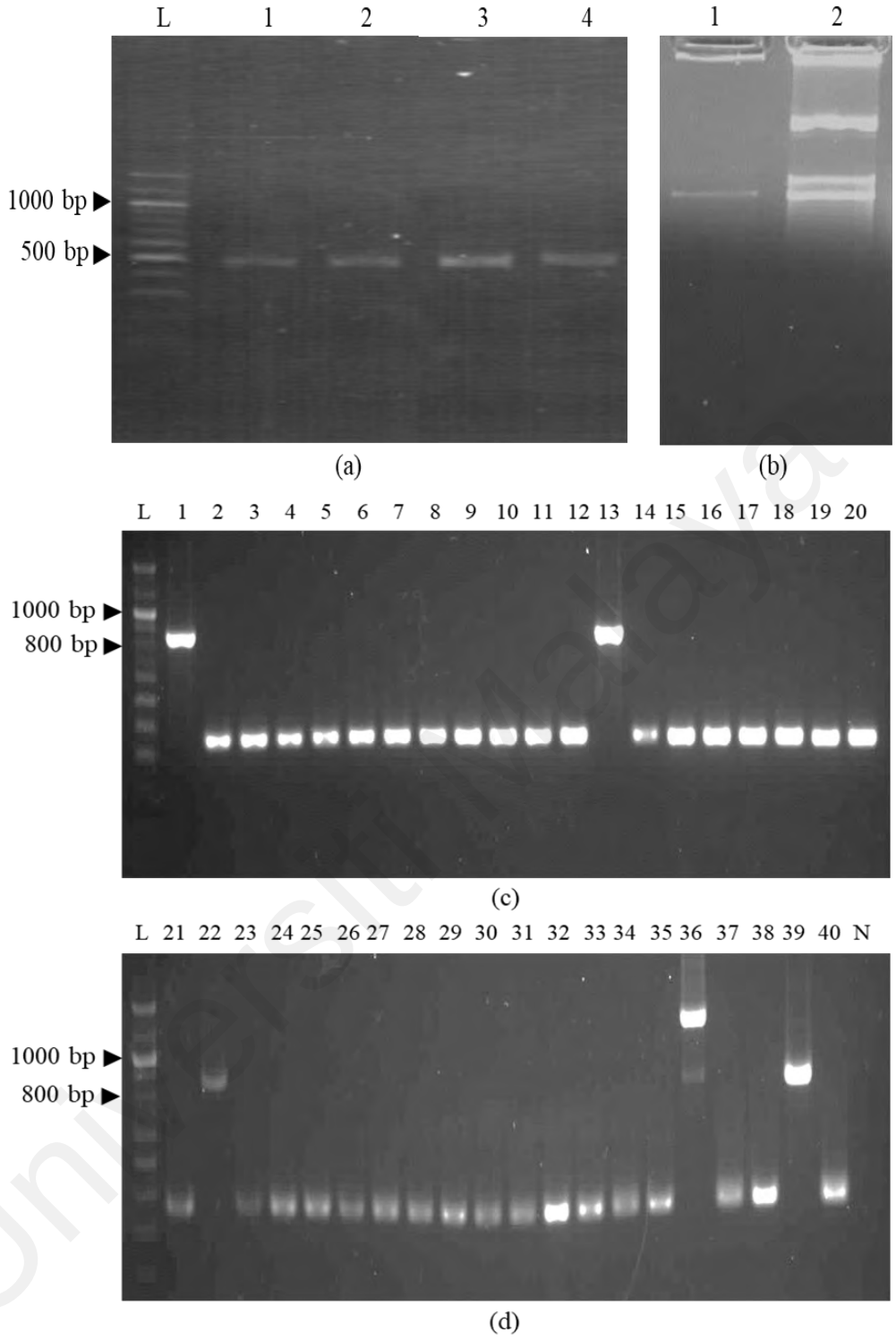

Figure 4.28: Purification of *Nco*I-digested *MaPR10-BeB5/GNA5* transcript fragment, *Nco*I restriction enzyme assay of pCAMBIA vector, and detection of cloned *MaPR10-BeB5* and *MaPR10-GNA5* transcript in *E. coli* strain JM109 cells via colony PCR. Agarose gel electrophoresis showing (a) DNA purification yielded a single distinct band of ~480 bp for *Nco*I-digested *MaPR10-BeB5* (Lanes 1 and 2) and *MaPR10-GNA5* (Lanes 3 and 4) transcript fragments, (b) a single, distinct band of *Nco*I-digested pCAMBIA vector (Lane 1), and undigested pCAMBIA1304 vector (Lane 2). PCR amplification yielded a high intensity band of ~800 bp for five bacterial colonies (Lanes 1, 13, 22, 36 and 39) indicating the presence of cloned fragment for (c) *MaPR10-BeB5* (Lanes 1–20), and (d) *MaPR10-GNA5* (Lanes 21–40) transcript fragments in the transformed *E. coli* strain JM109 cells. The size of amplicon was estimated using a 100 bp DNA ladder (Thermo Fisher Scientific, USA; Lane L). Negative control reactions yielded no PCR products (Lane N).

4.4.2 Isolation of pET30a(+)::T7promoter::6xHis::*MaPR10-BeB5/GNA5* vector from transformed *E. coli* strain JM109 cells and sequence characterisation of the isolated plasmids

Plasmids from the five bacterial colonies detected to contain the cloned fragment in Section 4.4.1 were isolated. Two colonies harboured *MaPR10-BeB5* transcript fragment while the rest harboured *MaPR10-GNA5* transcript fragment. Agarose gel electrophoresis analysis revealed the isolation of high molecular weight plasmid bands from all colonies (Figure 4.29). DNA quantification result revealed that A_{260}/A_{280} purity values of all isolated plasmids ranged from 1.8 to 2.0 while A_{260}/A_{230} values were more than 2.0. The concentrations of the isolated plasmids ranged from 1.7 to 4.8 µg/µL (Appendix B-13).

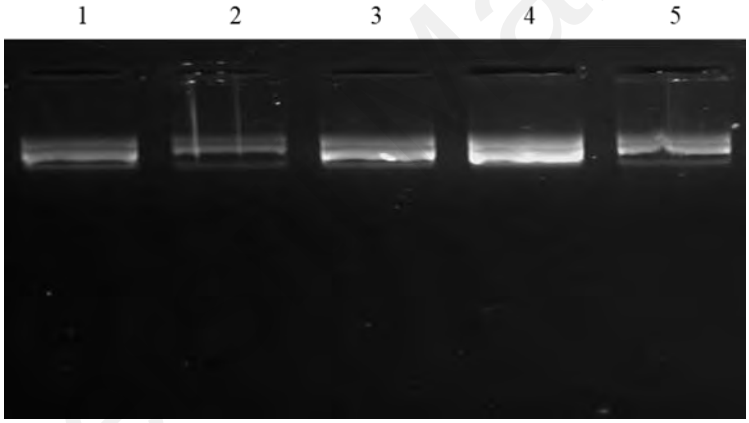

Figure 4.29: Plasmid isolation of pET30a(+) expression vector harbouring the *MaPR10-BeB5/GNA5* transcript. Agarose gel electrophoresis result showing the detection of high molecular weight bands indicating successful isolation of pET30a(+)::T7promoter::6xHis::*MaPR10-BeB5* (Lanes 1–2) and pET30a(+)::T7promoter::6xHis::*MaPR10-GNA5* (Lanes 3–5).

All ten chromatograms of the five cloned DNA fragments were of single peaks, indicating the presence of single DNA template (Figure 4.30) in the sequenced samples. Sequencing reactions using universal T7 promoter forward and reverse primer pair revealed that the length of all cloned fragments were ~620 bp. Nucleotide sequence alignment (Appendix B-14) showed that each variant cloned into pET30(a)+ expression vector shared 100 % homology with that of *MaPR10-BeB5* and *MaPR10-GNA5*

sequences. One verified recombinant plasmid from each variant was transformed into *E. coli* strain BL21 cells.

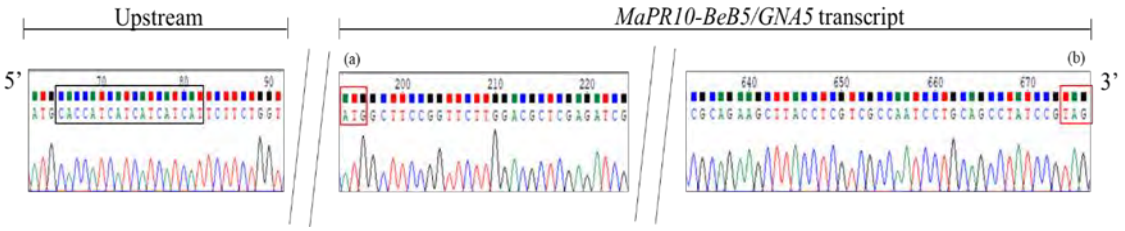

Figure 4.30: Sequence verification of *MaPR1-like* transcript fragment. An example of a concatenated chromatogram obtained after sequencing one of the pET30a(+)::T7promoter::6xHis::*MaPR10-BeB5/GNA5* vectors using a universal T7 promoter forward and reverse primer reaction showing (a) the presence of a start codon, ATG (boxed in red) and (b) the presence of a stop codon, TAG (boxed in red) indicating the 5' and 3' end of the *MaPR10-BeB5* and *MaPR10-GNA5* transcript. The presence of 6xHis tag sequence (CACCATCATCATCATCAT) at the upstream of the cloned fragment (boxed in black) confirmed the presence of the pET30(a)+ backbone sequence at the 5' end of the cassette.

4.4.3 Detection of pET30a(+)::T7promoter::6xHis::*MaPR10-BeB5/GNA5* in transformed *E. coli* strain BL21 cells via PCR

Colony PCR using universal T7 forward and reverse primer pair on *E. coli* strain BL21 cells transformed with pET30a(+)::T7Promoter::6xHis::*MaPR10-BeB5/GNA5* plasmids revealed the amplification of a ~800 bp band for all six transformed colonies of each variant (Figure 4.31). The negative control reaction showed no amplification. The presence of an unspecific band of ~1200 bp may indicate unspecific amplification or surplus amount of template used in the reactions.

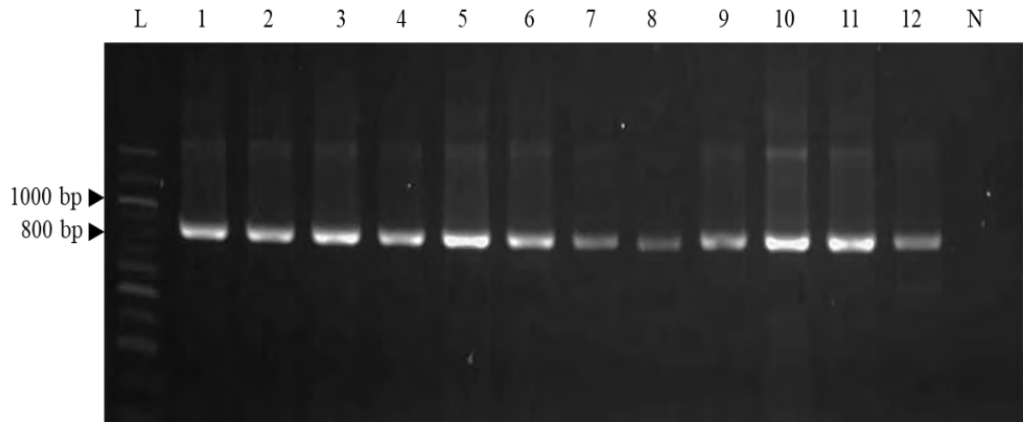

Figure 4.31: Detection of pET30a(+)::T7promoter::6xHis::*MaPR10-BeB5/GNA5* plasmids in *A. tumefaciens* strain LB4404 via colony PCR. PCR amplification yielded a high intensity band of ~800 bp indicating the presence of the cloned fragment in the transformed *E. coli* strain BL21 cells. These clones were propagated from *MaPR10-BeB5* (Lanes 1–6) and *MaPR10-GNA5* (Lanes 7–12) sequence variants. The size of amplicon was estimated using a 100 bp DNA ladder (Thermo Fisher Scientific, USA; Lane L). The negative control reaction yielded no PCR product (Lane N).

4.4.4 Expression and purification of pET30a(+)::T7promoter::6xHis::*MaPR10-BeB5/GNA5* heterologous proteins from *E. coli*

Escherichia coli strain BL21 cells which harbour the plasmids pET30a(+)::T7promoter::6xHis::*MaPR10-BeB5/GNA5* were harvested. Both soluble and insoluble crude protein samples were obtained with the former subjected to purification using nickel His Gravitrap™ affinity column. Protein quantification analysis (Table 4.1) revealed that the concentration of the soluble crude MaPR10-BeB5 protein sample was 50.87 µg/µL while 48.43 µg/µL for MaPR10-GNA5. The concentration of purified proteins was much lower with only 15.18 µg/µL for MaPR10-BeB5 variant and 11.19 µg/µL for MaPR10-GNA5 variant. SDS-PAGE of 3 µg purified protein samples showed the presence of a single protein band of ~25 kDA and a similar band size was obtained in western blot analysis. This analysis confirmed the successful expression and protein purification of MaPR10-BeB5 and MaPR10-GNA5 protein variants (Figure 4.32).

Table 4.1 Quantification of the soluble crude MaPR10 protein variants, and purified MaPR10 protein variants based on the standard curve generated from bovine serum albumin (BSA) standard solution.

Sample (Protein variants)	Concentration of crude protein (µg/µL)	Concentration of purified protein (µg/µL)
MaPR10-BeB5	50.87	15.18
MaPR10-GNA5	48.43	11.19

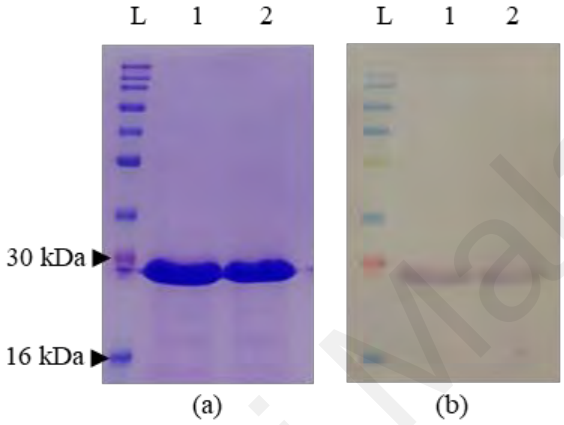

Figure 4.32: Detection of the purified MaPR10 protein variants. (a) SDS-PAGE gel separation estimated the molecular size of the MaPR10 protein variants at ~25kDa and (b) nitrocellulose membrane showing the detection of purified MaPR10-BeB5 (Lane 1) and MaPR10-GNA5 (Lane 2) protein variants using nickel His Gravitrap^{TM} affinity column showing the presence and detection of a specific protein band. Western blot analysis was conducted using anti-His primary antibody and anti-mouse IgG- alkaline phosphatase produced in goat, secondary antibody. Protein size was estimated (Lane L) based on the BLUltra Prestained Protein Ladder (Genedirex, UK).

4.5 Functional analyses of MaPR10-BeB5 and MaPR10-GNA5 protein variants

4.5.1 RNA isolation of *A. thaliana* (Col-0)

Total RNA sample was successfully isolated from the leaf tissues of *A. thaliana* (Col-0). Agarose gel electrophoresis result showed the presence of *28S* and *18S* bands (Figure 4.33). However, no DNA contaminations were observed in both samples, hence DNase treatment was not performed to the two samples. RNA quantification analysis revealed that the average concentration of the RNA samples was 0.5 µg/µL (Appendix B-15) with an average $A_{260/280}$ purity value of 2.08, indicating high amount of ribonucleic acids obtained. On the other hand, $A_{260/230}$ purity values for both samples were above 2.0,

indicating the occurrence of low amount of phenolic contamination in the samples. One of the samples was subsequently subjected to ribonuclease assay.

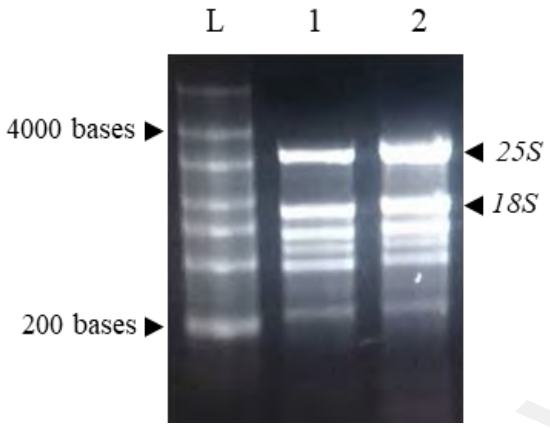

Figure 4.33: RNA extraction from *A. thaliana* (Col-0). Agarose gel electrophoresis result of the total RNA samples isolated from *A. thaliana* leaf tissues (Lane 1 & 2) showing 25S rRNA band estimated at 3200 bases and 18S rRNA band estimated at 1800 bases length. The size of RNA band was estimated using High Range RNA Riboruler (Thermo Fisher Scientific, USA; Lane L).

4.5.2 Ribonuclease (RNase) activity of MaPR10 protein variants

Most PR10 proteins in plants possess RNase activity that was associated with the presence of a P-loop domain in its gene structure. The amino acid alignment revealed that the highly conserved P-loop motif (Figure 4.19) was present in both MaPR10 protein variants, hence subjected to RNase activity analysis.

The RNase activity of the isolated protein variants MaPR10-BeB5 and MaPR10-GNA5 was evaluated by measuring the mean of A_{260} absorbance values for *A. thaliana* RNA sample that were treated with each protein isoform after 30 minutes of incubation at 50 ℃. *Arabidopsis thaliana* RNA sample without any treatment served as the negative control reaction to this experiment. This experiment revealed that the mean of A_{260} absorbance values of the treated samples increased upon treatment with each MaPR10 protein isoform (Table 4.2). The mean of absorbance unit was normalised by subtracting the absorbance value of the control sample from the mean of absorbance value of the treated sample. This analysis revealed that the total RNase activity of MaPR10-BeB5 was

at 575 U compared to only 375 U for MaPR10-GNA5. In addition, specific RNase activity for MaPR10-Be5B5 protein was 115 U μg^{-1}, and only 63 μg^{-1} for MaPR10-GNA5 protein. Specific RNase activity in this experiment was defined as the increase in A_{260} absorbance units caused by one microgram of MaPR10 protein. Therefore, this result suggested that both MaPR10 protein variants were able to function as an RNase with MaPR10-BeB5 protein possessing a higher specific RNase activity compared to MaPR10-GNA5 protein. *Arabidopsis thaliana* RNA samples used in the RNAse activity experiment were subjected to agarose gel electrophoresis (Figure 4.34) for a qualitative analysis in order to observe the degradation level of the RNA samples upon treatment with each MaPR10 protein isoform. In this analysis, all RNA samples were not visible in the agarose gel lanes when treated with MaPR10-BeB5 and MaPR10-GNA5 proteins when compared to the negative control lane (Figure 4.34b). Although the *25S* and *18S* gene bands of the untreated RNA sample appeared much fainter than that of freshly isolated RNA sample before treatment (Figure 4.34a), the bands were still present after treatment with each protein isoform and incubation at 50 ℃ for 30 minutes (Figure 4.34b). This result corroborated the quantitative data obtained in Table 4.2 and further confirmed the function of both MaPR10 protein variants as RNases.

Table 4.2 RNase activity of the purified MaPR1-BeB5 and MaPR10-GNA5 protein variants. The total RNA isolated from *A. thaliana* was digested using the two protein variants resulting in the release of free nucleotides that increased the value of A_{260} absorbance. This experiment revealed that the mean of A_{260} absorbance values of the treated samples increased upon treatment with each MaPR10 protein isoform. RNA samples were denatured when incubated in the presence of MaPR10 protein isoform for 30 minutes at 50 °C. One unit (U) of enzyme activity was defined as an increase in absorption of 0.001 caused by the amount of protein after 30 min of incubation. The mean of absorbance unit was normalised by subtracting the absorbance value of the control sample from the mean absorbance unit of the treated sample.

Purified protein variants	Absorbance Unit (AU) at A_{260}		Total RNase activity (U) for 5 µg purified protein	Specific RNase activity (U μg^{-1})
	Mean	Normalised Mean		
MaPR10-BeB5	0.751	0.575	575	115
MaPR10-GNA5	0.490	0.314	314	63
Untreated *A. thaliana* RNA (Negative control)	0.176	-	-	-

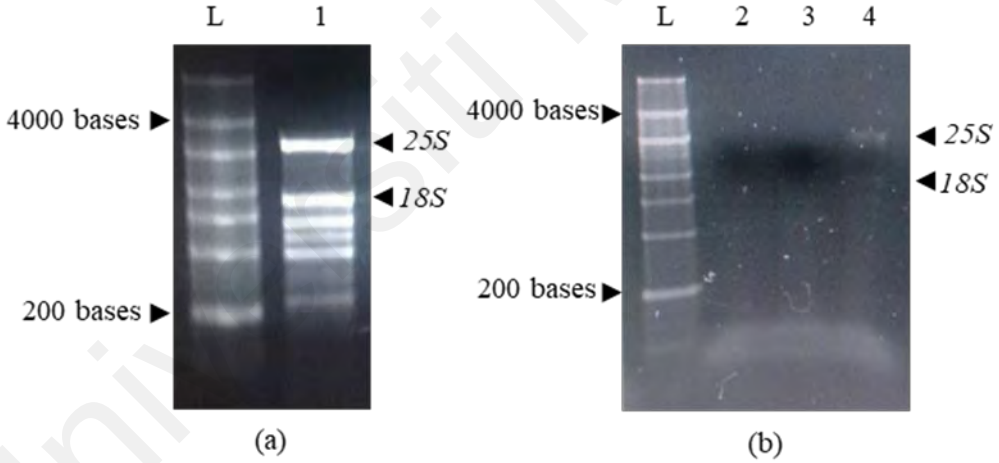

Figure 4.34 Agarose gel electrophoresis showing the denaturation of *A. thaliana* total RNA sample upon treatment with each MaPR10 protein isoform. (a) Untreated total RNA sample showed the presence of distinct 25S and 18S bands (Lane 1). (b) The loss of *25S* and *18S* rRNA bands upon treatment with MaPR10-BeB5 (Lane 2) and MaPR10-GNA5 (Lane 3) protein variants, indicating the degradation of the treated RNA samples. Compared to the freshly isolated RNA sample before treatment (Lane 1), the *25S* and *18S* bands were still present in the negative control reaction (no protein treatment; Lane 4), albeit faintly after 30 minutes incubation at 50 °C. The size of RNA band was estimated using High Range RNA Riboruler (Thermo Fisher Scientific, USA; Lane L).

4.5.3 β-1,3-glucanase activity of MaPR10-BeB5 and MaPR10-GNA5 protein variants

The presence of glycoside hydrolase group 16 (GH 16) domain in MaPR10 protein variants suggested the possibility of the protein variants to possess β-1,3-glucanase activity. Laminarin-dinitrosalicylic (DNS) acid assay revealed that both purified MaPR10 protein variants changed the colour of the substrate from bright yellow to reddish-brown after 10 minutes incubation at 50 ℃ using 3.5 µg and 10 µg protein samples (Figure 4.35). This change of colour signified the conversion of DNS into 3-amino-5-nitrosalicylic acid by β-1,3-glucanase. No colour change was observed in the negative control sample.

The intensity of reddish-brown colour was higher when laminarin was treated with MaPR10-BeB5 protein variant compared to that of MaPR10-GNA5, indicating higher concentration of glucose produced in the former. A common reducing sugar, glucose, was used as the standard sample for this experiment. Therefore, this qualitative result suggested that MaPR10 protein variants functioned as β-1,3-glucanase.

A quantitative analysis carried out on the DNS assay (Table 4.3) corroborated the qualitative result showing an increase of absorbance values at 540 nm wavelength in the presence of MaPR10 protein variants compared to the negative control, indicating the increase in β-1,3-glucanase activity in each treated sample. In this study, it was found that the 540 nm absorbance values for 3.5 µg and 10 µg MaPR10-BeB5 protein sample were 0.657 and 0.902, respectively. These values were higher than that obtained for 3.5 µg and 10 µg MaPR10-GNA5 protein sample measuring at 0.352 and 0.685, respectively. This

data suggested that MaPR10-BeB5 protein variant has higher β-1,3-glucanase activity compared to MaPR10-GNA5 protein variant.

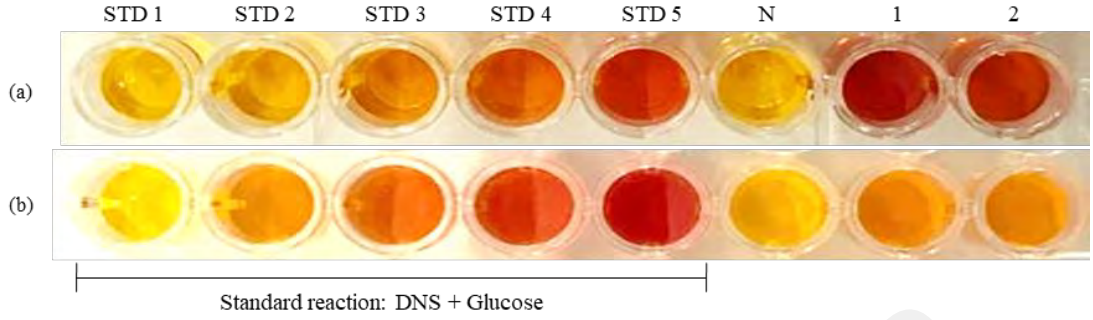

Figure 4.35 Laminarin-dinitrosalicylic (DNS) acid assay on the purified MaPR10 protein variants. The assay revealed that the purified (a) MaPR10-BeB5 and (b) MaPR10-GNA5 proteins were able to change the colour of the substrate, laminarin, from bright yellow to reddish-brown after 10 min incubation at 50 °C using 3.5 µg and 10 µg (Columns 1 and 2) of each protein sample. No colour change was observed in the negative control (Column N). The intensity of the converted laminarin colour was higher when laminarin is treated with protein variant MaPR10-BeB5 compared to that of MaPR10-GNA5, indicating a higher β-1,3-glucanase activity in the former. A common reducing sugar, glucose, was used as the standard (STD) reaction sample for this experiment. Concentrations of glucose used for the standard reactions were 0.00 mM (STD 1), 0.10 mM (STD 2), 0.25 mM (STD 3), 0.50 mM (STD 4), and 1.00 mM (STD 5).

Table 4.3 Quantitative analysis of the laminarin-DNS assay using purified MaPR10 protein variants. The table shows the absorbance value of the reduced dinitrosalicylic (DNS) acid complex measured at 540 nm wavelength indicating the reduction of laminarin into reducing sugar when treated with 3.5 µg and 10 µg MaPR10 protein variants, after incubation at 50 °C for 10 min. An increase in absorbance units (AU) at A_{540} indicates β-1,3-glucanase activity. The data showed that MaPR10-BeB5 protein variant has a higher β-1,3-glucanase activity compared to that of MaPR10-GNA5 protein variant.

Treatment on dinitrosalicylic acid complex	Absorbance unit (AU) at A_{540} for 3.5 µg protein	Absorbance unit (AU) at A_{540} for 10 µg protein	Absorbance unit (AU) at A_{540} with no protein
MaPR10-BeB5	0.657	0.902	0.151
MaPR10-GNA5	0.352	0.685	0.132

4.6 Antifungal susceptibility test of MaPR10 protein variants against human and plant opportunistic fungal pathogens

4.6.1 Morphological characterisation of *A. fumigatus*, *A. niger* and *F. oxysporum*

4.6.1.1 Morphological characterisation of *A. fumigatus* and *A. niger*

Morphological characterisation of *A. fumigatus* and *A. niger* was done as described in Nithiyaa *et al.* (2012). The formation of green-powdery and black hyphae was observed on the seven-day-old potato dextrose agar (PDA) plates cultured with *A. fumigatus*

(Figure 4.36a) and *A. niger* (Figure 4.36c) respectively. It was also observed that the spores of the cultured fungus were rounded and small (3.0-6.0 µm) (Figure 4.36b and d).

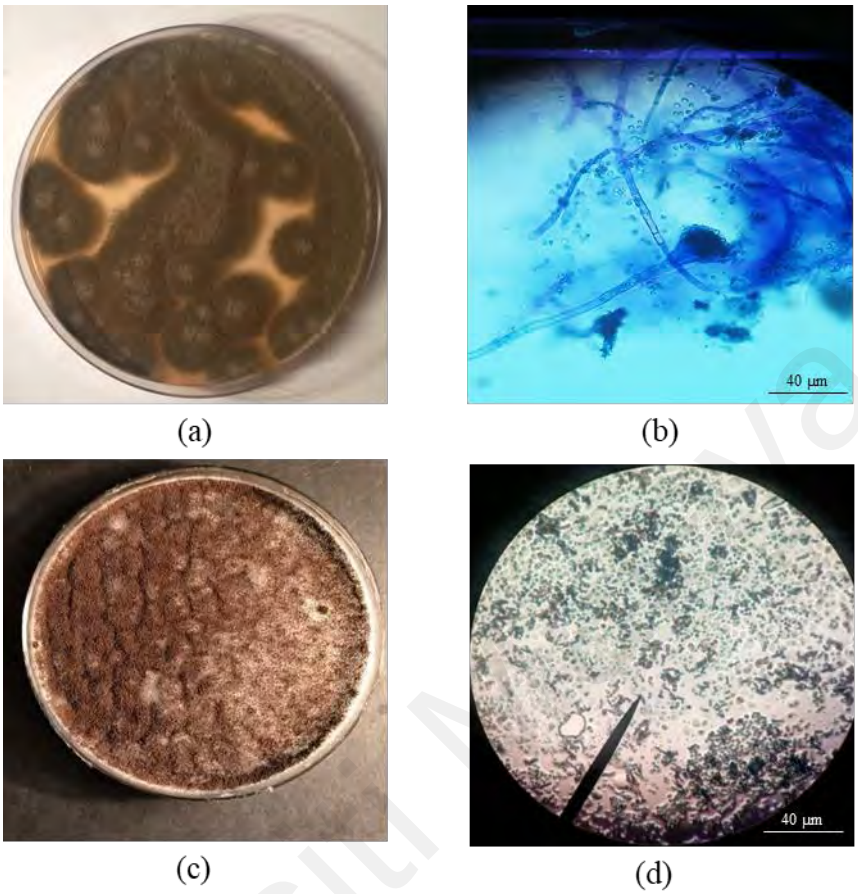

Figure 4.36 Morphological characteristics of *A. fumigatus* and *A. niger* observed under a compound microscope. The front image of PDA plates showing (a) the green-powdery hyphae of *A. fumigatus* and (c) the black hyphae of *A. niger* after seven days of culturing at 28 ℃. Under the compound microscope, the small round spores under a compound microscope with 10X magnification level were visible for both *Aspergillus* species (b & d). These morphological characteristics were consistent with that of found in *A. fumigatus* and *A. niger* as described in Nithiyaa *et al.* (2012).

4.6.1.2 Morphological characterisation of *F. oxysporum*

Morphological characterisation of *F. oxysporum* was done as described in Leslie & Summerell (2008). The formation of white hyphae was observed on the seven-day-old PDA plates cultured with *F. oxysporum* (Figure 4.37a). It was also observed that the spores of the cultured fungus were of small rod-like shape (Figure 4.37b).

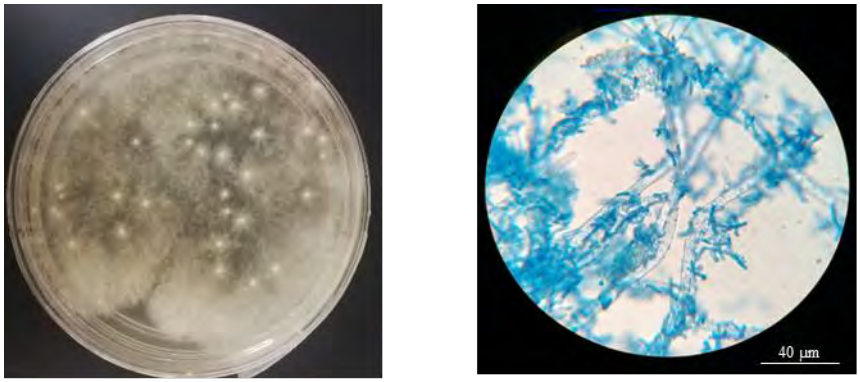

Figure 4.37 Morphological characteristics of *F. oxysporum* f. sp. *cubense*: TR4 observed under compound microscope. The front image of PDA plates showing (a) the white hyphae of *F. oxysporum* after seven days of culturing at 28 °C, and (b) the small rod- like spores under a compound microscope with 10X magnification level. These morphological characteristics were consistent with the description of *F. oxysporum* in Leslie & Summerell (2008).

4.6.2 Molecular characterisation of *A. fumigatus*, *A. niger* and *F. oxysporum*

4.6.2.1 DNA isolation from the three fungal species

Total genomic DNA was successfully isolated from *A. fumigatus*, *A. niger* and *F. oxysporum*. Agarose gel electrophoresis analysis (Figure 4.38) revealed that a high molecular weight band was obtained for each fungal species. DNA quantification showed that all three samples were of high concentration ranging from 0.3–0.5 µg/µL with an average $A_{260/280}$ value and $A_{260/230}$ value of 1.91 and 2.32, respectively (Appendix B-16).

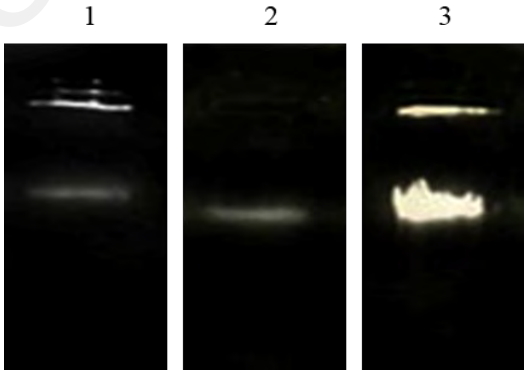

Figure 4.38 Fungal DNA extraction. Agarose gel electrophoresis result showing the detection of high molecular weight band indicating the presence of DNA sample isolated from *A. fumigatus* (Lane 1), *A. niger* (Lane 2) and *F. oxysporum* (Lane 3).

4.6.2.2 Molecular characterisation of *A.* fumigatus and *A. niger,* and *F. oxysporum*

PCR was carried out to isolate the Internal Transcribed Spacer 1 (ITS 1)-*5.8S* DNA fragment from *A. fumigatus* and *A. niger* cultures as described in Norlia *et al.* (2019).

Agarose gel electrophoresis of the PCR products showed the presence of a distinct band of ~500 bp for both *Aspergillus* species (Figure 4.39a). On the other hand, a primer pair published by Dita *et al.* (2010) was used to isolate the *28S*-intergenic spacer region (IGS)-*18S* ribosomal DNA (rDNA) fragment from *F. oxysporum* f. sp. *cubense*: TR4. Agarose gel electrophoresis revealed the amplification of a ~480 bp band for *F. oxysporum* DNA samples (Figure 4.39b). In addition, a faint band of ~1000 bp was observed in Lanes 5 and 6, indicating unspecific binding of the primers used. Note that no amplifications were obtained in the negative control reaction for both primer pairs. In addition, PCR products of *Aspergillus* spp. and *F. oxysporum* were purified and then sequenced using the designated primer pairs. All chromatograms obtained showed single peaks, indicating the presence of single DNA template (Appendix B-17) in all sequencing reactions. The length of sequences obtained for *A. fumigatus, A. niger and F. oxysporum* was 617 bp, 593 bp, and 471 bp, respectively.

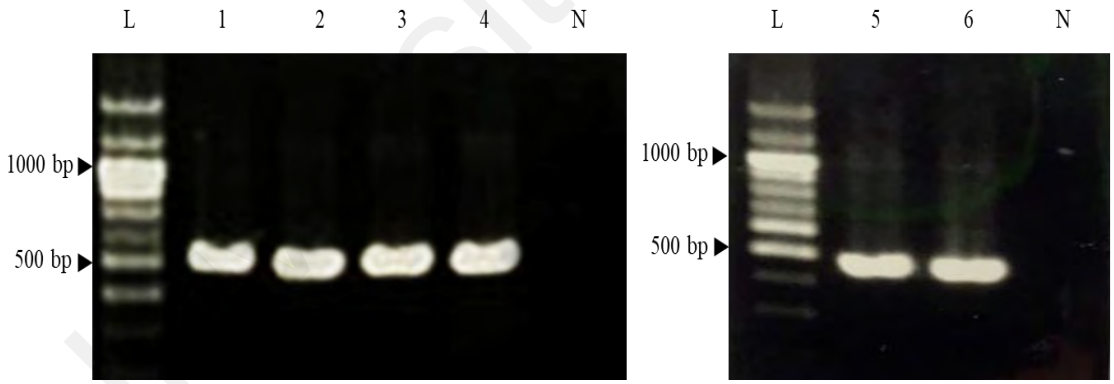

Figure 4.39 PCR amplification of isolated fragments from *A. fumigatus, A. niger and F. oxysporum*. Agarose gel electrophoresis showing the amplification of (a) a single distinct band at ~500 bp band corresponding to ITS1-*5.8S* gene fragment from *A. fumigatus* (Lanes 1 and 2) and *A. niger* (Lanes 3 and 4) DNA samples, and (b) a single distinct band of ~480 bp band corresponding to the *28S*-IGS-*18S* rDNA fragment isolated from *F. oxysporum* (Lanes 5 and 6) DNA samples. No amplification was obtained in all negative control reactions (Lane N). The size of amplicon was estimated using a 100 bp DNA ladder (Thermo Fisher Scientific, USA; Lane L).

4.6.2.3 Sequence homology analysis of ITS 1-*5.8S* rRNA fragment from *Aspergillus* spp. and *28S*-IGS-*18S* rRNA fragment isolated from *F. oxysporum*

BLASTn analysis conducted in the GenBank revealed that the query sequences shared 97–100 % similarities with ITS1-*5.8S* rRNA sequences from *A. fumigatus* (Figure 4.40a) and *A. niger* (Figure 4.40b), and *28S*-IGS-*18S* ribosomal RNA sequences from *F. oxysporum* (Figure 4.40c). This analysis suggested that the three isolated PCR amplicons isolated from *A. fumigatus*, *A. niger*, and *F. oxysporum* DNA samples indeed belong to the three fungal species, corroborating the morphological characterisation result obtained in Section 4.6.1.

Description	Max Score	Total Score	Query Cover	E value	Per. Ident	Accession
Aspergillus fumigatus isolate NIANP garden soil small subunit ribosomal RNA gene, partial sequence; internal transcribed spacer 1, 5.8S ribosomal RNA gene, and internal transcribed spac	972	972	100%	0.0	99.82%	gi|1591777491|MK640673.1
Aspergillus fumigatus isolate ZJ18 18S ribosomal RNA gene, partial sequence; internal transcribed spacer 1, 5.8S ribosomal RNA gene, and internal transcribed spacer 2, complete sequenc	972	972	100%	0.0	99.82%	gi|751136898|KP412259.1
Aspergillus fumigatus strain F1 internal transcribed spacer 1, partial sequence; 5.8S ribosomal RNA gene and internal transcribed spacer 2, complete sequence; and large subunit ribosomal	967	1123	100%	0.0	99.63%	gi|1372205463|MF276893.1
Aspergillus fumigatus strain MSEF106 internal transcribed spacer 1, partial sequence; 5.8S ribosomal RNA gene and internal transcribed spacer 2, complete sequence; and 28S ribosomal F	967	967	100%	0.0	99.63%	gi|948273721|KT311000.1
Aspergillus fumigatus strain LA18 18S ribosomal RNA gene, internal transcribed spacer 1, 5.8S ribosomal RNA gene, internal transcribed spacer 2, and 28S ribosomal RNA gene, region	967	967	100%	0.0	99.63%	gi|310947503|HQ392478.1

(a)

Description	Max Score	Total Score	Query Cover	E value	Per. Ident	Accession
Aspergillus niger strain MM1 small subunit ribosomal RNA gene, partial sequence; internal transcribed spacer 1, 5.8S ribosomal RNA gene, and internal transcribed spacer 2, complete seq	1050	1199	99%	0.0	100.00%	gi|1532309919|MH091025.1
Aspergillus sp. strain SS3 small subunit ribosomal RNA gene, partial sequence; internal transcribed spacer 1, 5.8S ribosomal RNA gene, and internal transcribed spacer 2, complete seque	1050	1050	99%	0.0	100.00%	gi|1131385151|KX928746.1
Aspergillus niger strain CMXY3556 small subunit ribosomal RNA gene, partial sequence; internal transcribed spacer 1, 5.8S ribosomal RNA gene, and internal transcribed spacer 2, comple	1047	1047	99%	0.0	100.00%	gi|1349756500|MG991583.1
Aspergillus niger isolate AP-2 small subunit ribosomal RNA gene, partial sequence; internal transcribed spacer 1, 5.8S ribosomal RNA gene, and internal transcribed spacer 2, complete se	1046	1046	99%	0.0	99.83%	gi|1693853335|MN100313.1
Aspergillus niger isolate BBRP small subunit ribosomal RNA gene, partial sequence; internal transcribed spacer 1, 5.8S ribosomal RNA gene, and internal transcribed spacer 2, complete se	1044	1044	99%	0.0	99.83%	gi|1815406122|MT123512.1

(b)

Description	Max Score	Total Score	Query Cover	E value	Per. Ident	Accession
Fusarium oxysporum f. sp. cubense strain B2-4 28S-18S ribosomal RNA intergenic spacer, partial sequence	808	808	99%	0.0	97.87%	MN830364.1
Fusarium oxysporum f. sp. cubense strain B2-2 28S-18S ribosomal RNA intergenic spacer, partial sequence	808	808	99%	0.0	97.87%	MN830363.1
Fusarium oxysporum f. sp. cubense strain B2-5 28S-18S ribosomal RNA intergenic spacer, partial sequence	808	808	99%	0.0	97.87%	MN830362.1
Fusarium oxysporum f. sp. cubense 28S-18S ribosomal RNA intergenic spacer, partial sequence	808	808	99%	0.0	97.87%	MN830361.1
Fusarium oxysporum f. sp. cubense strain B2-3 28S-18S ribosomal RNA intergenic spacer, partial sequence	808	808	99%	0.0	97.87%	MN830360.1

(c)

Figure 4.40 Sequence analysis of the isolated gene fragments from three fungal species in the GenBank. BLASTn result showing the top five BLASTn sequence hits possessing high similarity value with the query sequences. (a) ITS1-*5.8S* query sequence isolated from *A. fumigatus* culture showing 99 % similarity with garden soil *A. fumigatus* ITS1-*5.8S* gene sequences, (b) ITS1-*5.8S* query sequence isolated from *A. niger* culture showing 99–100 % similarity with *A. niger* strain MM1 ITS1-*5.8S* gene sequences, and (c) *28S*-IGS-*18S* ribosomal RNA query sequence isolated from *F. oxysporum* f. sp. *cubense*: TR4 showing 97 % similarity with *F. oxysporum* f. sp. *cubense* strain B2-4 (Tropical Race 4). All BLASTn hit results were with E-values of 0.00 and query coverage of 99–100 %, confirming the identity of the three fungal cultures obtained as *A. fumigatus*, *A. niger* and *F. oxysporum* f. sp. *cubense*: TR4.

4.6.3 Antifungal susceptibility test of MaPR10-BeB5 and MaPR10-GNA5 protein variants against *A. fumigatus*, *A. niger*, and *F. oxysporum*

The isolated MaPR10 protein variants shown to possess β-1,3-glucanase activity (Section 4.5.2). Since the fungal cell walls are made up of glucans, both protein variants were subjected to well-diffusion antifungal assay to assess their possible inhibitory effect on the three selected fungal species i.e., *A. fumigatus*, *A. niger,* and *F. oxysporum*. This

experiment revealed that 1 mg/mL of each protein variants inhibited the growth of *A. fumigatus* but not of *A. niger* and *F. oxysporum*. A clear halo region was observed on the PDA plates surrounding the well containing MaPR10-BeB5 and MaPR10-GNA5 protein variants as a result of inhibition on the growth of *A. fumigatus* colonies after four days of treatment (Figure 4.41a). When compared to the positive control plate, the inhibition level of both protein variants to *A. fumigatus*' growth was highly significant ($p < 0.01$; Figure 4.41b).

This susceptibility test suggested that both protein variants were able to exhibit antifungal effect with MaPR10-BeB5 protein variant showing higher level of inhibition compared to that of shown by MaPR10-GNA5 variant against *A. fumigatus*. However, neither MaPR10-BeB5 nor MaPR10-GNA5 showed significant inhibition level difference towards the fungal growth ($p < 0.05$). The mean of halo region diameter was 2.63 cm for MaPR10-BeB5 protein variant and 2.01 cm for MaPR10-GNA5 protein variant.

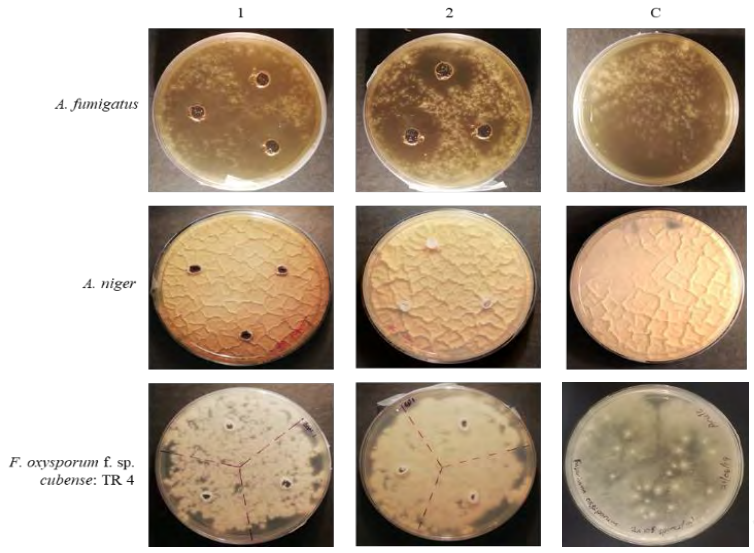

(a)

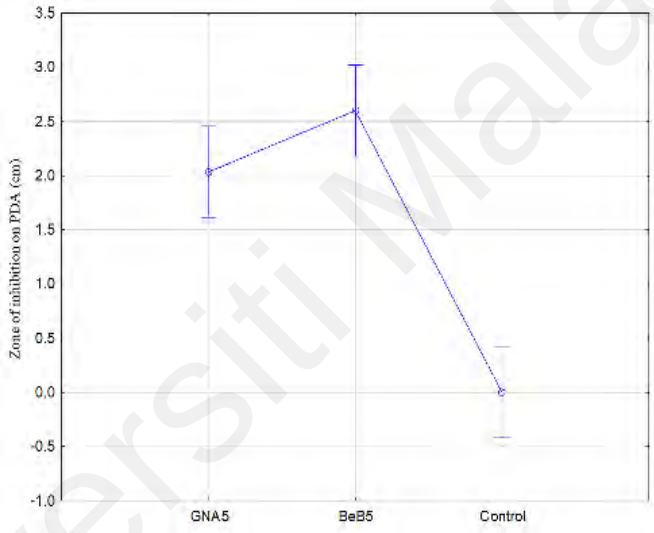

(b)

Figure 4.41 Antifungal susceptibility assay of MaPR10 protein variants against *A. fumigatus*, *A. niger* and *F. oxysporum*. (a) Well-diffusion antifungal assay of MaPR10-BeB5 and MaPR10-GNA5 protein variants against important fungi: *A. fumigatus*, *A. niger* and *F. oxysporum*. Halo regions were clearly visible on the potato-dextrose agar (PDA) plate when 1 mg/ml purified proteins (1) *Ma*PR10-BeB5, and (2) *Ma*PR10-GNA5 was treated on 2 x 10^5 *A. fumigatus* after four days of treatment at 28 °C, suggesting the existence of an antagonistic interaction between the two components. Fungal growth inhibition was not observed when the two purified proteins were treated on *A. niger* and *F. oxysporum*. In the positive control samples (C), the growth of all three fungi were observed and it was confirmed that no other factors inhibit the fungal growth. (b) The zone of inhibition (diameter of inhibition) on the growth of *A. fumigatus* against the MaPR10 proteins was measured using a ruler and was subjected to one-way ANOVA (STATISTICA 13.0) showing a significant difference ($p < 0.01$) between positive control PDA plate and PDA plate diffused with MaPR10-GNA5 and MaPR10-BeB5 protein variants. Neither MaPR10-GNA5 nor MaPR10-BeB5 protein variants showed a significant inhibition difference level ($p < 0.05$) unto the fungal growth with an average inhibition zone length of 2.01 cm-diameter for the former and 2.63 cm-diameter for the latter. Means with different letters on the bar graph are significantly different (Tukey's HSD, $p < 0.05$). Standard error bar was calculated based on the least squares mean method.

CHAPTER 5: DISCUSSION

The study on the isolation of *Pathogenesis-related 1-like* (*PR1-like*) gene from banana cultivars branched out from a study conducted by Al-Idrus *et al.* (2017) on a compatible interaction between Grand Naine (ITC 1256) and *Meloidogyne incognita*. From their proteomic data, ITC1587_Bchr9_P26466_MUSBA protein was hypothesised to be involved in banana defence against *M. incognita* infestation. tBLASTn analysis conducted on the protein sequence (Appendix B-1) revealed that this protein shared a high level of sequence similarity (81–97 %) with PR1 protein in bananas (Accession numbers of the *Musa* spp. reference sequences from the GenBank: JK271128.1 and LOC103998084, and from Banana Genome Hub database: Ma03_g08140, Ma03_g0815, Ma03_g08160 and Ma03_g15840). Therefore, a degenerate primer pair was designed (Figure 4.1) to isolate the *MaPR1-like* gene fragment from two banana cultivars namely Berangan and Grand Naine (ITC 1256). In addition, two specific primer pairs were designed to isolate the *MaPR1-like* transcript fragment of this gene from *M. incognita*-inoculated banana root tissues (Appendix B-6).

Suspicion on the gene identity was firstly triggered in the BLAST analysis conducted in the GenBank and Banana Genome Hub (BGH) databases. Although the BLASTn results of 44 genomic and 25 transcript clones in the GenBank and BGH databases suggested the identity of the isolated clones as banana *PR1* gene (Figure 4.8 and Figure 4.17) since they shared high sequence homology (84–95 %) with *MaPR1* gene sequences (Accession numbers: XM_009393226.2, XM_009393223.2, KF582558, JF271128.1 and XM_009393224.2), BLASTn analysis in the GenBank also showed result hits with *PR10* gene sequences from other plant species such as *E. guineensis* (HQ436525.1), *L. regale* (KF690636.1), and *T. aestivum* (EU908212.1) with at least 69.4 % sequence similarity (Figure 4.17d). This finding compelled the author to question the identity of the isolated genomic and transcript clones of the *PR* gene. Such misidentification has been reported

in Garino *et al.* (2015) when they discovered the misidentification of Pru du vicilin as Pru du 2S albumin for 17 years. This mistake was made since only the N-terminal region was subjected to the partial peptide sequence similarity analysis leading to the misidentification as Pru du 2S albumin peptide sequence, whereas the new bioinformatic tools such as CDD-NCBI revealed that the protein belongs to vicilin protein family. Therefore, sequence analysis was conducted using the deduced amino acid sequences instead to search for unique motifs for both PR1 and PR10 protein groups (Appendix B-9).

Two clonal variants i.e., BeB5 and GNA5 transcript fragments representing Berangan and Grand Naine (ITC 1256) cultivars, respectively, were subjected to conserved protein domain analysis using the conserved domain search tool available in the GenBank. This analysis revealed that the isolated clones belong to START/RHO alpha C/PITP/Bet v 1/CoxG/CalC (SRPBCC) protein superfamily (Figure 4.18). This protein superfamily consists of six highly similar protein domains namely the steroidogenic acute regulatory protein (StAR)-related lipid transfer (START) domains of mammalian STARD1-STARD15, C-terminal catalytic domains of the alpha oxygenase subunit of Rieske-type non-heme iron aromatic ring-hydroxylating oxygenases (RHOs_alpha_C), phosphatidylinositol transfer proteins (PITPs), Bet v 1 (the major pollen allergen of white birch, *Betula verrucosa*), CoxG, and CalC (Lu *et al.,* 2020). SRPBCC superfamily houses the Bet v 1 protein family that is generally associated with PR10 protein family. When the two cloned sequences were aligned with the deduced amino acid sequences of *PR10* genes from *L. regale* (AHG94650.1), *O. sativa* (AAL74406.1), *S. bicolor* (AAW83209.1), and *Z. mays* (ADA68331.1), it was found that these two cloned sequences shared the same conserved PR10 signature motifs with the reference sequences (Figure 4.19). These motifs were P-loop (GxGxxGxxK), Bet v I motif, and PR10 specific domain (KAXEXYL), thus confirming the identity of the isolated *MaPR1-like* gene and

transcript sequences as *PR10* gene. This finding corroborated earlier reports on PR10 proteins characterised in other plants such as *O. sativa* (Hashimoto *et al.*, 2004), *V. vinifera* (Lebel *et al.*, 2010), *Hypericum perforatum* (Karppinen *et al.*, 2016), and *Saccharum arundinaceum* (Mohan *et al*., 2019) to share the three conserved PR10 signature motifs. It is noteworthy that there were two studies conducted on *M. acuminata* PR10 proteins emphasising on the antifungal effect against *F. oxysporum* f. sp. *cubense* (Baharum *et al.*, 2018; Munusamy *et al*., 2019), but characterisation study was not performed in both studies. To further confirmed the identity of *PR10* gene studied, protein subcellular localisation assay was carried out.

Van Loon *et al.* (1994) reported that most PR proteins can either be secreted extracellularly or intracellularly localised in the vacuoles. The acidic PR proteins such as PR1 protein with N-terminal signal peptide are mostly secreted to the extracellular space (Breen *et al.,* 2017) while the basic forms are transported to the vacuole by a signal located at the C-terminus (Linthorst *et al.,* 1990). In contrast to this notion, PR10 protein family was reported as the only PR protein group that is secreted intracellularly (also termed cytosolic) (Chadha & Das, 2006). In the current study, two protein sequence variants i.e., MaPR10-BeB5 and MaPR10-GNA5 were subjected to an *in silico* prediction analysis using Plant-mPLoc. This analysis showed that both deduced amino acid sequences were intracellularly expressed due to the absence of signal peptides (Figure 4.21). An *in vivo* study was carried out to confirm the predicted result using inner epidermal cells of *A. cepa*. The latter study showed that both protein variants were indeed expressed intracellularly (Figure 4.27), further justifying the fact that the isolated clones indeed belong to *PR10* gene family, and henceforth denoted as *MaPR10* gene. Subcellular localisation studies conducted on *PR10* genes isolated from *Panax ginseng* (Moiseyev *et al.,* 1997), *Z. mays* (Zandvakili *et al.,* 2017) and *Salix matsudana* (Han *et al.,* 2017) also showed that *PR10* genes were intracellularly expressed.

The current study found that the confusion in classification of the isolated gene stemmed from mis-curation of deposited genes in the database. Although it is highly crucial for public sequence databases to be accurate, problems and challenges to manage and maintain data accuracy have long been reported (Lathe *et al.,* 2008). The possibility of coming across gene name errors in the database was known to be widespread in the scientific community (Ziemann *et al.,* 2016) due to incorrect gene identification of the organism studied (Valkiūnas *et al.,* 2008), or possible mistakes made at data-entry stage (Leray *et al.,* 2019). In relation to the finding in the current study, Fernandes *et al.* (2013) reported similar mistake such that found in the current study, of which, *PR10* gene from parsley was initially misidentified as *PR1* gene. Such circumstance may arise due to the fact that *PR10* gene was initially described as *PR1* gene when it was first isolated in parsley by Warner *et al.* (1992). This could be the reason why *PR10* gene sequences of bananas were instead curated as *PR1* sequences in both sequence databases used in the current study.

Grouping and numbering of *PR* gene families was initially based solely on their electrophoretic mobilities (Antoniw *et al.,* 1980). However, 14 years later Van Loon *et al.* (1994) discussed that the peptide sequences (or the deduced peptide sequence), serological relationship, and/or the peptide's enzymatic, or biological property(s) should be the factor(s) considered to determine the classification of a member into a *PR* gene family. This idea was adopted in this study where MaPR10 peptide sequences were first aligned with known PR10 peptide (Figure 4.19) to identify any conserved motifs found among the sequences. The sequence alignment and subcellular localisation analyses (Figure 4.27) conducted in this study confirmed that the isolated *PR* gene clones were indeed belong to the *PR10* gene family. Therefore, the author would like to suggest that the sequence data currently deposited in the GenBank (KF582558.1, JF271128.1) and

BGH database (Ma09_g15840, Ma03_g08160.1, Ma03_g08150.1 and Ma03_g08140) that were curated as *MaPR1* gene to be updated to *MaPR10* gene.

The current study identified at least three PR10 clonal variants present in Berangan and Grand Naine (ITC 1256) genomes. This was evident in the result obtained in both phylogenetic analysis (Figure 4.9) and Southern blot assays (Figure 4.10) that were carried out in this study. Dolatabadian *et al.* (2017) suggested that the occurrence of more than one copy number of a defence-related gene is advantageous to the plant in facing environmental changes. In addition, the presence of more than one *PR10* gene copy was also reported in *V. vinifera* (Lebel *et al.,* 2010), and *Lupinus luteus* genomes (Handschuh *et al.,* 2007). Walsh *et al.* (2001) suggested that these observations may be caused by multiple and independent gene duplication events in the common ancestors of a group of plant species, or a strong concerted evolution drive. However, although there were occurrences of more than one copy number of *PR10* gene in the genome of a plant, the current study found that a certain level of conservation exists in the gene as observed in the alignment analysis between the deduced amino acid sequence of *MaPR10* gene variants and *PR10* genes isolated from other plant species (Figure 4.19). Here, it was found that *PR10* gene sequence maintained three conserved motifs namely P-loop (GxGxxGxxK) domain, Bet v I motif, and PR10 specific domain (KAXEXYL) that served as the signature motifs to *PR10* gene family.

Of all the three conserved motifs present in the gene sequence, P-loop domain or also known as the glycine-rich motif (GXGGXGXXK) (Figure 4.19) plays an important role in conferring ribonuclease activity to a gene (Chadha & Das, 2006; Wu *et al.,* 2003). This motif is known as an RNA binding site. The ribonuclease activity assay conducted in the current study using the two purified protein variants MaPR10-BeB5 and MaPR10-GNA5 on *A. thaliana* total RNA sample confirmed that both variants possess ribonuclease activity, thus degrading the RNA sample used (Figure 4.34). It was found that the specific

RNase activity of the former was higher with the value of 115 U μg^{-1} compared to the latter with the value of 65 U μg^{-1} (Table 4.2). This finding corroborated other reports on PR10 proteins purified from other species e.g., pepper (Park *et al.*, 2004), peanut (Chadha & Das, 2006), and female ginseng (Pan *et al.*, 2018). Although PR10 is generally associated with ribonuclease function, Biesiadka *et al.* (2002) reported that only one of PR10 yellow lupine variants possessed RNase activity despite the other isoform having high homology level (77 %) with PR10 proteins, on account of the different conformation of P-loop domain found in each isoform. This finding suggested that not all PR10 proteins exhibit RNase activity (Pan *et al.,* 2018). In addition, Gao *et al.* (2019) proposed that PR10 protein family members may possess multiple functions.

It was suggested that PR10 protein family members are involved in numerous enzymatic properties such as in secondary metabolite biosynthesis, membrane binding process, phytohormone productions, and other hydrophobic ligand-binding mechanism for secondary metabolites storage and transport (Koistinen *et al.,* 2005). With previous reports suggesting the possible multifunctional role of PR10 proteins, the current study reports the finding of a possible novel function of the purified MaPR10 protein variants based on the presence of a unique catalytic domain EXDXXE in the two deduced amino acid sequences (Figure 4.19). This domain belongs to the glycosidase hydrolase family 16, which encodes for the β-1,3-glucanase activity (Behar *et al.,* 2018). Therefore, it was hypothesised that MaPR10-BeB5 and MaPR10-GNA5 protein variants function as β-1,3-glucanases. Interestingly, despite being a widely accepted dogma for *PR2* gene to confer β-1,3-glucanase function (Mestre *et al.,* 2017), the current study using the glucan-binding test (dinitrosalicylic acid assay) demonstrated that the two *PR10* clonal variants isolated from *M. acuminata* cultivars i.e., *MaPR10-BeB5* and *MaPR10-GNA5*, possess β-1,3-glucanase activity (Figure 4.35), thus confirming the hypothesis. This observation is the first to be reported thus far for the PR10 protein family member. Since PR10 amino acid

sequences isolated from other plants to date (Liu & Ekramoddoullah, 2006) lack the presence of the glycosidase family domain, hence, lacking β-1,3-glucanase activity, the finding on *PR10* clonal variants isolated from *M. acuminata* possessing β-1,3-glucanase activity is, to the author's knowledge, novel.

CHAPTER 6: CONCLUSION

6.1 Concluding remarks

The characterisation and functional analyses of *MaPR10* gene study revealed a successful isolation and characterisation of 69 genomic and transcript clonal sequences of *MaPR10* from Berangan and Grand Naine (ITC 1256) varieties. Although these clonal fragments were initially thought to be the members of the *PR1* gene group, further conserved domain analysis revealed that the isolated clones belong to *PR10* gene group. Phylogenetic analysis on the cloned sequences and Southern blot assays that were carried out on Berangan and Grand Naine (ITC 1256) varieties confirmed that the *MaPR10* gene exists in at least three copies in both banana genomes, reflecting its evolution as a gene that involves in plant defence.

Two clonal variants namely *MaPR10-BeB5* and *MaPR10-GNA5* were chosen for an *in vivo* sub-localisation study and further functional analyses i.e., ribonuclease and β-1,3-glucanase, representing the two banana genomes studied. The former assay concluded that both protein variants were present in cytoplasm and the latter confirmed their functions as a ribonuclease and a glucanase. It is noteworthy that the discovery of a member of the *PR10* gene group as β-1,3-glucanase is to the author's knowledge, novel. The current study also demonstrated that the two PR10 protein variants significantly inhibit the growth of *A. fumigatus* but not that of *A. niger* and *F. oxysporum* f. sp. *cubense*: TR4, which was another novel finding in this study as no other plant-based proteins have been reported to inhibit *A. fumigatus* growth, to the author's knowledge.

6.2 Future prospect

The discovery of the dual activity of MaPR10 protein variants in this study provides a new knowledge on the ability of a PR10 gene to function as both a glucanase and a ribonuclease. Although β-1,3-glucanase was synonymously associated only with the members of PR2 gene family, the current study proved that the isolated MaPR10 peptide

variants possess the same function (Figure 4.35 and Table 4.3), signifying its possible role in plant's defence against fungal pathogens. Therefore, this finding leads to the development of transgenic plant expressing this antifungal protein to demonstrate resistance against the fungi.

In addition, as previously demonstrated in this study, MaPR10 peptides were able to inhibit A. fumigatus growth. These peptides can further be subjected to the development of natural antifungal peptides using high-throughput screening (HTS) with many compounds will be evaluated to determine the biological active compounds. This finding could benefit the immunity-impaired populations against human opportunistic fungal infections. Furthermore, since synthetic antifungal peptides were reported to be less effective, the development of natural antifungal or its derivatives peptides will be promising targets to the production of antifungal drugs.

Besides that, the presence of ribonuclease activity in the isolated protein variants indicates an antiviral property of the proteins and can further be tested on economically important plant and mammalian viruses for future development of antiviral peptides using the peptide-based strategy has been used to design peptidic macrocyclic compounds with antagonistic effect against the viruses.

REFERENCES

Addy, H. S., Azizi, N. F., & Mihardjo, P. A. (2016). Detection of bacterial wilt pathogen and isolation of its bacteriophage from banana in Lumajang area, Indonesia. *International Journal of Agronomy*, *2016*, Article#5164846.

Agarwal, P., Bhatt, V., Singh, R., Das, M., Sopory, S. K., & Chikara, J. (2013). *Pathogenesis-related* gene, *JcPR-10a* from *Jatropha curcas* exhibit RNase and antifungal activity. *Molecular Biotechnology*, *54*(2), 412-425.

Agarwal, P., & Agarwal, P. K. (2014). Pathogenesis related-10 proteins are small, structurally similar but with diverse role in stress signaling. *Molecular Biology Reports*, *41*(2), 599-611.

Aglas, L., Soh, W. T., Kraiem, A., Wenger, M., Brandstetter, H., & Ferreira, F. (2020). Ligand binding of PR-10 proteins with a particular focus on the Bet v 1 allergen family. *Current Allergy and Asthma Reports*, *20*(7), 1-11.

Al-Abdalall, A. H. A. (2009). Production of aflatoxins by *Aspergillus flavus* and *Aspergillus niger* strains isolated from seeds of pulses. *Journal of Food Agriculture and Environment*, *7*, 33-39.

Al-Idrus, A., Carpentier, S. C., Ahmad, M. T., Panis, B., & Mohamed, Z. (2017). Elucidation of the compatible interaction between banana and *Meloidogyne incognita* via high-throughput proteome profiling. *PloS ONE, 12*(6), Article#e0178438.

Alastruey-Izquierdo, A., Melhem, M. S., Bonfietti, L. X., & Rodriguez-Tudela, J. L. (2015). Susceptibility test for fungi: Clinical and laboratorial correlations in medical mycology. *Revista do Instituto de Medicina Tropical de São Paulo*, *57*, 57-64.

Alberts, B., Johnson, A., Lewis, J., Raff, M., Roberts, K., & Walter, P. (2002). How genomes evolve. In *Molecular Biology of the Cell* (4th Edition). New York, USA: Garland Science.

Ali, S., Ganai, B. A., Kamili, A. N., Bhat, A. A., Mir, Z. A., Bhat, J. A., ... Grover, A. (2018). Pathogenesis-related proteins and peptides as promising tools for engineering plants with multiple stress tolerance. *Microbiological Research*, *212*, 29-37.

Alexander, D., Goodman, R. M., Gut-Rella, M., Glascock, C., Weymann, K., Friedrich, L., ... Ward, E. (1993). Increased tolerance to two oomycete pathogens in transgenic tobacco expressing pathogenesis-related protein 1a. *Proceedings of the National Academy of Sciences, 90*(15), 7327-7331.

Antoniw, J. F., Ritter, C. E., Pierpoint, W. S., & Van Loon, L. C. (1980). Comparison of three pathogenesis-related proteins from plants of two cultivars of tobacco infected with TMV. *Journal of General Virology*, *47*(1), 79-87.

Arnoys, E. J., & Wang, J. L. (2007). Dual localization: Proteins in extracellular and intracellular compartments. *Acta Histochemica*, *109*(2), 89-110.

Aurore, G., Parfait, B., & Fahrasmane, L. (2009). Bananas, raw materials for making processed food products. *Trends in Food Science & Technology, 20*(2), 78-91.

Baharum, N. A., Othman, R. Y., Mohd-Yusuf, Y., Tan, B. C., Zaidi, K., & Khalid, N. (2018). The effect of *Pathogenesis-Related 10* (*Pr-10*) gene on the progression of Fusarium wilt in *Musa acuminata* cv. Berangan. *Sains Malaysiana*, *47*(10), 2291-2300.

Bailey, M. J., Biely, P., & Poutanen, K. (1992). Interlaboratory testing of methods for assay of xylanase activity. *Journal of Biotechnology*, *23*(3), 257-270.

Ballard, E., Yucel, R., Melchers, W. J., Brown, A. J., Verweij, P. E., & Warris, A. (2020). Antifungal activity of antimicrobial peptides and proteins *against Aspergillus fumigatus*. *Journal of Fungi, 6*(2), Article#65.

Balint-Kurti, P. (2019). The plant hypersensitive response: Concepts, control, and consequences. *Molecular Plant Pathology, 20*(8), 1163-1178.

Banana Market Review Snapshot February 2020. (2020). Retrieved 2 January 2020, from http://www.fao.org/3/ca9212en/ca9212en.pdf

Bantignies, B., Séguin, J., Muzac, I., Dédaldéchamp, F., Gulick, P., & Ibrahim, R. (2000). Direct evidence for ribonucleolytic activity of a PR-10-like protein from white lupin roots. *Plant Molecular Biology*, *42*(6), 871-881.

Barber, A. E., Scheufen, S., Walther, G., Kurzai, O., & Schmidt, V. (2020). Low rate of azole resistance in cases of avian aspergillosis in Germany. *Medical Mycology*, *58*(8), 1187-1190.

Beadle, G. W., & Tatum, E. L. (1941). Genetic control of biochemical reactions in *Neurospora*. *Proceedings of the National Academy of Sciences of the United States of America*, *27*(11), 499.

Becker, S., Scheffel, A., Polz, M. F., & Hehemann, J. H. (2017). Accurate quantification of laminarin in marine organic matter with enzymes from marine microbes. *Applied and Environmental Microbiology*, *83*(9). Article#e03389-16.

Behar, H., Graham, S., & Brumer, H. (2018). Strength through diversity: The evolution of plant cell wall glucan-active enzymes in GH16. In *Glycobiology 28*(12), New York, USA: Oxford Univ. Press Inc.

Berger, S., El Chazli, Y., Babu, A. F., & Coste, A. T. (2017). Azole resistance in *Aspergillus fumigatus*: A consequence of antifungal use in agriculture? *Frontiers in Microbiology, 8*, Article#1024.

Berkow, E. L., Lockhart, S. R., & Ostrosky-Zeichner, L. (2020). Antifungal susceptibility testing: Current approaches. *Clinical Microbiology Reviews*, *33*(3), Article#e00069-19.

Biesiadka, J., Bujacz, G., Sikorski, M. M., & Jaskolski, M. (2002). Crystal structures of two homologous pathogenesis-related proteins from yellow lupine. *Journal of Molecular Biology*, *319*(5), 1223-1234.

Blomme, G., Dita, M., Jacobsen, K. S., Pérez Vicente, L., Molina, A., Ocimati, W., ... Prior, P. (2017). Bacterial diseases of bananas and enset: Current state of knowledge and integrated approaches toward sustainable management. *Frontiers in Plant Science*, *8*, Article#1290.

Bocate, K. P., Reis, G. F., de Souza, P. C., Junior, A. G. O., Durán, N., Nakazato, G., ... Panagio, L. A. (2019). Antifungal activity of silver nanoparticles and simvastatin against toxigenic species of Aspergillus. *International Journal of Food Microbiology*, *291*, 79-86.

Boning, C. R. (2006). *Florida's best fruiting plants*, Florida, USA: Pineapple Press, Inc.

Bouchez, D., & Höfte, H. (1998). Functional genomics in plants. *Plant Physiology*, *118*(3), 725-732.

Brakhage, A. A., Bruns, S., Thywissen, A., Zipfel, P. F., & Behnsen, J. (2010). Interaction of phagocytes with filamentous fungi. *Current Opinion in Microbiology*, *13*(4), 409-415.

Breen, S., Williams, S. J., Outram, M., Kobe, B., & Solomon, P. S. (2017). Emerging insights into the functions of Pathogenesis-Related protein 1. *Trends in Plant Science*, *22*(10), 871-879.

Breiteneder, H., Pettenburger, K., Bito, A., Valenta, R., Kraft, D., Rumpold, H., Scheiner, O., & Breitenbach, M. (1989). The gene coding for the major birch pollen allergen Bet v 1, is highly homologous to a pea disease resistance response gene. *The EMBO journal*, *8*(7), 1935-1938.

Britannica, Editors of Encyclopaedia (2020, October 29). *Banana*. Retrieved from https://www.britannica.com/plant/banana-plant

Cairns, T. C., Nai, C., & Meyer, V. (2018). How a fungus shapes biotechnology: 100 years of *Aspergillus niger* research. *Fungal Biology and Biotechnology*, *5*(1), 1-14.

Calderan-Rodrigues, M. J., Fonseca, J. G., Clemente, H. S., Labate, C. A., & Jamet, E. (2018). Glycoside hydrolases in plant cell wall proteomes: Predicting functions that could be relevant for improving biomass transformation processes. *Advances in Biofuels and Bioenergy, 1*, 165-182.

Carlier, J., De Waele, D., & Escalant. J. V. (2002). Global evaluation of *Musa* germplasm for resistance to Fusarium wilt, Mycosphaerella leaf spot diseases and nematodes. In A. Vézina & C. Picq (Eds.), *INIBAP Technical Guidelines 6* (pp 1-64). Montpellier, France: The International Network for the Improvement of Banana and Plantain.

Castro, A., Vidal, S., & Ponce de León, I. (2016). Moss pathogenesis-related-10 protein enhances resistance to *Pythium irregulare* in *Physcomitrella patens* and *Arabidopsis thaliana*. *Frontiers in Plant Science, 7*, Article#580.

CDC, Isolate submission opportunity: Monitoring for Azole resistance in *Aspergillus fumigatus,* resources, fungal Diseases, CDC (2019). Retrieved 18 September 2020, from https://www.cdc.gov/fungal/aspergillus-resistance.html

Chadha, P., & Das, R. H. (2006). A pathogenesis related protein, AhPR10 from peanut: An insight of its mode of antifungal activity. *Planta, 225*(1), 21 3-222.

Chamnongpol, S., Willekens, H., Moeder, W., Langebartels, C., Sandermann, H., Van Montagu, … Van Camp, W. (1998). Defense activation and enhanced pathogen tolerance induced by H_2O_2 in transgenic tobacco. *Proceedings of the National Academy of Sciences*, *95*(10), 5818-5823.

Chen, Z. Y., Brown, R. L., Rajasekaran, K., Damann, K. E., & Cleveland, T. E. (2006). Identification of a maize kernel pathogenesis-related protein and evidence for its involvement in resistance to *Aspergillus flavus* infection and aflatoxin production. *Phytopathology*, *96*(1), 87-95.

Chester, K. S. (1933). The problem of acquired physiological immunity in plants. *The Quarterly Review of Biology*, *8*(3), 275-324.

Choudhary, D. K., Prakash, A., & Johri, B. N. (2007). Induced systemic resistance (ISR) in plants: Mechanism of action. *Indian Journal of Microbiology*, *47*(4), 289-297.

Coleman, J. J., Ghosh, S., Okoli, I., & Mylonakis, E. (2011). Antifungal activity of microbial secondary metabolites. *PloS ONE*, *6*(9), Article#e25321.

Costa, J. H., Wassano, C. I., Angolini, C. F. F., Scherlach, K., Hertweck, C., & Fill, T. P. (2019). Antifungal potential of secondary metabolites involved in the interaction between citrus pathogens. *Scientific Reports*, *9*(1), 1-11.

Coyne, D. (2016). Sustainable agricultural intensification in Sub-Saharan Africa and the role of nematodes. In B. Habtegebriel (Ed.), *Post-harvest Pest Management Research, Education and Extension in Ethiopia: The Status and Prospects, Proceedings of the 22nd Annual Conference* (pp. 61-69), Ethiopia: Plant Protection Society of Ethiopia.

Dai, L., Wang, D., Xie, X., Zhang, C., Wang, X., Xu, Y., … & Zhang, J. (2016). The novel gene *VpPR4-1* from *Vitis pseudoreticulata* increases powdery mildew resistance in transgenic *Vitis vinifera* L. *Frontiers in Plant Science*, *7*, Article#695.

Danchin, E. G., Arguel, M. J., Campan-Fournier, A., Perfus-Barbeoch, L., Magliano, M., Rosso, M. N., … Abad, P. (2013). Identification of novel target genes for safer and more specific control of root-knot nematodes from a pan-genome mining. *PLoS Pathogen*, *9*(10), Article#e1003745.

Dangl, J. L., & Jones, J. D. (2001). Plant pathogens and integrated defence responses to infection. *Nature*, *411*(6839), 826-833.

Datta, K., Velazhahan, R., Oliva, N., Ona, I., Mew, T., Khush, G. S., … & Datta, S. K. (1999). Over-expression of the cloned rice thaumatin-like protein (PR-5) gene in transgenic rice plants enhances environmental friendly resistance to *Rhizoctonia solani* causing sheath blight disease. *Theoretical and Applied Genetics*, *98*(6-7), 1138-1145.

Davide, R. G. (1996). Overview of nematodes as a limiting factor in *Musa* production. In E. A. Frison, J. P. Horry & D. De Waele (Eds.), *New Frontiers in Resistance Breeding for Nematode, Fusarium and Sigatoka* (pp. 27-31). Montpellier, France: The International Network for the Improvement of Banana and Plantain.

De la Cruz, J., Pintor-Toro, J. A., Benitez, T., & Llobell, A. (1995). Purification and characterization of an endo-beta-1, 6-glucanase from *Trichoderma harzianum* that is related to its mycoparasitism. *Journal of Bacteriology*, *177*(7), 1864-1871.

De Vries, R. P., & Visser, J. (2001). Aspergillus enzymes involved in degradation of plant cell wall polysaccharides. *Microbiology and Molecular Biology Reviews*, *65*(4), 497-522.

De Waele, D., & Davide, R. G. (1998). *The root-knot nematodes of banana*: International Network for the Improvement of Banana and Plantain [Electronic version]. *Musa Pest Fact Sheet*, *3*. Retrieved from https://www.bioversityinternational.org/fileadmin/user_upload/online_library/publications/pdfs/697.pdf

Dita, M. A., Waalwijk, C., Buddenhagen, I. W., Souza Jr, M. T., & Kema, G. H. J. (2010). A molecular diagnostic for tropical race 4 of the banana fusarium wilt pathogen. *Plant Pathology*, *59*(2), 348-357.

Dolatabadian, A., Patel, D. A., Edwards, D., & Batley, J. (2017). Copy number variation and disease resistance in plants. *Theoretical Applied Genetics, 130*(12), 2479-2490.

Dönnes, P., & Höglund, A. (2004). Predicting protein subcellular localization: Past, present, and future. *Genomics, Proteomics & Bioinformatics*, *2*(4), 209-215.

Ebrahim, S., Usha, K., & Singh, B. (2011). Pathogenesis related (PR) proteins in plant defense mechanism. In A. M ndez-Vilas (Ed.), *Science against microbial pathogens: Communicating current research and technological advances*, *3* (pp. 1043-1054), Badajoz, Spain: Formatex Research Center.

Edreva, A. (2005). Pathogenesis-related proteins: Research progress in the last 15 years. *General and Applied Plant Physiology, 31*(1-2), 105-124.

EST: Bananas. (2019). Retrieved 11 October 2020, from http://www.fao.org/economic/est/est-commodities/bananas/en/

Fallath, T., Rosli, A. B., Kidd, B., Carvalhais, L. C., & Schenk, P. M. (2017). Toward plant defense mechanisms against root pathogens. *Agriculturally Important Microbes for Sustainable Agriculture*, 293-313.

Fan, S., Jiang, L., Wu, J., Dong, L., Cheng, Q., Xu, P., & Zhang, S. (2015). A novel pathogenesis-related class 10 protein Gly m 4l, increases resistance upon *Phytophthora sojae* infection in soybean (*Glycine max* [L.] Merr.). *PLoS ONE*, 10(10), Article#e0140364.

Favery, B., Quentin, M., Jaubert-Possamai, S., & Abad, P. (2016). Gall-forming root-knot nematodes hijack key plant cellular functions to induce multinucleate and hypertrophied feeding cells. *Journal of Insect Physiology*, *84*, 60-69.

Fernandes, H., Michalska, K., Sikorski, M., & Jaskolski, M. (2013). Structural and functional aspects of PR-10 proteins. *The FEBS Journal, 280*(5), 1169-1199.

Ferreira, R. B., Monteiro, S. A. R. A., Freitas, R., Santos, C. N., Chen, Z., Batista, L. M., ... Teixeira, A. R. (2007). The role of plant defence proteins in fungal pathogenesis. *Molecular Plant Pathology*, *8*(5), 677-700.

Ferreira, S. A., Trujillo, E. E., & Ogata, D. Y. (1997). Banana bunchy top virus. In *Plant Disease PD-12* (pp. 1-4), College of Tropical Agriculture and Resources, University of Hawaii, Honolulu, Hawaii, USA.

Filipenko, E. A., Kochetov, A. V., Kanayama, Y., Malinovsky, V. I., & Shumny, V. K. (2013). PR-proteins with ribonuclease activity and plant resistance against pathogenic fungi. *Russian Journal of Genetics: Applied Research*, *3*(6), 474-480.

Finkina, E.I., Melnikova, D.N., Bogdanov, I.V., & Ovchinnikova, T. (2017). Plant pathogenesis-related proteins PR-10 and PR-14 as components of innate immunity system and ubiquitous allergens. *Current Medicinal Chemistry, 24*(17), 1772-1787.

Fischer, M. S., & Glass, N. L. (2019). Communicate and fuse: how filamentous fungi establish and maintain an interconnected mycelial network. *Frontiers in Microbiology*, *10*(619).

Fones, H. N., Bebber, D. P., Chaloner, T. M., Kay, W. T., Steinberg, G., & Gurr, S. J. (2020). Threats to global food security from emerging fungal and oomycete crop pathogens. *Nature Food, 1*(6), 332-342.

Fourie, G., Steenkamp, E. T., Ploetz, R. C., Gordon, T. R., & Viljoen, A. (2011). Current status of the taxonomic position of *Fusarium oxysporum* formae specialis *cubense* within the *Fusarium oxysporum* complex. *Infection, genetics, and evolution, 11*(3), 533–542.

Frisvad, J. C., Larsen, T. O., De Vries, R., Meijer, M., Houbraken, J., Cabañes, F. J., ... Samson, R. A. (2007). Secondary metabolite profiling, growth profiles and other tools for species recognition and important *Aspergillus* mycotoxins. *Studies in mycology*, *59*, 31-37.

Fu, Z. Q., & Dong, X. (2013). Systemic acquired resistance: Turning local infection into global defense. *Annual Review of Plant Biology*, *64*, 839-863.

Fujimoto, Y., Nagata, R., Fukasawa, H., Yano, K., Azuma, M., Iida, A., Sugimoto, S., Shudo, K., & Hashimoto, Y. (1998). Purification and cDNA cloning of cytokinin-specific binding protein from mung bean (*Vigna radiata*). *European Journal of Biochemistry*, *258*(2), 794-802.

Gao, L. (2019). Structure Analysis of a Pathogenesis-Related 10 Protein from *Gardenia jasminoides*. In *IOP Conference Series: Earth and Environmental Science, 242*(p. 042005). United Kingdom : IOP Publishing.

Garino, C., De Paolis, A., Coïsson, J. D., & Arlorio, M. (2015). Pru du 2S albumin or Pru du vicilin? *Computational Biology and Chemistry*, *56*, 30-32.

Gautam, A. K., Sharma, S., Avasthi, S., & Bhadauria, R. (2011). Diversity, pathogenicity, and toxicology of *A. niger*: An important spoilage fungi. *Research Journal of Microbiology*, *6*(3), 270-280.

Ghose, T. K. (1987). Measurement of cellulase activities. *Pure Applied Chemistry*, *59*(2), 257-268.

Gianinazzi, S., Martin, C., & Vallee, J. (1970). Hypersensitivity to viruses, temperature, and soluble proteins in *Nicotiana xanthi* n.c. Appearance of new macromolecules at the repression of viral synthesis. *Weekly reports of the sessions of the Academy of Sciences: Series D, 270*, 2383-2386.

Gimenez-Ibanez, S., Chini, A., & Solano, R. (2016). How microbes twist jasmonate signaling around their little fingers. *Plants*, *5*(1), Article#9.

Gold, C. S., Karamura, E. B., Kiggundu, A., Bagamba, F., & Abera, A. M. (1999). Geographic shifts in the highland cooking banana (*Musa* spp., group AAA-EA) production in Uganda. *International Journal of Sustainable Development & World Ecology, 6*(1), 45-59.

Gonneau, M., Pagant, S., Brun, F., & Laloue, M. (2001). Photoaffinity labelling with the cytokinin agonist azido-CPPU of a 34 kDa peptide of the intracellular pathogenesis-related protein family in the moss *Physcomitrella patens*. *Plant Molecular Biology*, *46*(5), 539-548.

Gonzlez Mendoza, D., Argumedo Delira, R., Morales Trejo, A., Pulido Herrera, A., Cervantes Daz, L., Grimaldo Juarez, O., & Alarcón, A. (2010). A rapid method for isolation of total DNA from pathogenic filamentous plant fungi. *Genetics Molecular Research, 9*(1), 162-166.

Gowen, S., Quénéhervé, P., & Fogain, R. (2005). Nematode parasites of bananas and plantains. In M. Luc, R. A. Sikora & J. Bridge (Eds.), *Plant parasitic nematodes in subtropical and tropical agriculture, 2* (pp. 611-643), Oxfordshire, United Kingdom: CABI Publishing.

Green, M. R., & Sambrook, J. (2020). Cloning in plasmid vectors: Directional cloning. *Cold Spring Harbor Protocols*, *2020*(11).

Guerra-Guimarães, L., Pinheiro, C., Chaves, I., Barros, D. R., & Ricardo, C. P. (2016). Protein dynamics in the plant extracellular space. *Proteomes*, *4*(3), Article#22.

Gumus, T., Demirci, A. S., Sagdic, O., & Arici, M. (2010). Inhibition of heat resistant molds: *Aspergillus fumigatus* and *Paecilomyces variotii* by some plant essential oils. *Food Science and Biotechnology*, *19*(5), 1241-1244.

Gururani, M. A., Venkatesh, J., Upadhyaya, C. P., Nookaraju, A., Pandey, S. K., & Park, S. W. (2012). Plant disease resistance genes: Current status and future directions. *Physiological and Molecular Plant Pathology*, *78*, 51-65.

Gusakov, A. V., Kondratyeva, E. G., & Sinitsyn, A. P. (2011). Comparison of two methods for assaying reducing sugars in the determination of carbohydrase activities. *International Journal of Analytical Chemistry*, Article#283658.

Hamid, R., Khan, M. A., Ahmad, M., Ahmad, M. M., Abdin, M. Z., Musarrat, J., & Javed, S. (2013). Chitinases: an update. *Journal of Pharmacy & Bioallied Sciences*, *5*(1), 21-29.

Han, G. Z. (2019). Origin and evolution of the plant immune system. *New Phytologist*, *222*(1), 70-83.

Han, X., He, X., Qiu, W., Lu, Z., Zhang, Y., Chen, S., Liu, M., Qiao, G., and Zhuo, R. (2017). Pathogenesis-related protein PR10 from *Salix matsudana* Koidz exhibits resistance to salt stress in transgenic *Arabidopsis thaliana*. *Environmental and Experimental Botany, 141*, 74-82.

Handschuh, L., Femiak, I., Kasperska, A., Figlerowicz, M., & Sikorski, M. M. (2007). Structural and functional characteristics of two novel members of pathogensis-related multigene family of class 10 from yellow lupine. *Acta Biochimica Polonica, 54*(4), 783-796.

Hashimoto, M., Kisseleva, L., Sawa, S., Furukawa, T., Komatsu, S., & Koshiba, T. (2004). A novel rice PR10 protein, RSOsPR10, specifically induced in roots by biotic and abiotic stresses, possibly via the jasmonic acid signaling pathway. *Plant and Cell Physiology*, *45*(5), 550-559.

Hatanaka, C., & Kobara, Y. (1980). Determination of glucose by a modification of Somogyi-Nelson method. *Agricultural and Biological Chemistry*, *44*(12), 2943-2949.

Heslop-Harrison, J. S., & Schwarzacher, T. (2007). Domestication, genomics, and the future for banana. *Annals of Botany, 100*(5), 1073-1084.

Hieter, P., & Boguski, M. (1997). Functional genomics: it's all how you read it. *Science*, *278*(5338), 601-602.

Hoffmann-Sommergruber, K., Vanek-Krebitz, M., Radauer, C., Wen, J., Ferreira, F., Scheiner, O., & Breiteneder, H. (1997). Genomic characterization of members of the Bet v 1 family: genes coding for allergens and pathogenesis-related proteins share intron positions. *Gene*, *197*(1-2), 91-100.

Holbein, J., Grundler, F. M., & Siddique, S. (2016). Plant basal resistance to nematodes: an update. *Journal of Experimental Botany, 67*(7), 2049-2061.

Hombach, M., Zbinden, R., & Böttger, E. C. (2013). Standardisation of disk diffusion results for antibiotic susceptibility testing using the sirscan automated zone reader. *BMC Microbiology*, *13*(1), 1-8.

Hope, J. (2013). A review of the mechanism of injury and treatment approaches for illness resulting from exposure to water-damaged buildings, mold, and mycotoxins. *The Scientific World Journal*, *2013*.

Jain, A., Jain, R., & Jain, S. (2020). Quantitative analysis of reducing sugars by 3, 5-dinitrosalicylic acid (DNSA method). In *Basic Techniques in Biochemistry, Microbiology and Molecular Biology* (pp. 181-183). New York, USA: Humana.

Jain, D., & Khurana, J. P. (2018). Role of pathogenesis-related (PR) proteins in plant defense mechanism. In *Molecular aspects of plant-pathogen interaction* (pp. 265-281). Singapore: Springer.

Jain, S., & Kumar, A. (2015). The pathogenesis related class 10 proteins in plant defense against biotic and abiotic stresses. *Advances in Plants & Agriculture Research, 2*(7), 305-314.

Jalil, M., Khalid, N., & Othman, R. Y. (2003). Plant regeneration from embryogenic suspension cultures of *Musa acuminata* cv. Mas (AA). *Plant Cell, Tissue and Organ Culture*, *75*(3), 209-214.

Jaouannet, M., Perfus-Barbeoch, L., Deleury, E., Magliano, M., Engler, G., Vieira, P., … Abad, P. (2012). A root-knot nematode-secreted protein is injected into giant cells and targeted to the nuclei. *New Phytologist, 194*(4), 924-931.

Jarvis, P., & Robinson, C. (2004). Mechanisms of protein import and routing in chloroplasts. *Current Biology*, *14*(24), R1064-R1077.

Jepson, S. B. (1987). *Identification of root-knot nematodes (*Meloidogyne *species).* Wallingford, United Kingdom: CAB International.

Jones, D. T., Taylor, W. R., & Thornton, J. M. (1992). The rapid generation of mutation data matrices from protein sequences. *Bioinformatics*, *8*(3), 275-282.

Jones, J. T., Haegeman, A., Danchin, E. G., Gaur, H. S., Helder, J., Jones, M. G., … Perry, R. N. (2013). Top 10 plant-parasitic nematodes in molecular plant pathology. *Molecular Plant Pathology, 14*(9), 946-961.

Jooste, A., Wessels, N., & Van der Merwe, M. (2016). First Report of Banana bunchy top virus in Banana (*Musa* spp.) from South Africa. *Plant Disease, 100*(6).

Karppinen, K., Derzsó, E., Jaakola, L., & Hohtola, A. (2016). Molecular cloning and expression analysis of *hyp-1 type PR-10* family genes in *Hypericum perforatum*. *Frontiers in Plant Science*, *7*, Article#526.

Kaur, A., Pati, P. K., Pati, A. M., & Nagpal, A. K. (2020). Physico-chemical characterization and topological analysis of pathogenesis-related proteins from *Arabidopsis thaliana* and *Oryza sativa* using *in-silico* approaches. *PloS ONE*, *15*(9), Article#e0239836.

Kaur, P. K., Joshi, N., Singh, I. P., & Saini, H. S. (2017). Identification of cyclic lipopeptides produced by *Bacillus vallismortis* R2 and their antifungal activity *against Alternaria alternata*. *Journal of Applied Microbiology*, *122*(1), 139-152.

Khan, M. F., & Umar, U. U. D. (2021). Application of a robust microplate assay to determine induced β-1, 3-glucanase and chitinase activity in the cotton plant. *BioTechniques*, (0).

Khayat, E., Duvdevani, A., Lahav, E., & Ballesteros, B. (2004). Somaclonal variation in banana (*Musa acuminata* cv. Grande Naine). Genetic mechanism, frequency, and application as a tool for clonal selection. In *Banana improvement: Cellular, Molecular Biology, and Induced Mutations* (pp. 97-109). Leuven, Belgium: Science Publishers, Inc.

Kistner, C., & Matamoros, M. (2005). RNA isolation using phase extraction and LiCl precipitation. In *Lotus* japonicus handbook (pp. 123-124). Springer, Dordrecht.

Koistinen, K. M., Soininen, P., Venäläinen, T. A., Häyrinen, J., Laatikainen, R., Peräkylä, M., Tervahauta, A. I., & Kärenlampi, S. O. (2005). Birch PR-10c interacts with several biologically important ligands. *Phytochemistry*, *66*(21), 2524-2533.

Koonin, E. V., & Galperin, M. Y. (2003). Principles and methods of sequence analysis. In *Sequence—Evolution—Function* (pp. 111-192). Boston, Massachusetts, USA: Springer.

Kombrink, E., & Schmelzer, E. (2001). The hypersensitive response and its role in local and systemic disease resistance. *European Journal of Plant Pathology, 107*(1), 69-78.

Kumar, S., Stecher, G., Li, M., Knyaz, C., & Tamura, K. (2018). MEGA X: Molecular evolutionary genetics analysis across computing platforms. *Molecular Biology Evolution 35*(6), 1547-1549.

Lass-Flörl, C., Cuenca-Estrella, M., Denning, D. W., & Rodriguez-Tudela, J. L. (2006). Antifungal susceptibility testing in *Aspergillus* spp. according to EUCAST methodology. *Medical Mycology*, *44*(Supplement_1), S319-S325.

Latgé, J. P., & Chamilos, G. (2019). *Aspergillus fumigatus* and Aspergillosis in 2019. *Clinical Microbiology Reviews*, *33*(1).

Lathe, W., Williams, J., Mangan, M., & Karolchik, D. (2008). Genomic data resources: Challenges and promises. *Nature Education*, *1*(3), Article#2.

Lebel, S., Schellenbaum, P., Walter, B., & Maillot, P. (2010). Characterisation of the *Vitis vinifera PR10* multigene family. *BMC Plant Biology, 10*(1), 1-13.

Leray, M., Knowlton, N., Ho, S. L., Nguyen, B. N., & Machida, R. J. (2019). GenBank is a reliable resource for 21st century biodiversity research. *Proceedings of the National Academy of Sciences*, *116*(45), 22651-22656.

Leslie, J. F., & Summerell, B. A. (2008). *The Fusarium laboratory manual*. Hoboken, New Jersey, USA: John Wiley & Sons.

Li, Y. Z., Zheng, X. H., Tang, H. L., Zhu, J. W., & Yang, J. M. (2003). Increase of beta-1, 3-glucanase and chitinase activities in cotton callus cells treated by salicylic acid and toxin of *Verticillium dahliae*. *Acta Botanica Sinica-Chinese Edition, 45*(7), 802-808.

Li, W. M., Dita, M., Wu, W., Hu, G. B., Xie, J. H., & Ge, X. J. (2015). Resistance sources to *Fusarium oxysporum* f. sp. *cubense* tropical race 4 in banana wild relatives. *Plant Pathology*, *64(5)*, 1061-1067.

Lim, G. H., Shine, M. B., de Lorenzo, L., Yu, K., Cui, W., Navarre, D., … Kachroo, P. (2016). Plasmodesmata localizing proteins regulate transport and signaling during systemic acquired immunity in plants. *Cell Host & Microbe*, *19*(4), 541-549.

Lima, M. A. S., Oliveira, M. D. C. F. D., Pimenta, A. T., & Uchôa, P. K. (2019). *Aspergillus niger*: A hundred years of contribution to the natural products chemistry. *Journal of the Brazilian Chemical Society*, *30*(10), 2029-2059.

Linthorst, H. J., Van Loon, L., van Rossum, C. M., Mayer, A., Bol, J. F., van Roekel, J. S., Meulenhoff, E.J., and Cornelissen, B. J. (1990). Analysis of acidic and basic chitinases from tobacco and petunia and their constitutive expression in transgenic tobacco. *Molecular Plant Microbe Interaction, 3*(4), 252-258.

Linthorst, H. J., & Van Loon, L. (1991). Pathogenesis-related proteins of plants. *Critical Reviews in Plant Sciences, 10*(2), 123-150.

Liu, J.-J., & Ekramoddoullah, A. K. (2006). The family 10 of plant pathogenesis-related proteins: Their structure, regulation, and function in response to biotic and abiotic stresses. *Physiological Molecular Plant Pathology, 68*(1-3), 3-13.

Liu, Z. H., Wang, Y. C., Qi, X. T., & Yang, C. P. (2010). Cloning and characterization of a chitinase gene *Lbchi31* from *Limonium bicolor* and identification of its biological activity. *Molecular Biology Reports*, *37*(5), 2447-2453.

Lo Presti, L., Lanver, D., Schweizer, G., Tanaka, S., Liang, L., Tollot, … Kahmann, R. (2015). Fungal effectors and plant susceptibility. *Annual Review of Plant Biology, 66*, 513-545.

Lotan, T., Ori, N., & Fluhr, R. (1989). Pathogenesis-related proteins are developmentally regulated in tobacco flowers. *The Plant Cell, 1*(9), 881-887.

Lu, S., Wang, J., Chitsaz, F., Derbyshire, M. K., Geer, R. C., Gonzales, N. R., ... Marchler-Bauer, A. (2020). CDD/SPARCLE: The conserved domain database in 2020. *Nucleic Acids Research, 48*(D1), D265-D268.

Luo, K., Kim, N. G., You, S. M., & Kim, Y. R. (2019). Colorimetric determination of the activity of starch-debranching enzyme via modified tollens' reaction. *Nanomaterials*, *9*(9), Article#1291.

Macreadie, I. G., Johnson, G., Schlosser, T., & Macreadie, P. I. (2006). Growth inhibition of *Candida* species and *Aspergillus fumigatus* by statins. *FEMS Microbiology Letters*, *262*(1), 9-13.

Magaldi, S., Mata-Essayag, S., De Capriles, C. H., Perez, C., Colella, M. T., Olaizola, C., & Ontiveros, Y. (2004). Well diffusion for antifungal susceptibility testing. *International Journal of Infectious Diseases*, *8*(1), 39-45.

Malamy, J., & Klessig, D. F. (1992). Salicylic acid and plant disease resistance. *The Plant Journal*, *2*(5), 643-654.

Mantelin, S., Thorpe, P., & Jones, J. T. (2015). Suppression of plant defences by plant-parasitic nematodes. *Advances in Botanical Research, 73*, 325-337.

Marković-Housley, Z., Degano, M., Lamba, D., von Roepenack-Lahaye, E., Clemens, S., Susani, M., ... Breiteneder, H. (2003). Crystal structure of a hypoallergenic isoform of the major birch pollen allergen Bet v 1 and its likely biological function as a plant steroid carrier. *Journal of Molecular Biology*, *325*(1), 123-133.

Maymon, M., Sela, N., Shpatz, U., Galpaz, N., & Freeman, S. (2020). The origin and current situation of *Fusarium oxysporum* f. sp. *cubense* tropical race 4 in Israel and the Middle East. *Scientific Reports*, *10*(1), 1-11.

McBride, J. K., Cheng, H., Maleki, S. J., & Hurlburt, B. K. (2019). Purification and Characterization of Pathogenesis Related Class 10 Panallergens. *Foods, 8*(12), 609.

McCleary, B. V., & McGeough, P. (2015). A comparison of polysaccharide substrates and reducing sugar methods for the measurement of endo-1, 4-β-xylanase. *Applied Biochemistry and Biotechnology*, *177*(5), 1152-1163.

Meissner, B., Rogalski, T., Viveiros, R., Warner, A., Plastino, L., Lorch, A., … Moerman, D. G. (2011). Determining the sub-cellular localization of proteins within *Caenorhabditis elegans* body wall muscle. *PloS ONE*, *6*(5), Article#e19937.

Mejias, J., Truong, N. M., Abad, P., Favery, B., & Quentin, M. (2019). Plant proteins and processes targeted by parasitic nematode effectors. *Frontiers in Plant Science, 10*, 970.

Menna, A., Nguyen, D., Guttman, D. S., & Desveaux, D. (2015). Elevated temperature differentially influences effector-triggered immunity outputs in *Arabidopsis*. *Frontiers in Plant Science*, *6*, 995.

Mestre, P., Arista, G., Piron, M. C., Rustenholz, C., Ritzenthaler, C., Merdinoglu, D., & Chich, J. F. (2017). Identification of a *Vitis vinifera* endo-β-1, 3-glucanase with antimicrobial activity against *Plasmopara viticola*. *Molecular Plant Pathology*, *18*(5), 708-719.

Mogensen, J. E., Wimmer, R., Larsen, J. N., Spangfort, M. D., & Otzen, D. E. (2002). The major birch allergen, Bet v 1, shows affinity for a broad spectrum of physiological ligands. *Journal of Biological Chemistry*, *277*(26), 23684-23692.

Mohamad, R., Tengku, A. M., & Sharif, H. (2012). Challenges to banana production in Malaysia: A threat to food security. *Planter*, *88*(1030), 13-21.

Mohamed, S. A. E. H., Elloumi, M., & Thompson, J. D. (2016). Motif discovery in protein sequences. *Pattern Recognition-Analysis and Applications*.

Mohan, C., Santos Júnior, C. D., & Chandra, S. (2020). *In silico* characterisation and homology modelling of a pathogenesis-related protein from *Saccharum arundinaceum*. *Archives of Phytopathology and Plant Protection*, *53*(5-6), 199-216.

Moiseyev, G. P., Fedoreyeva, L. I., Zhuravlev, Y. N., Yasnetskaya, E., Jekel, P. A., & Beintema, J. J. (1997). Primary structures of two ribonucleases from ginseng calluses: New members of the PR-10 family of intracellular pathogenesis-related plant proteins. *FEBS Letters, 407*(2), 207-210.

Mokrini, F., Viaene, N., Waeyenberge, L., Dababat, A. A., & Moens, M. (2019). Root-lesion nematodes in cereal fields: importance, distribution, identification, and management strategies. *Journal of Plant Diseases and Protection*, *126*(1), 1-11.

Mostert, D., Molina, A. B., Daniells, J., Fourie, G., Hermanto, C., Chao, C. P., … Viljoen, A. (2017). The distribution and host range of the banana Fusarium wilt fungus, *Fusarium oxysporum* f. sp. *cubense*, in Asia. *PLoS one*, *12*(7), e0181630.

Munusamy, U., Mohd-Yusuf, Y., Baharum, N. A., Zaidi, K., & Othman, R. Y. (2019). RT-qPCR profiling of pathogenesis related genes in *Musa acuminata* cv. 'Berangan' seedlings challenged with *Fusarium oxysporum* f. sp. *cubense* tropical race 4. *Pakistan Journal of Agricultural Sciences*, *56*(1), 37-42.

Mur, L. A., Kenton, P., Lloyd, A. J., Ougham, H., & Prats, E. (2008). The hypersensitive response; The centenary is upon us but how much do we know? *Journal of Experimental Botany, 59*(3), 501-520.

Mware, B. O. (2016). *Development of Banana bunchy top virus resistance in bananas: RNAi approach* (Doctoral dissertation, Queensland University of Technology). Retrieved from https://eprints.qut.edu.au/95736/

N'guessan, C. A., Brisse, S., Le Roux-Nio, A.-C., Poussier, S., Koné, D., & Wicker, E. (2013). Development of variable number of tandem repeats typing schemes for *Ralstonia solanacearum*, the agent of bacterial wilt, banana Moko disease and potato brown rot. *Journal of Microbiological Methods, 92*(3), 366-374.

Nelson-Vasilchik, K., Hague, J., & Kausch, A. (2016, July 20). *X-Gluc Gus Assay Protocol.* Retrieved on 1st January 2019 from https://www.x-gluc.com/2016/07/gus-assay-protocol/

Neucere, J. N., Brown, R. L., & Cleveland, T. (1995). Correlation of Antifungal Properties and. beta.-1, 3-Glucanases in Aqueous Extracts of Kernels from Several Varieties of Corn. *Journal of Agricultural Food Chemistry*, *43*(2), 275-276.

Neumann, U., Brandizzi, F., & Hawes, C. (2003). Protein transport in plant cells: In and out of the Golgi. *Annals of Botany*, *92*(2), 167-180.

Nithiyaa, P., Nur Ain Izzati, M., Umi Kalsom, Y., & Salleh, B. (2012). Diversity and Morphological Characteristics of *Aspergillus* Species and *Fusarium* Species Isolated from Cornmeal in Malaysia. *Pertanika Journal of Tropical Agricultural Science, 35*(1), 103-116.

Noonim, P., Mahakarnchanakul, W., Nielsen, K. F., Frisvad, J. C., & Samson, R. A. (2009). Fumonisin B2 production by *Aspergillus niger* in Thai coffee beans. *Food Additives and Contaminants*, *26*(1), 94-100.

Norlia, M., Jinap, S., Nor-Khaizura, M. A. R., Radu, S., Chin, C. K., Samsudin, N. I. P., & Farawahida, A. H. (2019). Molecular characterisation of aflatoxigenic and non-aflatoxigenic strains of *Aspergillus* section *Flavi* isolated from imported peanuts along the supply chain in Malaysia. *Toxins, 11*(9), Article#501.

Okongo, R. N., Puri, A. K., Wang, Z., Singh, S., & Permaul, K. (2019). Comparative biocontrol ability of chitinases from bacteria and recombinant chitinases from the thermophilic fungus *Thermomyces lanuginosus*. *Journal of Bioscience and Bioengineering*, *127*(6), 663-671.

Ongena, M., & Jacques, P. (2008). Bacillus lipopeptides: Versatile weapons for plant disease biocontrol. *Trends in Microbiology*, *16*(3), 115–125.

Ortiz, R. (2013). Conventional Banana and Plantain Breeding. *Acta Hortic, 986*, 177-194.

Pagán, I., & García-Arenal, F. (2018). Tolerance to plant pathogens: Theory and experimental evidence. *International Journal of Molecular Sciences*, *19*(3), Article#810.

Paiva, P. M. G., Gomes, F. S., Napoleão, T. H., Sá, R. A., Correia, M. T. S., & Coelho, L. C. B. B. (2010). Antimicrobial activity of secondary metabolites and lectins from plants. In A. M ndez-Vilas (Ed.), *Science against microbial pathogens: Communicating current research and technological advances*, *1* (pp. 396-406), Badajoz, Spain: Formatex Research Center.

Palencia, E. R., Hinton, D. M., & Bacon, C. W. (2010). The black *Aspergillus* species of maize and peanuts and their potential for mycotoxin production. *Toxins, 2*(4), 399-416.

Pan, J., Wang, X., Li, L., Li, X., Ye, X., Lv, D., Chen, C., Liu, S., & He, H. (2018). Purification and characterization of two pathogenesis-related class 10 protein isoforms with ribonuclease activity from the fresh *Angelica sinensis* roots. *Plant Physiology and Biochemistry*, *128*, 66-71.

Park, C. J., Kim, K. J., Shin, R., Park, J. M., Shin, Y. C., & Paek, K. H. (2004). Pathogenesis-related protein 10 isolated from hot pepper functions as a ribonuclease in an antiviral pathway. *The Plant Journal*, *37*(2), 186-198.

Patel, Z. M., Mahapatra, R., & Jampala, S. S. M. (2020). Role of fungal elicitors in plant defense mechanism. In *Molecular Aspects of Plant Beneficial Microbes in Agriculture* (pp. 143-158). Cambridge, Massachusetts, USA: Elsevier.

Perrier, X., De Langhe, E., Donohue, M., Lentfer, C., Vrydaghs, L., Bakry, F., . . . Jenny, C. (2011). Multidisciplinary perspectives on banana (*Musa* spp.) domestication. *Proceedings of the National Academy of Sciences, 108*(28), 11311-11318.

Pieterse, C. M., Zamioudis, C., Berendsen, R. L., Weller, D. M., Van Wees, S. C., & Bakker, P. A. (2014). Induced systemic resistance by beneficial microbes. *Annual Review of Phytopathology*, *52*, 347-375.

Ploetz, R. C. (2000). Panama disease: a classic and destructive disease of banana. *Plant Health Progress, 1*(1), Article#10.

Ploetz, R. C. (2005). Panama disease: An old nemesis rears its ugly head: Part 1. The beginnings of the banana export trades. *Plant Health Progress, 6*(1), Article#18.

Ploetz, R. C. (2015). Fusarium wilt of banana. *Phytopathology, 105*(12), 1512-1521.

Pokotylo, I., Kravets, V., & Ruelland, E. (2019). Salicylic acid binding proteins (SABPs): The hidden forefront of salicylic acid signalling. *International Journal of Molecular Sciences*, *20*(18), Article#4377.

Pollmächer, J., & Figge, M. T. (2014). Agent-based model of human alveoli predicts chemotactic signaling by epithelial cells during early *Aspergillus fumigatus* infection. *PloS ONE*, *9*(10), Article#e111630.

Ponzio, C., Weldegergis, B. T., Dicke, M., & Gols, R. (2016). Compatible and incompatible pathogen–plant interactions differentially affect plant volatile emissions and the attraction of parasitoid wasps. *Functional Ecology*, *30*(11), 1779-1789.

Porazinska, D. L., Morgan, M. J., Gaspar, J. M., Court, L. N., Hardy, C. M., & Hodda, M. (2014). Discrimination of plant-parasitic nematodes from complex soil communities using ecometagenetics. *Phytopathology, 104*(7), 749-761.

Powell, K. A., Renwick, A., & Peberdy, J. F. (2013). *The genus Aspergillus: From taxonomy and genetics to industrial application* (69), Berlin, Germany: Springer Science & Business Media.

Pumplin, N., & Voinnet, O. (2013). RNA silencing suppression by plant pathogens: defence, counter-defence, and counter-counter-defence. *Nature Reviews Microbiology*, *11*(11), 745-760.

Rahman, S. A. S. A., Mohamed, Z., Othman, R. Y., Swennen, R., Panis, B., De Waele, D., Remy, S., & Carpentier, S. C. (2010). *In planta* PCR-based detection of early infection of plant-parasitic nematodes in the roots: A step towards the understanding of infection and plant defence. *European Journal of Plant Pathology*, *128*(3), 343-351.

Rahman, S., Zain, S. M., Mat, M. B., Sidam, A., Othman, R., & Mohamed, Z. (2014). Population distribution of plant-parasitic nematodes of bananas in Peninsular Malaysia. *Sains Malaysiana, 43*(2), 175-183.

Raskin, I., Skubatz, H., Tang, W., & Meeuse, B. J. (1990). Salicylic acid levels in thermogenic and non-thermogenic plants. *Annals of Botany*, *66*(4), 369-373.

Read, N. D., & Roca, M. G. (2006). Vegetative hyphal fusion in filamentous fungi. In *Cell-Cell Channels* (pp. 87-98). New York, USA: Springer.

Richter, L., Wanka, F., Boecker, S., Storm, D., Kurt, T., Vural, Ö., Süßmuth, R., & Meyer, V. (2014). Engineering of *Aspergillus niger* for the production of secondary metabolites. *Fungal Biology and Biotechnology*, *1*(1), 1-13.

Riley, M. B., Williamson, M. R., & Maloy, O. (2002). Plant disease diagnosis. *The Plant Health Instructor,* Article#10.

Robinson, A. D. (1974). An Evaluation of Garrod's Contribution to the One Gene-One Enzyme Hypothesis. *BioScience*, *24*(6), 357-358.

Rodriguez-Tudela, J. L., Alcazar-Fuoli, L., Mellado, E., Alastruey-Izquierdo, A., Monzon, A., & Cuenca-Estrella, M. (2008). Epidemiological cutoffs and cross-resistance to azole drugs in *Aspergillus fumigatus*. *Antimicrobial Agents Chemotherapy, 52*(7), 2468-2472.

Ross, A. F. (1961). Localized acquired resistance to plant virus infection in hypersensitive hosts. *Virology*, *14*(3), 329-339.

Sarowar, S., Kim, Y. J., Kim, E. N., Kim, K. D., Hwang, B. K., Islam, R., & Shin, J. S. (2005). Overexpression of a pepper basic pathogenesis-related protein 1 gene in tobacco plants enhances resistance to heavy metal and pathogen stresses. *Plant Cell Reports, 24*(4), 216-224.

Sambrook, J., & Russell, D. W. (Eds.) (2006) *Cold Spring Harb Protocols, 2006(1).* New York, NY: Cold Spring Harbor Laboratory.

Sato, K., Kadota, Y., & Shirasu, K. (2019). Plant immune responses to parasitic nematodes. *Frontiers in Plant Science*, *10*, 1165.

Schatz, G., & Dobberstein, B. (1996). Common principles of protein translocation across membranes. *Science*, *271*(5255), 1519-1526.

Schuster, E., Dunn-Coleman, N., Frisvad, J. C., & Van Dijck, P. W. (2002). On the safety of *Aspergillus niger*–a review. *Applied Microbiology and Biotechnology*, *59*(4), 426-435.

Sels, J., Mathys, J., De Coninck, B. M., Cammue, B. P., & De Bolle, M. F. (2008). Plant pathogenesis-related (PR) proteins: A focus on PR peptides. *Plant Physiology and Biochemistry, 46*(11), 941-950.

Sharma, R. (2012). Pathogenecity of *Aspergillus niger* in plants. *Cibtech Journal of Microbiology, 1*(1), 47-51.

Shigenaga, A. M., & Argueso, C. T. (2016, August). No hormone to rule them all: Interactions of plant hormones during the responses of plants to pathogens. In *Seminars in Cell & Developmental Biology* (Vol. 56, pp. 174-189). USA: Elsevier.

Sinha, M., Singh, R. P., Kushwaha, G. S., Iqbal, N., Singh, A., Kaushik, S., ... Singh, T. P. (2014). Current overview of allergens of plant pathogenesis related protein families. *The Scientific World Journal,* Article#543195.

Speijer, P. R., & De Waele, D. (1997). Screening of Musa germplasm for resistance and tolerance to nematodes. In *INIBAP Technical Guidelines 1*. Montpellier, France: The International Network for the Improvement of Banana and Plantain.

Spoel, S. H., & Dong, X. (2012). How do plants achieve immunity? Defence without specialized immune cells. *Nature Reviews Immunology*, *12*(2), 89-100.

Stothard, P. (2000). The sequence manipulation suite: JavaScript programs for analyzing and formatting protein and DNA sequences. *Biotechniques*, *28*(6), 1102-1104.

Sun, W., Cao, Z., Li, Y., Zhao, Y., & Zhang, H. (2007). A simple and effective method for protein subcellular localization using *Agrobacterium*-mediated transformation of onion epidermal cells. *Biologia*, *62*(5), 529-532.

Tang, Y., Liu, Q., Liu, Y., Zhang, L., & Ding, W. (2017). Overexpression of *NtPR-Q* up-regulates multiple defense-related genes in *Nicotiana tabacum* and enhances plant resistance to *Ralstonia solanacearum*. *Frontiers in Plant Science*, *8*, Article#1963.

Tekaia, F., & Latgé, J. P. (2005). *Aspergillus fumigatus*: Saprophyte or pathogen? *Current Opinion in Microbiology*, *8*(4), 385-392.

Teng, S.-K., Aziz, N. A. A., Mustafa, M., Laboh, R., Ismail, I. S., Sulaiman, S. R., ... Devi, S. (2016). The occurrence of blood disease of banana in Selangor, Malaysia. *International Journal of Agriculture and Biology, 18*, 92-97.

Terras, F. R., Eggermont, K., Kovaleva, V., Raikhel, N. V., Osborn, R. W., Kester, A., ... Vanderleyden, J. (1995). Small cysteine-rich antifungal proteins from radish: their role in host defense. *The Plant Cell*, *7*(5), 573-588.

Thakur, M., & Sohal, B. S. (2013). Role of elicitors in inducing resistance in plants against pathogen infection: A review. *International Scholarly Research Notices*, Article#762412.

Timper, P. (2014). Conserving and enhancing biological control of nematodes. *Journal of Nematology*, *46*(2), 75-89.

Tran, D. M., Sugimoto, H., Nguyen, D. A., Watanabe, T., & Suzuki, K. (2018). Identification and characterization of chitinolytic bacteria isolated from a freshwater lake. *Bioscience, Biotechnology, and Biochemistry*, *82*(2), 343-355.

Tumin, S., & Ahmad Shaharudin, A. (2019). Banana: The World's Most Popular Fruit. Retrieved 2 May 2020, from http://www.krinstitute.org/Views-@-Banana-;_The_Worlds_Most_Popular_Fruit.aspx

Valkiūnas, G., Atkinson, C. T., Bensch, S., Sehgal, R. N., & Ricklefs, R. E. (2008). Parasite misidentifications in GenBank: how to minimize their number?. *Trends in Parasitology*, *24*(6), 247-248.

Vallad, G. E., & Goodman, R. M. (2004). Systemic acquired resistance and induced systemic resistance in conventional agriculture. *Crop Science*, *44*(6), 1920-1934.

Van Baarlen, P., Van Belkum, A., Summerbell, R. C., Crous, P. W., & Thomma, B. P. (2007). Molecular mechanisms of pathogenicity: How do pathogenic microorganisms develop cross-kingdom host jumps? *FEMS Microbiology Reviews, 31*(3), 239-277.

Van Der Linden, J. W., Warris, A., & Verweij, P. E. (2011). *Aspergillus* species intrinsically resistant to antifungal agents. *Medical Mycology, 49*(Supplement_1), S82-S89.

Van Loon, L., & Van Kammen, A. (1970). Polyacrylamide disc electrophoresis of the soluble leaf proteins from *Nicotiana tabacum* var.'Samsun'and 'Samsun NN': II. Changes in protein constitution after infection with tobacco mosaic virus. *Virology, 40*(2), 199-211.

Van Loon, L., Pierpoint, W., Boller, T., & Conejero, V. (1994). Recommendations for naming plant pathogenesis-related proteins. *Plant Molecular Biology Reporter, 12*(3), 245-264.

Van Loon, L. C. (1983). The induction of pathogenesis-related proteins by pathogens and specific chemicals. *Netherlands Journal of Plant Pathology*, *89*(6), 265-273.

Van Loon, L. C., Rep, M., & Pieterse, C. M. (2006). Significance of inducible defense-related proteins in infected plants. *Annual Review of Phytopathology*, *44*, 135-162.

Vieira, P., & Gleason, C. (2019). Plant-parasitic nematode effectors—insights into their diversity and new tools for their identification. *Current Opinion in Plant Biology, 50*, 37-43.

Voora, V., Larrea, C., & Bermudez, S. (2020). Global Market Report: Bananas. In S. Baliño (Ed.), *Sustainable Commodities Marketplace Series 2019 (May)*, Manitoba, Canada: International Institute for Sustainable Development.

Walker, M., & Rapley, R. (2009). *Route maps in gene technology*. Hoboken, New Jersey, USA: John Wiley & Sons.

Walsh, J. B., & Stephan, W. (2001). Multigene families: Evolution. In *Encylopedia of Life Sciences,* Hoboken, New Jersey, USA: John Wiley & Sons.

Warner, S. A., Scott, R., & Draper, J. (1992). Characterisation of a wound-induced transcript from the monocot asparagus that shares similarity with a class of intracellular pathogenesis-related (PR) proteins. *Plant Molecular Biology, 19*(4), 555-561.

Watanabe, S., & Bressan, A. (2013). Tropism, compartmentalization, and retention of banana bunchy top virus (Nanoviridae) in the aphid vector *Pentalonia nigronervosa*. *Journal of General Virology, 94*(1), 209-219.

Wessel, D. M., & Flügge, U. I. (1984). A method for the quantitative recovery of protein in dilute solution in the presence of detergents and lipids. *Analytical Biochemistry*, *138(1)*, 141-143.

Wiederhold, N. P., & Verweij, P. E. (2020). *Aspergillus fumigatus* and pan-azole resistance: Who should be concerned? *Current Opinion in Infectious Diseases*, *33*(4), 290-297.

Wise, A. A., Liu, Z., & Binns, A. N. (2006). Three methods for the introduction of foreign DNA into Agrobacterium. In *Agrobacterium Protocols* (pp. 43-54), Berlin, Germany: Springer.

Wu, F., Yan, M., Li, Y., Chang, S., Song, X., Zhou, Z., & Gong, W. (2003). cDNA cloning, expression, and mutagenesis of a PR-10 protein SPE-16 from the seeds of *Pachyrrhizus erosus*. *Biochemical and Biophysical Research Communications, 312*(3), 761-766.

Wu, J., Kim, S. G., Kang, K. Y., Kim, J. G., Park, S. R., Gupta, R., Kim ... Kim, S. T. (2016). Overexpression of a pathogenesis-related protein 10 enhances biotic and abiotic stress tolerance in rice. *The Plant Pathology Journal*, *32*(6), 552.

Xie, C., Wen, S., Liu, H., Chen, X., Li, H., Hong, Y., & Liang, X. (2013). Overexpression of ARAhPR10, a member of the PR10 family, decreases levels of *Aspergillus flavus* infection in peanut seeds. *American Journal of Plant Sciences, 4(3),* 602-607.

Xu, T. F., Zhao, X. C., Jiao, Y. T., Wei, J. Y., Wang, L., & Xu, Y. (2014). A pathogenesis related protein, VpPR-10.1, from *Vitis pseudoreticulata*: an insight of its mode of antifungal activity. *PLoS ONE*, *9*(4), Article#e95102.

Xu, X., Feng, Y., Fang, S., Xu, J., Wang, X., & Guo, W. (2016). Genome-wide characterization of the *β-1, 3-glucanase* gene family in *Gossypium* by comparative analysis. *Scientific Reports*, *6*(1), 1-15.

Xu, Y. I., Chang, P. F. L., Liu, D., Narasimhan, M. L., Raghothama, K. G., Hasegawa, P. M., & Bressan, R. A. (1994). Plant defense genes are synergistically induced by ethylene and methyl jasmonate. *The Plant Cell*, *6*(8), 1077-1085.

Yakura, H. (2020). Cognitive and memory functions in plant immunity. *Vaccines*, *8*(3), Article#541.

Yi, S. Y., Shirasu, K., Moon, J. S., Lee, S. G., & Kwon, S. Y. (2014). The activated SA and JA signaling pathways have an influence on flg22-triggered oxidative burst and callose deposition. *PloS ONE*, *9*(2), Article#e88951.

Zarember, K. A., Sugui, J. A., Chang, Y. C., Kwon-Chung, K. J., & Gallin, J. I. (2007). Human polymorphonuclear leukocytes inhibit *Aspergillus fumigatus* conidial growth by lactoferrin-mediated iron depletion. *The Journal of Immunology*, *178*(10), 6367-6373.

Zandvakili, N., Zamani, M., Motallebi, M., & Jahromi, Z. M. (2017). Cloning, overexpression, and in vitro antifungal activity of *Zea mays* PR10 protein. *Iranian Journal of Biotechnology*, *15*(1), 42-49.

Zhang, J., & Zhou, J.-M. (2010). Plant immunity triggered by microbial molecular signatures. *Molecular Plant, 3*(5), 783-793.

Zhang, S. B., Zhang, W.-J., Zhai, H.-C., Lv, Y.-Y., Cai, J.-P., Jia, F., . . . Hu, Y.-S. (2019). Expression of a wheat β-1, 3-glucanase in *Pichia pastoris* and its inhibitory effect on fungi commonly associated with wheat kernel. *Protein Expression Purification, 154*, 134-139.

Zhou, J., Li, Z., Wu, J., Li, L., Li, D., Ye, X., ... Cao, H. (2017). Functional analysis of a novel β-(1, 3)-glucanase from *Corallococcus* sp. strain EGB containing a fascin-like module. *Applied and Environmental Microbiology*, *83*(16), Article#e01016-17.

Zhou, X. J., Lu, S., Xu, Y.-H., Wang, J. W., & Chen, X. Y. (2002). A cotton cDNA (*GaPR-10*) encoding a pathogenesis-related 10 protein with in vitro ribonuclease activity. *Plant Science, 162*(4), 629-636.

Ziemann, M., Eren, Y., & El-Osta, A. (2016). Gene name errors are widespread in the scientific literature. *Genome Biology*, *17*(1), 1-3.